COMPUTATIONAL STUDIES OF SELECTED RUTHENIUM CATALYSIS REACTIONS

Khaldoon A. Barakat, B.S., M.S.

Dissertation Prepared for the Degree of

DOCTOR OF PHILOSOPHY

UNIVERSITY OF NORTH TEXAS

December 2007

APPROVED:

Thomas R. Cundari, Major Professor
Mohammad A. Omary, Committee Member
Martin Schwartz, Committee Member
Angela K. Wilson, Committee Member
Michael G. Richmond, Chair of the Department of Chemistry
Sandra L. Terrell, Dean of the Robert B. Toulouse School of Graduate Studies

Barakat, Khaldoon, A., Computational studies of selected ruthenium catalysis reactions. Doctor of Philosophy (Chemistry), December 2007, 108 pp., 6 tables, 21 illustrations, references, 214 titles.

Computational techniques were employed to investigate pathways that would improve the properties and characteristics of transition metal (*i.e.*, ruthenium) catalysts, and to explore their mechanisms. The studied catalytic pathways are particularly relevant to catalytic hydroarylation of olefins. These processes involved the +2 to +3 oxidation of ruthenium and its effect on ruthenium-carbon bond strengths, carbon-hydrogen bond activation by 1,2-addition/reductive elimination pathways appropriate to catalytic hydrogen/deuterium exchange, and the possible intermediacy of highly coordinatively unsaturated (*e.g.*, 14-electron) ruthenium complexes in catalysis.

The calculations indicate a significant decrease in the Ru-CH_3 homolytic bond dissociation enthalpy for the oxidation of TpRu(CO)(NCMe)(Me) to its Ru^{III} cation through both reactant destabilization and product stabilization. This oxidation can thus lead to the olefin polymerization observed by Gunnoe and coworkers, since weak Ru^{III}-C bonds would afford quick access to alkyl radical species.

Calculations support the experimental proposal of a mechanism for catalytic hydrogen/deuterium exchange by a Ru^{II}-OH catalyst. Furthermore, calculational investigations reveal a probable pathway for the activation of C-H bonds that involves phosphine loss, 1,2-addition to the Ru-OH bond and then reversal of these steps with deuterium to incorporate it into the substrate. The presented results offer the indication

for the net addition of aromatic C-H bonds across a Ru^{II}-OH bond in a process that although thermodynamically unfavorable is kinetically accessible.

Calculations support experimental proposals as to the possibility of binding of weakly coordinating ligands such as dinitrogen, methylene chloride and fluorobenzene to the ”14-electron” complex $[(PCP)Ru(CO)]^+$ in preference to the formation of agostic Ru-H-C interactions. Reactions of $[(PCP)Ru(CO)(\eta^1\text{-}ClCH_2Cl)][BAr'_4]$ with N_2CHPh or phenylacetylene yielded conversions that are exothermic to both terminal carbenes and vinylidenes, respectively, and then bridging isomers of these by C-C bond formation resulting from insertion into the Ru-C_{ipso} bond of the phenyl ring of PCP. The QM/MM and DFT calculations on full complexes $[(PCP)(CO)Ru{=}(C)_{0,1}{=}CHPh]^+$ and on small models $[(PCP')(CO)Ru{=}(C)_{0,1}{=}CH_2]^+$, respectively, offered data supportive of the thermodynamic feasibility of the suggested experimental mechanisms and their proposed intermediates.

ACKNOWLEDGEMENTS

I would like to thank God for giving me the health and ability to complete this research. My special gratitude and appreciation are to my advisor Dr. Thomas R. Cundari. I am also very obliged for all the research collaborators with whom I worked in the last four years. I expressly thank my entire family who helped me through all my school years.

Finally, the National Science Foundation, the United States Department of Education and the United States Department of Energy are acknowledged for partial support of this research.

TABLE OF CONTENTS

Page

LIST OF TABLES

Page

LIST OF ILLUSTRATIONS

Page

CHAPTER 1

INTRODUCTION

Catalysis is amongst the most important areas of modern chemistry research. Catalysis is defined as a process whereby the rate of a chemical reaction is increased (or decreased, although such catalysts are typically of little economical value; hence, we focus on the former in this dissertation). By definition, the catalyst speeds up the reaction without itself being consumed in the overall chemical reaction. Most useful catalysts help lower the activation barrier for the reaction; however, a catalyst does not make a forbidden reaction allowed, it only lowers otherwise high activation barriers for thermodynamically allowed reactions (Figure 1.1).

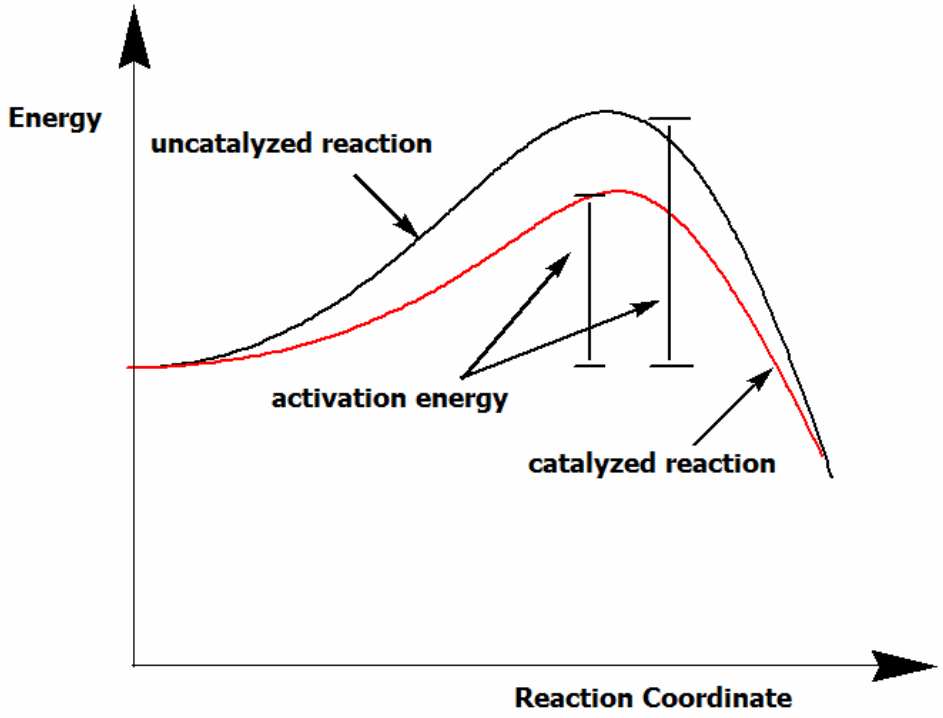

Figure 1.1. Hypothetical exothermic chemical reaction, before and after the introduction of a catalyst.

The importance of catalysis has grown in magnitude recently, especially in

organic synthesis and industrial chemistry, due to the obvious economic demand for producing more valuable products in shorter times. However, catalysis is also beneficial from an ecological and environmental viewpoint, given the necessity to selectively make desired chemical products with less wasteful (and expensive to dispose of) side products. One also wishes to employ a catalyst that is atom economical in order to make the most efficient use of dwindling natural resources like oil and natural gas. In addition to their industrial importance, catalytic reactions are also indispensable to sustain life, where enzymes, for example, are vital in most metabolic pathways.[1] The significance of catalytic techniques thus brings together many of the important economic and environmental issues that face modern chemistry.

Catalytic reactions are central to many industrial processes that involve the making of useful products from petrochemical feedstocks, which are fundamentally comprised of hydrocarbons. Just one example that is appropriate to the current dissertation is styrene (*i.e.*, vinyl-benzene), which is used primarily for making polystyrene for insulation foams and the making of thermoset and thermoplastic materials.

Undoubtedly, for the aforementioned applications, catalysts must continuously be developed and improved to meet performance standards in terms of activity (amount of product produced per unit catalyst also called turnover number (TON)) and selectivity (percentage of desired product versus unwanted side products, in terms of regioselectivity, chemoselectivity, and/or stereoselectivity depending on the particular application). In an ideal world, the catalyst would promote a pathway that is completely

specific to its target molecule, be chemically stable under the conditions required for the process, and would emerge from the completed reaction fully intact and ready for facile reuse. The desired catalysts must also be economical to manufacture.[2,3]

There are many catalysts available for use both in academic research and in industry; many of these catalysts involve transition metals such as ruthenium.[4,5,6,7] Ruthenium (Ru) is a second row transition metal. The chemical versatility of ruthenium complexes contributes to their use as catalyst precursors in many organic and organometallic reactions. One of the chemical characteristics of ruthenium catalysts within the realm of organometallic chemistry is their ability to react with unsaturated organic compounds containing carbon-carbon double and aromatic bonds, and the stability of ruthenium organometallics in the presence of different functional groups (unlike early metal catalysts based on, for example, titanium, ruthenium is a soft acid, and thus quite tolerant of oxygen- and nitrogen-based functional groups).[4,5,6]

In this dissertation, emphasis is given to the study of processes and materials relevant to the catalytic production of alkyl-arenes such as ethyl-benzene (used primarily for the production of styrene), cumene (or isopropyl-benzene, used for the manufacture of phenol and acetone), isobutyl-benzene (a starting material for the analgesic ibuprofen). Historically, alkyl-arenes are produced via Friedel-Crafts catalysis using a strong acid (typically aluminum chloride) catalyst. This example is discussed in the following paragraph.

For more than five centuries, organic reactions have been responsible for many useful chemical products. However, a lot of these reactions produced environmentally

hazardous byproducts.[2] A prime example of such a reaction is Friedel-Crafts (FC) acid-catalyzed alkylation.[2] The production of alkyl-arenes using a Friedel-Crafts catalyst involves multiple chemical steps (*i.e.*, ArH → ArX → Ar-R, where Ar, X and R are generic aryl, halide and alkyl groups, respectively), which is inherently less efficient than a single step process (*i.e.*, ArH → Ar-R). The first step of Friedel-Crafts catalysis involves functionalizing the arene substrate through a variety of methods, most notably free-radical halogenation to give an aryl-halide (*e.g.*, chlorobenzene). The halogenation step can be problematic given the lack of specificity sometimes seen for free-radical halogenation, *e.g.*, the formation of products that are multiply halogenated. This step is then followed by a carbon-carbon bond formation reaction using an aluminum chloride catalyst and an alkyl halide reagent to produce the desired alkyl-arene. The FC process for the manufacture of alkyl-arenes also has issues relating to linear versus branched alkyl-arene products (selectivity) (Figure 1.2) and multiple alkylation (*e.g.*, producing diethyl-benzene instead of ethyl-benzene). Friedel-Crafts chemistry often gives the branched isomer as the major product since a carbocation (R^+) is an intermediate in the catalytic cycle. The FC chemistry also entails the use of very acidic catalysts, which limit functional group tolerance.[2,7]

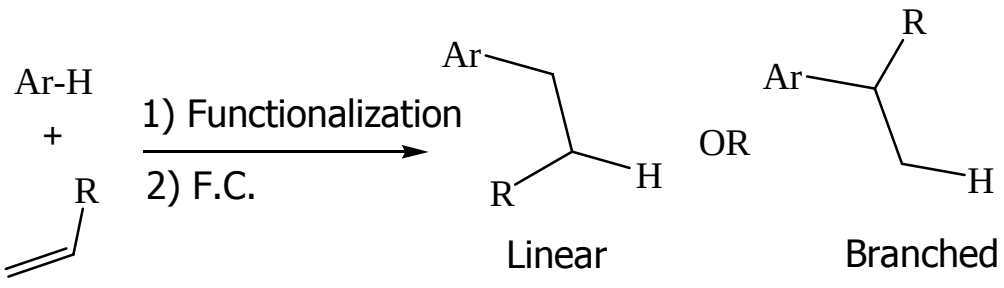

Figure 1.2. A simplified scheme for the linear vs. branched products of a Friedel-Crafts reaction.

Reaction pathways involving transition metal catalysts like ruthenium complexes may be of benefit to solve the problems inherent in Friedel-Crafts catalysis of alkyl-arenes, most notably functional group tolerance and control of the linear:branched product ratio. Trost *et al*. have extensively used coordinatively unsaturated ruthenium complexes to perform reactions such as alkyl addition and ligand dissociation and bond coupling.[3] Their research resulted in the suggestion of more than twenty new processes such as the addition of a terminal alkyne to a coordinatively and electronically unsaturated ruthenium complex to make a vinylidene ruthenium complex (*i.e.*, [Ru] + R-C≡C-H → [Ru]=C=C(H)R) where [Ru] signifies a generic ruthenium complex), giving a wide range of possibilities for improvement in the area of oxidation-reduction and C-C bond formation.[3] Additionally, other ruthenium-aryl and -alkyl complexes have been shown to activate aromatic C-H bonds together with functionalization of unsaturated C-C bonds leading to coupling of an olefin to an aryl in what is known as catalytic hydroarylation of olefins (Figure 1.3 shows a few representative examples).[7,8,9]

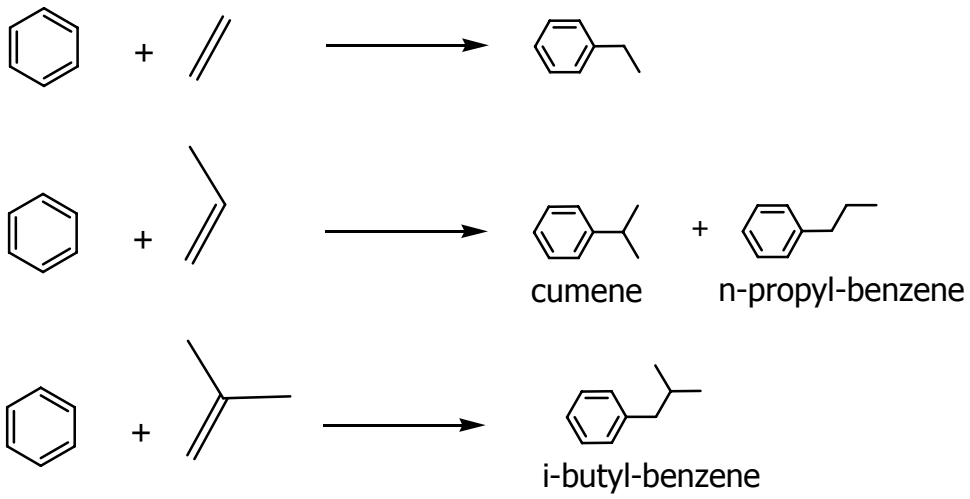

Figure 1.3. Hydroarylation of ethylene to produce ethyl-benzene (top), propylene to produce cumene and n-propyl-benzene (middle) and isobutylene to produce isobutyl-benzene.

Gunnoe *et al*. have proposed a catalytic cycle for the hydroarylation of olefins as a result of experiments (synthesis, spectroscopy, and mechanistic studies) in conjunction with density functional theory calculations (by our research group) for a ruthenium catalyst of the type TpRu(CO)(R)(NCMe) (Tp = hydridotris(pyrazolyl)borate, R = alkyl or aryl group), that activates arenes C-H bonds, and promotes the addition of arenes to unsaturated carbon-carbon bonds.[7] The reported hydroarylation reactions of olefins are catalyzed by the complex TpRu(CO)(NCMe)(Ph), via a pathway that involves the exchange of acetonitrile/olefin ligands to produce TpRu(CO)(η^2-olefin)(Ph), which is then followed by the insertion of the olefin ligand into the ruthenium-phenyl bond to produce a 16-electron intermediate, *e.g.*, TpRu(CO)(CH_2CH_2Ph) when the olefin is ethylene. Subsequently, metal-mediated C-H activation of arene reforms the ruthenium-aryl bond of the TpRu(CO)(Ph) active species and also releases an alkyl-arene to complete the catalytic cycle (Figure 1.4). The TpRu(CO)(Ph) active species has not been

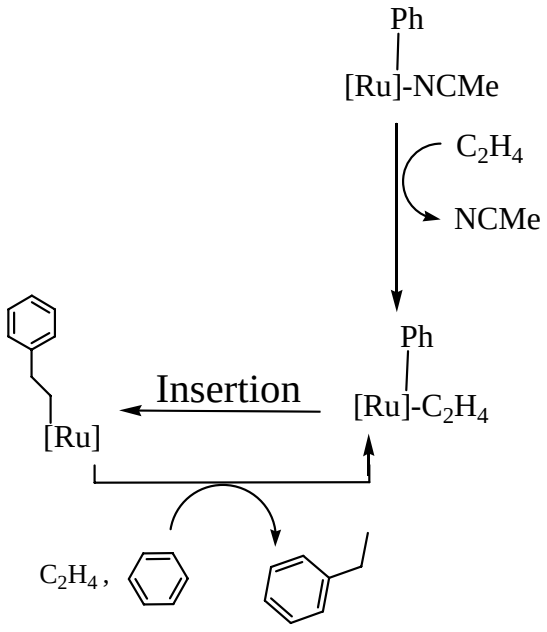

Figure 1.4. A scheme for the catalytic cycle of benzene ethylene addition.

experimentally isolated, nor is it likely to be given its 16-electron count; the catalyst resting state is 18-electron TpRu(CO)(η^2-olefin)(Ph).[7] Hence, proposed intermediates such as TpRu(CO)(Ph) are interesting subjects for computational chemistry study.

The proposed catalytic cycle provides an interesting pathway to arene alkylation as it involves fewer steps than would be used in a typical Friedel-Crafts process (*i.e.*, there is no need for functionalization via free-radical halogenation). A TpRu catalyzed process may also be directed towards the more selective production of linear versus branched alkyl-arene products by modifying the ligands (*e.g.*, replacing Tp with a more bulky derivative might be expected to enhance formation of the sterically less hindered linear product) and other aspects of the ruthenium catalyst's coordination environment (*e.g.*, replace CO with a phosphine, PR_3, ligand).

An important reaction in many organometallic catalytic cycles is reductive elimination. Metal-carbon bonds in transition metal complexes ($L_nM(R')R$) may undergo reductive elimination, in which the organic molecule (R-R') is eliminated from the transition metal complex leading to the metal center being reduced by a value of 2 (in the case of a monometallic complex).[10,11,12,13,14,15,16,17] Both the less common intermolecular and the more common intramolecular processes are observed for reductive elimination from two metal centers, which can be thought of as the simplest model for bond activation/formation on a metal surface.[10,11,12,13] Sherry *et al*. and Cui *et al*. have also studied oxidative addition, which is the microscopic reverse of reductive elimination, for both intermolecular and intramolecular reactions from two metal centers.[18,19] Furthermore, in addition to concerted pathways, reductive elimination of

hydrocarbons can be initiated by the homolysis of a metal-carbon bond resulting in a single electron reduction of the metal center.[14,15,16,17] The production of alkyl radicals can thus initiate radical-based polymerization or, may lead to activation of aromatic C-H bonds as in the case of hydroarylation of olefins.[7,8,9,14,15,16,17] Gunnoe *et al*. have previously studied catalyst precursors for hydroarylation of olefins and polymerization of olefins, such as TpRu(CO)(NCMe)(R) (Tp = hydridotris(pyrazolyl)borate; R = Me or aryl). The complex $TpRu^{II}(CO)(NCMe)(Me)$ was shown to initiate olefin polymerization through either a radical or an insertion pathway. The acetonitrile (MeCN) ligand's ability to undergo exchange reactions provided access to the coordinatively unsaturated, 16-electron TpRu(CO)(Me) active species, which permitted binding of the olefin and insertion of its C=C bond into the Ru-C_{alkyl} bond, allowing for oligomerization (L_nRu-CH_2CH_2-Ph) and polymerization (L_nRu-$(CH_2CH_2)_x$-Ph, x » 2) to occur.[7,8,9,20]

Early and late transition metals (including ruthenium) are also involved in catalytic hydrocarbon functionalization (*i.e.*, RH → RX where X can be a heteroatom or hydrocarbyl functional group).[21,22,23,24,25,26,27,28,29,30,31,32,33,34,35,36,37,38] In addition to the Gunnoe complexes just discussed, ruthenium amido complexes such as *trans*-$(DMPE)_2Ru(H)(NH_2)$ (DMPE = 1,2-dimethylphosphinoethane) have been shown to abstract hydrogen from acidic C-H bonds due to the presence of the highly basic NH_2 ligand,[39] thus, participating in selective activation of hydrocarbons, albeit not via a concerted C-H bond activation pathway.

Coordinatively unsaturated divalent (*i.e.*, Ru^{2+}) ruthenium complexes with 14- or 16-electron counts have been receiving increasing attention because of their possible

role as intermediates in catalytic processes,[40,41] for example, the Grubbs-type 16-electron ruthenium catalysts (Figure 1.5) have been widely used for olefin metathesis, (*e.g.*, $H_2C=CR_2 + H_2C=C(R')_2 \rightarrow H_2C=CH_2 + R_2C=C(R')_2$).[5]

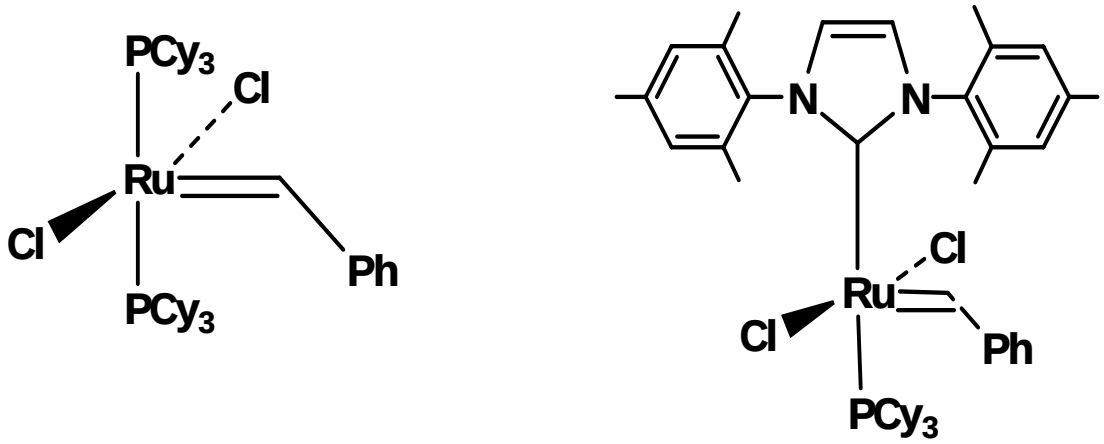

Figure 1.5. Ruthenium Grubbs-type catalysts for olefin metathesis.

Previous reports in the area of Ru catalysis have provided details of the synthesis and reactivity of ruthenium amido complexes with bulky ligands such as (PCP)Ru(CO)(NHR) where (PCP = 2,6-$(CH_2P^tBu_2)_2C_6H_3$) (Figure 1.6) and (R = H or Ph).[42,43,44] These types of complexes containing bulky ligands are of interest in this research since the presence of the tridentate PCP fragment may have steric consequences that could enhance the system's ability to activate C-H bonds.

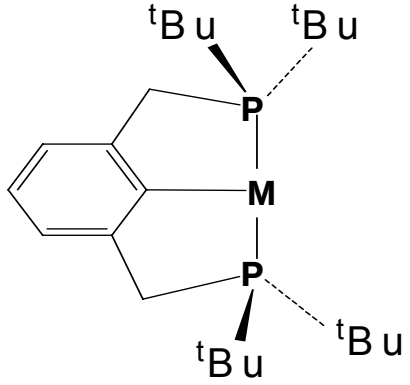

Figure 1.6. PCP ligand. M = ruthenium.

In support of experiments, constant advances in computer technology and computational chemistry methods can aid in the improvement of catalysts and the study of catalytic reactions. Computational techniques have the potential to provide for the faster and more economical development of novel catalysts by using modeling capabilities to predict catalyst performance (activity and selectivity) and hence fewer experiments would be needed to assess the influence of metal/ligand modification on the rates and product ratios of catalytic reactions. Computational chemistry is also an ideal approach to study the properties of transition states and short-lived reactive intermediates, whose direct study is typically very difficult with experimental techniques, and to extract chemical patterns (*e.g.*, which ligand gives the highest activity and/or greatest selectivity) from among many possible catalyst candidates that typically differ in metals and/or ligands.

This dissertation research is inspired by the interesting challenges arising in the study of catalytic pathways that involve the oxidation of ruthenium (from the +2 to +3 oxidation state), carbon-hydrogen bond activation by 1,2-addition/reductive elimination pathways, and the possible intermediacy of highly coordinatively unsaturated (*e.g.*, 14-electron) ruthenium complexes in catalytic processes that are particularly relevant to catalytic hydroarylation of olefins. In this research, computational and experimental techniques were employed in tandem to investigate pathways that would improve the properties and characteristics of transition metal (*i.e.*, ruthenium) catalysts, and to explore the mechanisms involved in these catalytic processes. The detailed experimental preparation of the ruthenium complexes in the herein discussed projects

and their reactions were carried out in collaboration with the experimental group of Prof. T. Brent Gunnoe (Department of Chemistry, North Carolina State University) and have been published elsewhere.[45,46,47,48] This dissertation focuses on the computational studies carried out in our laboratory at the University of North Texas (Department of Chemistry) in conjunction with the experimental studies of Gunnoe and coworkers. The remainder of this dissertation covers three other projects in computational chemistry.

CHAPTER 2

COMPUTATIONAL METHODS

Unless stated otherwise, all of the quantum calculations in this research were performed using the Gaussian98 suite of programs.[49] Quantum mechanical (QM) and hybrid quantum mechanics/molecular mechanics (QM/MM) calculations were utilized as needed for the type of complexes studied. Depending on availability, crystal structures for ruthenium complexes were used to initiate the geometry optimizations.

2.1 Quantum Mechanical (QM) Calculations

The QM calculations employed density functional theory (DFT),[50] precisely, the B3LYP hybrid functional.[51] Ruthenium and main group elements were described with the Stevens (CEP-31G) relativistic effective core potentials (ECPs) in addition to valence basis sets (VBSs).[52] The valence basis sets of main group elements (boron, carbon, nitrogen, oxygen, chlorine, fluorine) were augmented with a d polarization function with an exponent (ξ_d = 0.80), and a d polarization function with an exponent (ξ_d = 0.55) was used on the phosphorus. The full tris(pyrazolyl)borate (Tp^-) ligand was replaced by the tris(azo)borate (Tab) ligand $[HB(-N=NH)_3]^-$ for simplicity (Figure 2.1). The use of the Tab model was supported by results from previous research where the use of the Tab ligand was demonstrated to reproduce the structure and energetics of the full Tp ligand.[7] Also, for models containing the PMe_3 ligand, the less bulky PH_3 ligand was used instead of PMe_3 ligand, again for the sake of simplicity and to speed up the simulations.

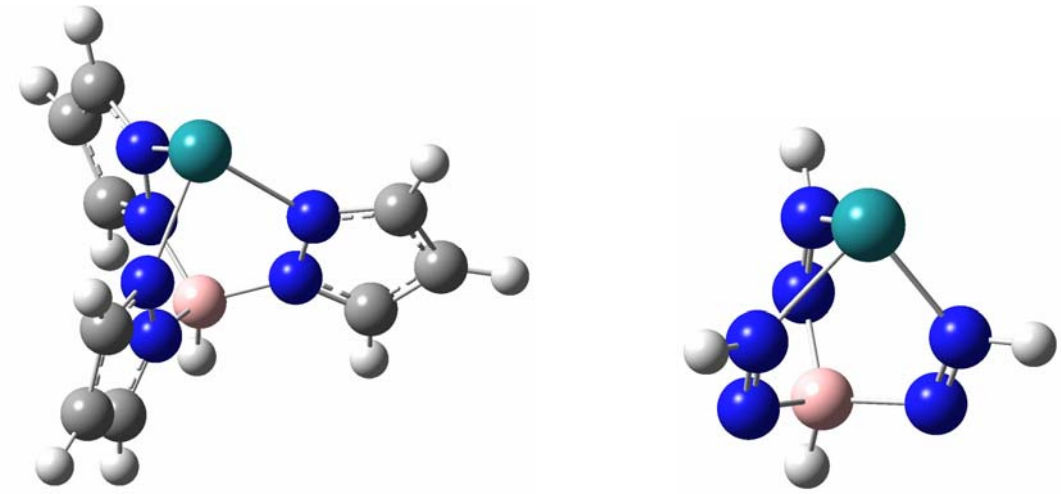

Figure 2.1. Tp = hydridotris(pyrazolyl)borate (left), and Tab = tris(azo)borate (right).

The present blending of ECPs and VBSs, termed SBK(d), has been validated by calculations on a broad selection of transition metal complexes and properties,[53,54,55] as well as specifically with scorpionate compounds of ruthenium.[56] Truncated experimental models of the Ru-PCP complexes were also calculated at the same QM level of theory described above, *i.e.*, B3LYP/SBK(d). These simplified models involved the replacement of (a) tert-butyl groups on the PCP ligand with hydrogen (Figure 1.6), and (b) the phenyl substituent on the carbene/vinylidene with a hydrogen atom.

All stationary points for the models explored in this research were fully optimized without any symmetry constraints. The energy Hessian was calculated at all stationary points to confirm the geometries thus obtained as minima (*i.e.*, no imaginary frequencies), or transition states (one and only imaginary frequency). Closed-shell complexes were calculated using the restricted Kohn-Sham formalism, while open-shell

complex were calculated within the unrestricted Kohn-Sham formalism. The energies calculated included zero point, enthalpic, and entropic corrections (1 atm, 298.15 K) found by employing unscaled vibrational frequencies determined at the B3LYP/CEP-31(d) level of theory.

2.2 Hybrid Quantum Mechanical/Molecular Mechanical (QM/MM) Calculations

Calculations of the hybrid QM/MM type were carried out on full experimental models of the Ru-PCP complexes only. The QM/MM approach was utilized according to the ONIOM methodology.[57] In order to scrutinize ligand (*i.e.*, N_2, CH_2Cl_2, PhF) binding and compare it to agostic Ru···H-C bonding, the MM region contained only three out of the four tert-butyl groups of the PCP ligand (*i.e.*, those not involved in agostic interaction) attached to the phosphorus atoms in each complex; the tert-butyl group with an agostic interaction was QM modeled (at the same B3LYP/CEP-31(d) level of theory) with the remainder of the complex. The MM region was described with the Universal Force Field (UFF).[58] Calculations on the QM core employed the B3LYP hybrid functional, and ruthenium and main group elements were described with the Stevens (CEP-31G(d)) relativistic effective core potentials (ECPs) and valence basis sets (VBSs). The Opt=NoMicro option was used to prevent microiterations during the geometry optimization steps.

CHAPTER 3

RESULTS AND DISCUSSION

3.1 $Ru^{III} \rightarrow Ru^{II}$ Complexes by Ru-C_{alkyl} Bond Homolysis

Ruthenium complexes of the type TpRu(CO)(NCMe)(R) (Tp = hydridotris(pyrazolyl)borate; R = Me or aryl) have been reported as catalyst precursors for the hydroarylation of olefins.[7,8,9] However, when the olefins involved in the reactions are electron-deficient, the Ru^{II} catalysts instigate radical polymerization reactions.[20] Electron-deficient olefins are compounds with at least one double bond and a terminal electron-withdrawing group attached to it, *e.g.*, acrylonitrile (H_2C=CH-CN). In this research, we explore the stability and structure of Ru^{III} complexes of the type [TpRu(L)(L')(R)][OTf] (L = CO, L' = NCMe and R = Me or CH_2CH_2Ph; L = L' = PMe_3 and R = Me) (OTf = trifluoromethanesulfonate), in particular their inclination to return to a Ru^{II} formal oxidation state after going through reductive transformations, specifically pathways involving Ru-C_{alkyl} bond homolysis. Of particular interest is the change in Ru-C_{alkyl} bond dissociation enthalpies with a change in the ruthenium oxidation state (*i.e.*, Ru^{2+} versus Ru^{3+}). TpRu(CO)(NCMe)(OTF) was isolated by Gunnoe and coworkers.[45] The reaction was hypothesized to involve the formation of Ag(s) through a single-electron transfer (from the ruthenium complex to a silver(I) salt) and the loss of a methyl ligand from the presumed Ru^{III} intermediate [TpRu(CO)(Me)(NCMe)][OTf]. Gunnoe *et al.* suggested that the active species is a free radical.[45] Efforts to study the effect of auxiliary ligands on the oxidation/reduction processes led to the experimental study of $TpRuL_2(R)$ type complexes and their oxidation reactions.[45] The results from

studying the $TpRu(PMe_3)_2(Me)$ complex were nearly the same as those results found for the comparable reactions of TpRu(CO)(NCMe)(Me).[45] These pieces of evidence thus imply a mechanism in the oxidation of $TpRu^{II}$ complexes that involves the formation of organic free radicals, and thus presumably Ru^{III} intermediates.

Gunnoe and coworkers[45] proposed that Ru-C_{alkyl} bond homolysis could be a likely path for the observed $Ru^{II/III}$ elimination sequences to produce free radicals. Organometallic complexes of Ru^{III} are quite rare and the inability of Gunnoe and coworkers to experimentally isolate a Ru^{III} complex thus makes them ideal candidates for computational analysis. If the C-H bond dissociation enthalpy (BDE) for CH_2Cl_2 (~100 kcal/mol) and the C-H BDE of methane (~105 kcal/mol) are taken into consideration, the breaking of the methane C-H bond is more difficult than that of CH_2Cl_2 making the former more stable and favorable to be formed in methylene chloride solution.[59] Therefore, it is thermodynamically favorable to produce methane from methyl radical and methylene chloride. The formation of ethane, which is likely an outcome of carbon-carbon bond coupling of two methyl radicals, appears to be kinetically competing with hydrogen atom abstraction from the solvent by the methyl radical. Reaction processes that produce methyl radical, similar to the reaction type studied by Gunnoe *et al.*, are expected to display increased production of methane (or deuterated methane) in solvents that have weaker C-H (or C-D) bonds. Consistent with this expectation, the oxidation of TpRu(CO)(Me)(NCMe) or $TpRu(PMe_3)_2(Me)$ in toluene-d_8, which has BDE for its benzylic C-H bond of ~88 kcal/mol, resulted in greater production of methane than ethane than comparable reactions in methylene chloride.

In support of the experiments by Gunnoe and coworkers, we performed B3LYP/SBK(d) calculations on full models of neutral $TpRu^{II}(CO)(NCMe)(Me)$, and $\{TpRu^{I}(CO)(NCMe)\}$ complexes as well as the cationic $[TpRu^{III}(CO)(NCMe)(Me)]^{+}$ and $[TpRu^{II}(CO)(NCMe)]^{+}$ complexes, and the methyl radical, to determine the Ru-CH_3 BDEs. In general, the corresponding neutral and cationic complexes of TpRu had no major geometrical differences. For example, inspection of the bond lengths resulted in the following: the calculated Ru^{II}-Me bond length of $TpRu^{II}(CO)(NCMe)(Me)$ was 2.15 Å, and the calculated Ru^{III}-Me bond length of $[TpRu^{III}(CO)(NCMe)(Me)]^{+}$ was 2.14 Å. Using the available ionic radii in the literature for Ru^{II} and Ru^{III},[60] it is envisaged that bond lengths involving Ru^{III} should be ~0.06 Å shorter than similar bonds involving Ru^{II}. However, the calculated $\Delta Ru^{III/II}$-CH_3 bond length is just 0.01 Å, indicating that the Ru^{III}-Me bond is intrinsically weaker than the Ru^{II}-Me bond. The Mulliken bond orbital population (BOP) was carried out to support this inference. The Mulliken BOP is a measure of the orbital overlap and the amount of electron density in the overlap region between two atoms; as such, when comparing similar bond types (ruthenium-carbon in the present case) a higher BOP indicates an intrinsically stronger bond. The BOP should, however, not be confused with the bond order. BOP analysis values were 0.45 for the Ru^{II}-Me bond of $TpRu^{II}(CO)(NCMe)(Me)$, and 0.36 for the Ru^{III}-Me bond of $[TpRu^{III}(CO)(NCMe)(Me)]^{+}$. Consequently, the DFT-derived BOPs are in support of the supposition that the metal-Me bond in the Ru^{III} complex is intrinsically weaker than that in the analogous Ru^{II} complex. When viewing the Ru-C bond scission in thermodynamic

terms, this implies a destabilization of the reactant (the TpRu-methyl complex) upon oxidation of the ruthenium from the 2+ to the 3+ formal oxidation state.

Oxidation of the Ru^{II} (calculated Ru-Me homolytic BDE of 48.6 kcal/mol) to Ru^{III} (calculated Ru-Me homolytic BDE of 23.2 kcal/mol) resulted in a significant decrease in the calculated Ru-Me homolytic BDEs of 25.4 kcal/mol. For closely related pseudo-octahedral Cp*Fe(dppe)X complexes (Cp* = pentamethylcyclopentadienyl; dppe = 1,2-bis(diphenylphosphino)ethane; X = halide, H, or Me), BDEs were studied experimentally, and it was concluded that the oxidation from Fe^{II} to Fe^{III} also reduced the homolytic Fe-X BDEs by 9 to 17 kcal/mol.[17] This result is similar in direction to the current computational predictions for ruthenium (which like iron is a Group 8 transition metal), although the magnitude is calculated to be much larger for the heavier ruthenium metal, perhaps due to the greater degree of covalent bond character expected for Ru-C versus Fe-C.

The reduction in Ru-methyl BDE is echoed by the calculated ionization potentials (IPs). From the B3LYP/SBK(d) calculations, it takes 6.3 eV to ionize the d^6-Ru^{II}-Me complex to the analogous d^5-$[Ru^{III}]^+$-Me complex. Similarly, it takes 5.2 eV to ionize the d^7-Ru^{I} complex to the d^6-$[Ru^{II}]^+$ complex (Figure 3.1). The difference between the IPs of d^6-Ru^{II}-Me complex of 6.3 eV and the d^7-Ru^{I} complex of 5.2 eV is ~1.1 eV, which amounts to the same 25 kcal/mol difference found for the change in ruthenium-methyl BDEs upon oxidation. Thus, the product of ionizing d^7-Ru^{I} is intrinsically more stable than the product of ionizing d^6-Ru^{II}. The calculational result seems plausible since for a heavier, second row transition metal like ruthenium (which has a larger ligand field

splitting and a preference for low spin configurations), a d^7 complex represents one "extra" electron above and beyond the stable d^6 configuration, which should make d^7 complexes relatively easy to oxidize.

From our calculations, it is found that the Ru-C bond becomes weaker upon oxidation of Ru from the 2+ to the 3+ oxidation state (reactant destabilization) and, the return to a d^6 configuration for the Ru^{III} complex after Ru-C bond homolysis leads to a more facile ionization process (product stabilization). Gunnoe *et al.* estimate a barrier of $\Delta G^{\ddagger} \leq 20$ kcal/mol at room temperature for Ru-C bond scission, consistent with our calculated estimate of 23.2 kcal/mol for the BDE of Ru^{III}-C. For the Ru^{III} oxidation state of the TpRu complexes studied, Ru^{III}-C_{alkyl} bonds emerge as weak bonds from the calculations, a result that supports the experimental hypothesis that Ru^{III} complexes are plausible intermediates in the radical initiated polymerization reactions of electron-deficient olefins.

Controlling metal-carbon bond energies are fundamental to the development of synthetic methodologies as well as understanding catalytic processes.[61,62,63,64] In this research, we have seen potential oxidation/reduction pathways to control this important chemical descriptor via both reactant destabilization (*i.e.*, metal-carbon bond weakening) and product stabilization (*i.e.*, return of a radical species to the preferred metal oxidation state upon oxidation).

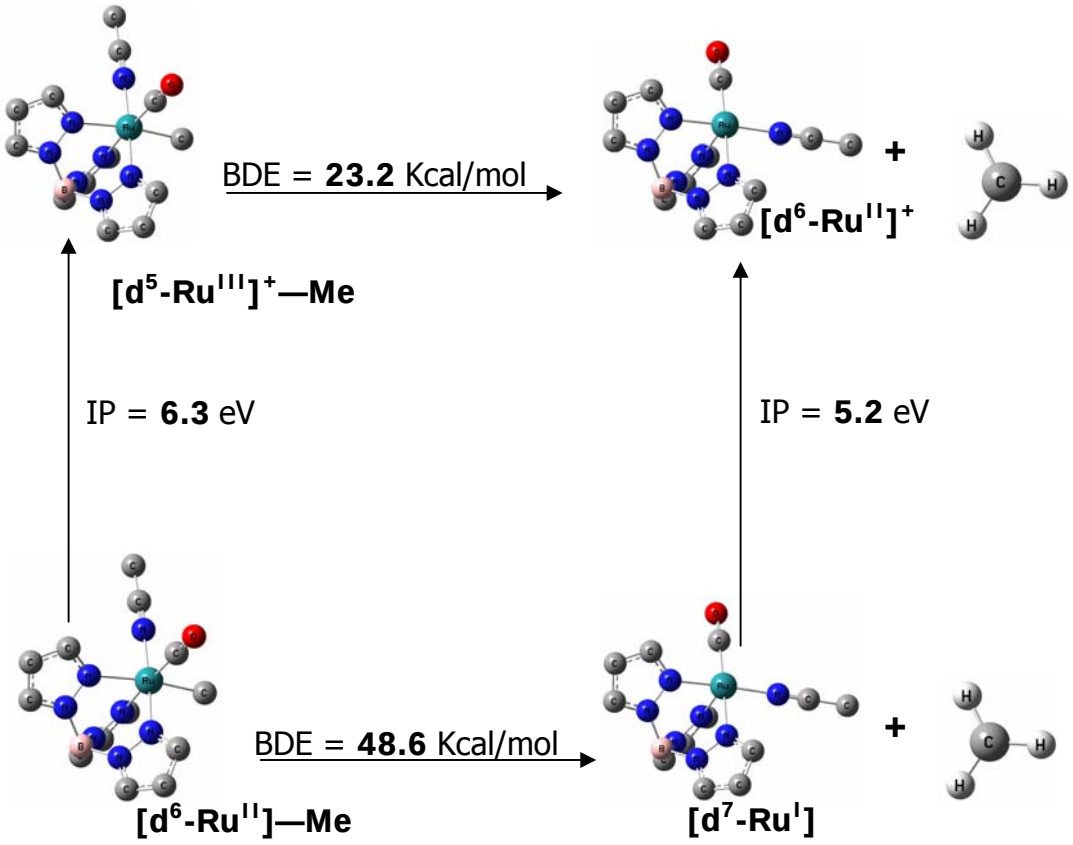

Figure 3.1. Calculated BDEs and IPs for $(TpRu(CO)(NCMe)(Me))^+$ (top), and TpRu(CO)(NCMe)(Me) (bottom). Hydrogen atoms omitted for clarity.

3.2 Addition of Arene C-H Bonds Across a Ru^{II}-OH Bond

Activation of C-H bonds by means of systems containing transition metals is observed via several pathways including the 1,2-addition of C-H bonds across early transition metal imido bonds ($L_nM{=}NX$ where L_n is a supporting ligand and X is a substituent, typically an alkyl, aryl or silyl group) to yield amido ($L_nM(R)$-N(H)X) complexes.[35,36,37,38] This type of transformation is important because the ensuing N-C reductive elimination from the amido complex would generate a free amine (NR(H)X),

and a reduced metal complex (L_nM). However, reductive elimination is a high-energy reaction for most early transition metals as they typically do not have stable oxidation states separated by two oxidation units. Moreover, issues would still remain in terms of regeneration of the active imido species via imido/nitrene (NX) transfer to the reduced metal complex. On the other hand, reductive eliminations of O-C and N-C bonds employing late transition metal catalysts are quite prevalent and form the basis of synthetic and catalytic pathways to aryl ethers and aryl amines.[65,66] Accordingly, it is projected that accessing the net addition of C-H bonds across late transition metal M-X bonds (X = anionic O- or N-based ligand) (*i.e.*, $L_nM\text{-}X + R\text{-}H \rightarrow L_nM(R)\text{---}X(H)$) could eventually lead to improved routes for catalytic hydrocarbon functionalization given the tendency of these metals to undergo facile reductive elimination.

Several pathways for C-H bond activation by late metal complexes seem viable. Hydrogen atom abstraction is known to occur via late transition metal oxo and related systems,[67] although this transformation does not entail direct interaction of the C-H bond with the metal center. As mentioned above, some ruthenium-amido complexes have been verified to abstract acidic hydrogen from C-H bonds.[39] However, nonconcerted bond activation pathways are often nonselective. What is desirable in terms of a selective catalytic pathway to hydrocarbon functionalization would therefore be a process that proceeds via a concerted C-H bond activation mechanism such as 1,2-addition to a metal-ligand bond. To this end, Gunnoe and coworkers investigated Ru-OH complexes.[46,48]

Specifically, Gunnoe's group has synthesized the monomeric Ru^{II} complex $TpRu(PMe_3)_2(OH)$.[46] Upon heating of $TpRu(PMe_3)_2(OH)$ in C_6D_6, H/D exchange resulted at the hydroxide ligand to produce $TpRu(PMe_3)_2(OD)$ as established by both ^1H and ^2H NMR. Metal catalyzed H/D exchange reactions that involve H_2O are rather rare.[68] Mixing the complex $TpRu(PMe_3)_2(OH)$ with H_2O and C_6D_6 also resulted in catalytic H/D exchange to make $C_6D_xH_y$ ($x + y = 6$).[46] No H/D exchange was observed between H_2O and C_6D_6 when the reaction was carried out without ruthenium or when using $TpRu(PMe_3)_2(OTf)$ implying that $TpRu(PMe_3)_2(OH)$ is the required catalyst or catalyst precursor.[46]

A mechanism of H/D exchange was proposed by Gunnoe and coworkers[46] to progress by means of initial ligand dissociation; the dissociated ligand being the PMe_3 ligand of the 18-electron complex, $TpRu(PMe_3)_2(OH)$. This is then followed by reversible addition of a benzene C-D bond across the Ru-OH bond to generate the undetected intermediate $TpRu(PMe_3)(Ph)(HOD)$. Reversing the aforementioned steps would produce $TpRu(PMe_3)_2(OH(D))$ and offer a pathway for the scrambling of H/D among C_6D_6 and the hydroxide ligand.

For the proposed pathway to be feasible, the complex $TpRu(PMe_3)_2(OH)$ has to be able to access a five-coordinate, 16-electron moiety (*i.e.*, $TpRu(PMe_3)(OH)$) on a reasonable timescale. Additionally, the conversion of $TpRu(PMe_3)_2(OH)$ plus benzene to free PMe_3 and the unobserved $TpRu(PMe_3)(Ph)(HOD)$ and/or the unobserved $TpRu(PMe_3)_2(Ph)$ and water has to be kinetically accessible (obviously, or H/D exchange would not be observed), but thermodynamically disfavored.

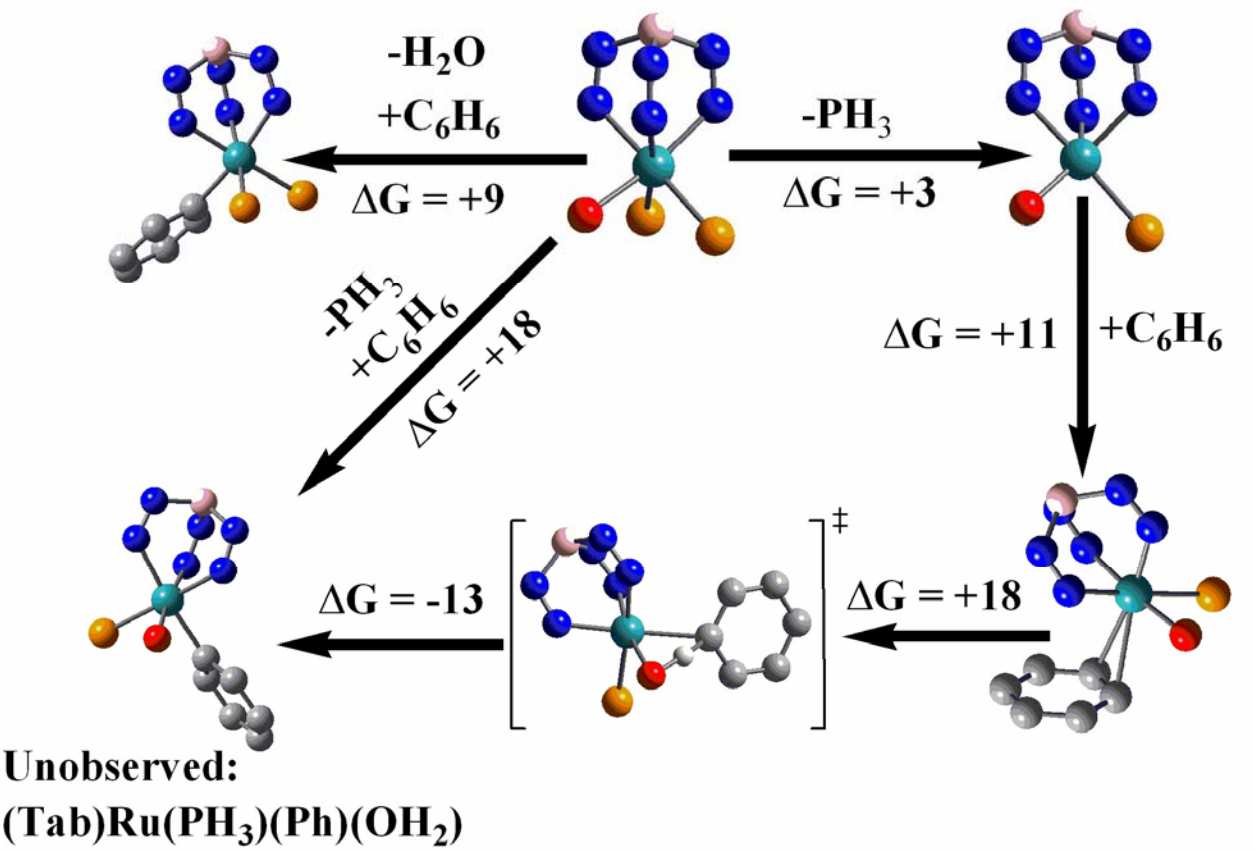

Figure 3.2. DFT calculated reaction pathway. Calculated free energies are in kcal/mol. Hydrogen atoms are omitted for clarity.

The latter may seem paradoxical at first, but if the reaction was thermodynamically favored, one would expect that TpRu(PMe_3)(Ph)(HOD) would be isolatable from the reaction mixture. Previous calculations and experimental results supported this thermodynamic hypothesis; Conner *et al*. have suggested that adding methane to (PCP)Ru(CO)(NH_2) to make (PCP)Ru(CO)(Me)(NH_3) is thermally disfavored, however, for this case the reaction was observed by calculations to be both thermodynamically and kinetically unfavorable.[42] Further it was proposed on the basis

of this preliminary research that the use of a more basic ligand (*i.e.*, NH_2 → OH) would further facilitate 1,2-addition of C-H bonds to ruthenium complexes.

In the computational studies performed as part of this dissertation research, the full Tp ligand was modeled by Tab (Figure 2.1), where DFT (B3LYP/CEP-31G(d)) methods were employed.[7] From the calculations, it was found that the process of a PH_3 ligand dissociation from (Tab)Ru(PH_3)$_2$OH to form the five-coordinate (Tab)Ru(PH_3)OH was only mildly thermodynamically disfavored with a calculated ΔG of +2.8 kcal/mol. Forming (Tab)Ru(PH_3)(η^2-C_6H_6)(OH) by coordinating benzene to (Tab)Ru(PH_3)OH was computed to be mildly exothermic but endergonic when entropic factors were included, ΔG = +11.2 kcal/mol.

Reacting benzene with the model complex (Tab)Ru(PH_3)$_2$OH to produce PH_3 and the complex (Tab)Ru(PH_3)(Ph)(OH_2) was also calculated to be significantly endergonic with a free energy of +18.4 kcal/mol. This computational result supports the deduction from the experiments that thermodynamics are the reason for the deficiency in the experimental observation of a (Tab)Ru(PH_3)(Ph)(OH_2) intermediate. Similarly, the reaction

(Tab)Ru(PH_3)$_2$OH + benzene → (Tab)Ru(PH_3)$_2$(Ph) + water (1)

was also calculated to be endergonic with ΔG = +9.1 kcal/mol (Figure 3.2). Taken together, these results imply that use of TpRu(PMe_3)$_2$OH as a catalyst for H/D exchange should yield only the starting material as an isolable ruthenium intermediate. However, the use of TpRu(PMe_3)$_2$(Ph) as the catalyst precursor should result in both

$TpRu(PMe_3)_2(Ph)$ and $TpRu(PMe_3)_2OH$ as isolable species (since the latter is thermodynamically downhill from the former, see Figure 3.2).

The calculated free energy barrier of the transition state for C-H activation of benzene by the Ru-OH bond was +17.6 kcal/mol relative to the complex $(Tab)Ru(PH_3)(\eta^2\text{-}C_6H_6)(OH)$. Previously, the C-H activation of benzene by the $Ru\text{-}CH_3$ bond of (Tab)Ru(CO)(Me), was reported to have an analogous computed free energy barrier of +21.2 kcal/mol.[7] The overall barrier to C-H activation from the starting materials ($TpRu(PMe_3)_2OH$ plus benzene) is thus ~32 kcal/mol, which is comparable to experimental estimates for other ruthenium complexes,[7] and hence presumably accessible under typical experimental conditions.

The calculations in this project are therefore consistent with the experimentally proposed pathway of Gunnoe and coworkers. The computational results offer the indication that the net addition of aromatic C-H bonds across a Ru^{II}-OH bond is thermodynamically unfavorable but kinetically accessible.

Another process that may be proposed for this H/D exchange process involves the formation of a Ru^{IV}-oxo complex, $TpRu^{IV}(O)(H)(PMe_3)$. After PMe_3 ligand dissociation from $TpRu(PMe_3)_2OH$, then hydrogen migration, C-H addition may occur across the Ru=O bond. However, the Ru^{IV}-oxo complex is anticipated to quickly generate $Me_3P{=}O$ as it is formed. The removal of H^+ from the complex $TpRu(PMe_3)_2(OH)$ to make $[TpRu(PMe_3)_2(O)]^-$ also appears implausible because, the product would be a d^6 Ru^{II}-oxo complex, which is calculated (Barakat, K. A. – unpublished results) to be a high-energy species. The calculated results, as well as the

experimental findings, offer as the most likely scenario for the activation of C-H bonds a pathway that proceeds through a 16-electron Ru-OH complex, even though, not all the C-H activation events can be directly probed by experiment. This proposed pathway, which is supported by our computations, involves the 1,2-addition of a carbon-hydrogen bond (benzene in the present case) across a metal-ligand bond, where the metal is a late transition metal (Ru) and the ligand is a non-dative heteroatom-based chemical group (hydroxyl). Furthermore, this computational research highlights that while thermodynamic favorability is important, what is more essential is kinetic accessibility.

3.3 Exploring Five-Coordinate Ru^{II}-PCP Complexes

Coordinatively and electronically unsaturated divalent ruthenium complexes with 14- or 16-electron counts have been of interest as possible intermediates in catalytic reactions in addition to being of fundamental interest in terms of understanding the structure and bonding of unsaturated metal complexes. [41,69] For instance, the Grubbs-type 16-electron ruthenium catalysts (see Figure 1.5) have been useful for olefin metathesis.[5,70,71] Others have comprehensively investigated the coordinatively unsaturated half-sandwich ruthenium systems having amidinate, phosphine or carbene ligands,[72,73,74,75,76,77,78,79] and numerous unsaturated Ru complexes have been synthesized to probe C-H···Ru agostic interactions.[80,81,82,83] Systematic studies have been carried out on the synthesis and reactivity of four-coordinate complexes such as $[L_2Ru(CO)(R)][BAr'_4]$ (R = H, Me or Ph; Ar' = 3,5-$(CF_3)_2C_6H_3$; L = phosphine ligands)

and their five-coordinate precursors with the extension to systems with chelating PNP (PNP = $N(SiMe_2CH_2PR_2)_2$, R = Cy or ^tBu) ligands.[80,84,85,86,87,88,89]

The reactivity of coordinatively unsaturated ruthenium complexes with a bulky PCP pincer ligand (PCP = 2,6-$(CH_2P^tBu_2)_2C_6H_3$) (Figure 1.6) are of interest in this research. Previously, the synthesis of the amido complexes (PCP)Ru(CO)(NHR) (R = H or Ph) and their reactivity with polar and non-polar substrates have been reported.[42,43,44] Among these, the complex (PCP)Ru(CO)(NH_2), which is a rare example of the parent amido (*i.e.*, L_nM-NH_2) complex, was shown to activate dihydrogen and C-H bonds (the latter in an intramolecular not intermolecular fashion).[42] In this research, computational chemistry methods – specifically density functional theory and effective core potentials – were employed to study a very electron-deficient, four-coordinate Ru complex that is proposed to be generated from the stable (although itself still only a 16-electron complex) five-coordinate precursor (PCP)Ru(CO)(Cl) via halide abstraction. These attempts led Gunnoe and coworkers to propose the experimental production of complexes of the type $[(PCP)Ru(CO)(L)]^+$ (L = η^1-$ClCH_2Cl$, η^1-N_2, C_6H_5F, or μ-Cl-Ru(PCP)(CO)) in weakly coordinating solvents such as methylene chloride.[90]

3.3.1 Comparison of $[(PCP)Ru(CO)(L)]^+$ (L = η^1-$ClCH_2Cl$, η^1-N_2, η^1-FC_6H_5, or agostic) Complexes: Synthesis and Calculations

The synthesis and structural characterization of the air-stable, formally 16-electron compound (PCP)Ru(CO)(Cl) has been reported in the literature by Gusev *et al.*[90] A four-coordinate ruthenium complex could result if the chloride ligand is abstracted from (PCP)Ru(CO)(Cl). The reaction of (PCP)Ru(CO)(Cl) with excess $NaBAr'_4$

resulted in a mixture of $[\{(PCP)Ru(CO)\}_2(\mu\text{-}Cl)][BAr'_4]$ and a second (not isolated) product.[47] Treating a CH_2Cl_2 solution of (PCP)Ru(CO)(OTf) with one equivalent of $NaBAr'_4$ leads to the formation of $[(PCP)Ru(CO)(\eta^1\text{-}ClCH_2Cl)][BAr'_4]$. Thus, this complex has a molecule of CH_2Cl_2 coordinated to the ruthenium center through a chlorine atom rather than forming the four-coordinate species $[(PCP)Ru(CO)]^+$. The synthesis of the methylene chloride complex was confirmed using NMR and IR spectroscopy as well as X-ray crystallography.[47]

The X-ray structural analysis of $[(PCP)Ru(CO)(\eta^1\text{-}ClCH_2Cl)][BAr'_4]$ revealed the presence of a monohapto coordinated $\eta^1\text{-}CH_2Cl_2$ ligand, plus one agostic interaction, with one short $Ru/C_{agostic}$ distance and a significantly smaller bond angle (100.9°) of the agostic C-H bond when compared to comparable bond angles of the other three *tert*-butyl group.[47] This observation of agostic bonding is consistent with previous reports of double agostic interactions in $[Ru(Ph)(CO)(P^tBu_2Me)_2][BAr'_4]$, which was synthesized by the Caulton group, and possesses comparable $Ru/C_{agostic}$ bond lengths and Ru-P-C bond angles to the Gunnoe group's complex.[80] Also, the Milstein group has observed an agostic interaction in the solid-state structure of $[(PCP)Ru(CO)_2]^+$.[91] Examples of structurally characterized complexes with CH_2Cl_2 ligands in the literature are known.[85,92,93,94,95,96,97,98,99] Systems with related chlorobenzene or chloroalkane ligands have also been published.[96,100,101,102]

In a synthetic attempt to eliminate CH_2Cl_2 coordination, (PCP)Ru(CO)(OTf) was treated with $NaBAr'_4$ in fluorobenzene; the latter is expected to be more weakly coordinating than CH_2Cl_2.[47] IR spectroscopy implies an equilibrium between a five-

coordinate complex, [(PCP)Ru(CO)(N_2)][BAr'$_4$], (N_2 was used as the inert gas in the synthesis), which was confirmed by X-ray diffraction, and a second complex that is either the four-coordinate complex [(PCP)Ru(CO)][BAr'$_4$] or a fluorobenzene adduct [(PCP)Ru(CO)(FC_6H_5)][BAr'$_4$]. Efforts to grow crystals of the latter complex were not successful.[47] Like [(PCP)Ru(CO)(η^1-$ClCH_2Cl$)][BAr'$_4$], one agostic interaction was confirmed by X-ray crystallography. A N-N bond length of about (1.069 Å) was measured, which is shorter than N-N bond length in free N_2 (~1.097 Å).[103] Many late metal dinitrogen complexes have been reported.[104,105,106,107,108,109,110,111,112,113,114,115,116]

Vibrational frequency analyses (subsequent to DFT geometry optimization) were carried out in our lab for truncated 16-electron [(PCP')Ru(CO)(L)]$^+$ models to discover their CO absorptions ν_{CO} (cm^{-1}) as this stretching mode is often indicative of the electronic structure of a complex. Moreover, calculations were performed to lend support to the proposed but not isolated fluorobenzene adduct. Truncated models involved replacement of (a) tert-butyl groups on the PCP ligand with hydrogen (Figure 1.6), and (b) the phenyl substituent on the carbene/vinylidene with a hydrogen atom. The experimental ν_{CO} (cm^{-1}) reported for [(PCP)Ru(CO)(L)]$^+$ is 1987 with (L = η^1-N_2), and 1964 with (L = η^1-CH_2Cl_2), and the equilibrium studies deduced 1953 with (L = PhF).[47] The calculation of ν_{CO} (cm^{-1}) for the corresponding PCP' model complexes gave 2085 (L = η^1-N_2), 2066 (L = η^1-CH_2Cl_2) and 2054 (L = PhF). Applying a typical vibrational frequency scaling factor of 0.95,[117] results in estimated CO stretching frequencies for [(PCP')Ru(CO)(L)]$^+$; ν_{CO} (cm^{-1}) of 1981 (L = η^1-N_2), 1963 (L = η^1-CH_2Cl_2) and 1951 (L = PhF). The trends in calculated CO stretching frequencies thus

CH_2Cl_2) and 1951 (L = PhF). The trends in calculated CO stretching frequencies thus support the experimental assignments and the latter value is comparable to the experimental ν_{CO} of 1953 cm^{-1} for the putative fluorobenzene adduct [(PCP)Ru(CO)(FC_6H_5)][BAr'_4]. Hence, our calculations support the feasibility of [(PCP)Ru(CO)(FC_6H_5)]$^+$ in solution equilibrium when fluorobenzene is the solvent.

Examples of unsaturated ruthenium complexes containing one or more agostic interaction(s) have been reported.[83,84,85,90,91,115] Thus, it is not inconceivable that the Ru in (PCP)Ru(CO)(Cl) may be stabilized by an agostic interaction.[118,119] Nevertheless, for the unsaturated (PCP)Ru(CO)(Cl) complex, no agostic interactions were reported, perhaps, it was proposed, due to the π-donor chloride ligand.[47]

The [(PCP)Ru(CO)(L)]$^+$ (L = η^1-$ClCH_2Cl$, η^1-N_2, η^1-FC_6H_5, or agostic carbon-hydrogen bond of the phosphine t-butyl substituent) complexes were evaluated computationally using DFT. Full experimental models were subjected to computations employing hybrid quantum mechanics/molecular mechanics (QM/MM) calculations. The binding of weak bases to [(PCP)Ru(CO)]$^+$ to generate [(PCP)Ru(CO)(L)]$^+$ (L = η^1-$ClCH_2Cl$, η^1-N_2, η^1-FC_6H_5, C-H agostic) was assessed. All geometry optimizations were begun from crystallographic coordinates, without conducting conformational analyses of these species. Both agostic and non-agostic conformers of the 14-electron, four-coordinate complex [(PCP)Ru(CO)]$^+$ were studied. The *tert*-butyl group with the agostic interaction was modeled using the B3LYP/CEP-31G(d) level of theory (similar to the other quantum atoms), while the other three tert-butyl groups were modeled classically, *i.e.*, using molecular mechanics (MM).

The QM/MM geometry optimization revealed that the complex $[(PCP)Ru(CO)]^+$ contained a weak agostic interaction with a Ru•••$C_{agostic}$ distance of 3.25 Å, in addition to a smaller than tetrahedral Ru-P-C bond angle of 102.1° for the phosphine with the agostic tert-butyl group. The compressed Ru-P-C bond angle is analogous to that illustrated in the crystal structures of the agostic interactions for $[(PCP)Ru(CO)(L)]^+$ complexes as mentioned above.[91] The calculated electronic energy for the agostic conformer was 6 kcal/mol less than that of the non-agostic conformer of $[(PCP)Ru(CO)]^+$ placing an upper bound on the strength of the Ru•••H-C interaction. Furthermore, the stability of the agostic conformer is the first piece of evidence that a true 14-electron $[(PCP)Ru(CO)]^+$ complex may be a very high energy intermediate, and not a true reflection of the active species in the carbene/vinylidene chemistry explored by Gunnoe and coworkers.

From the QM/MM geometry optimization calculations of the five-coordinate, "16-electron" (we are neglecting the contribution of agostic interactions, if any, in electron counting) complexes $[(PCP)Ru(CO)(L)]^+$, it was found that agostic conformers would result only for two (L = CH_2Cl_2, FC_6H_5 but not L = N_2) ligands. In each of these complexes there was formed one agostic Ru···H-C interaction. Hence, even these 16-electron species may be viewed as electron deficient given their tendency to form agostic complexes.

It is interesting that no agostic conformer could be found for L = N_2. Several attempts at varying the starting guess geometry to form agostic interactions for the complex $[(PCP)Ru(CO)(\eta^1\text{-}N_2)]^+$ resulted in energy minimized geometries with no

agostic interactions. Likewise, starting with agostic conformers of $[(PCP)Ru(CO)(L)]^+$ for the fluorobenzene and methylene chloride complexes, and replacing these with N_2, followed by DFT geometry optimization, also yielded non-agostic stationary points for $[(PCP)Ru(CO)(\eta^1\text{-}N_2)]^+$. The calculated agostic $Ru\bullet\bullet\bullet C_{agostic}$ distances for the agostic conformers of $[(PCP)Ru(CO)(L)]^+$ with L = CH_2Cl_2 and FC_6H_5 were 3.20 Å for the methylene chloride complex and 3.22 Å for the fluorobenzene complex.

In an additional series of computational "experiments" binding of the fifth ligand (L) to the non-agostic $[(PCP)Ru(CO)]^+$ conformer produced non-agostic complexes upon QM/MM geometry optimization. By comparison of the energies of nonagostic and agostic conformers of $[(PCP)Ru(CO)(L)]^+$, it was possible to estimate the binding energies of both L and agostic C-H bonds, which are summarized in Table 3.1.

Table 3.1. Calculated binding energies relative to the non-agostic $[(PCP)Ru(CO)]^+$ isomer.[a]

Ligand type	ΔE (kcal/mol)
$\eta^1\text{-}CH_2Cl_2$	-12
FC_6H_5	-13
$\eta^1\text{-}N_2$	-18

[a] These are the calculated energies for the process, nonagostic-$[(PCP)Ru(CO)]^+$ + L → nonagostic-$[(PCP)Ru(CO)(L)]^+$

Arranging the binding energies for the $[(PCP)Ru(CO)]^+$ and $[(PCP)Ru(CO)(L)]^+$ complexes in a relative order would give the decreasing trend N_2 > PhF ~ CH_2Cl_2 > $CH_{agostic}$ (for the latter we used the difference in energy of the agostic and nonagostic conformers of $[(PCP)Ru(CO)]^+$ as the measure of the agostic binding energy). This

decreasing order in ligand (L) binding energies is also seen when small models are subjected to full QM calculations (*i.e.*, PCP' is used instead of PCP, where PCP' is the model ligand in which hydrogen atoms replace the tert-butyl groups of the full PCP). Moreover, the magnitude of the binding energies for the PCP' models are commensurate with those for PCP (± 1 - 2 kcal/mol), which indicates that the role of steric factors in ligand binding preference to the ruthenium center amongst the bases N_2, PhF and CH_2Cl_2 is less important than electronic considerations.

Therefore, the calculations indicate that both agostic and non-agostic conformers of the 14-electron unsaturated $[(PCP)Ru(CO)]^+$ four-coordinate complex, are higher in energy and less stable than the conformers of the type $[(PCP)Ru(CO)(L)]^+$ (L = η^1-N_2, η^1-CH_2Cl_2, or PhF), and that fluorobenzene is a suitable base for $[(PCP)Ru(CO)(L)]^+$.

For the process agostic-$[(PCP)Ru(CO)]^+$ + L → agostic-$[(PCP)Ru(CO)(L)]^+$ with L = CH_2Cl_2, N_2 and FC_6H_5, there was no agostic product found for L = N_2, and altering the geometry manually as was done in the nonagostic case resulted in a nonagostic compound. It is possible that the large (compared to that for PhF and CH_2Cl_2) binding energy of N_2 to $[(PCP)Ru(CO)]^+$ essentially "quenches" the reactivity of the ruthenium in the resulting dinitrogen complex, forestalling the formation of an agostic entity. Meanwhile, agostic-$[(PCP)Ru(CO)(L)]^+$ products were found for L = CH_2Cl_2 and FC_6H_5 with calculated binding energies of –17 and –19 Kcal/mol respectively, (relative to the non-agostic $[(PCP)Ru(CO)]^+$ isomer).

The density functional and QM/MM computational investigations on Ru-PCP complexes afford results that are consistent with the experimental hypotheses of

Gunnoe and coworkers with respect to the unlikelihood of a 14-electron $[(PCP)Ru(CO)]^+$ complex in solution, but the likelihood of a fluorobenzene adduct of this complex in solution. More importantly, the QM and QM/MM calculations carried out in our lab provide additional insight that is not available from experiment. Firstly, the calculations indicate that there is greater thermodynamic preference for even the very weakly coordinating ligands η^1-N_2, η^1-CH_2Cl_2 and PhF to coordinate to the ruthenium of $[(PCP)Ru(CO)]^+$ versus the tert-butyl C-H bonds of a four-coordinate, "14-electron" complex $[(PCP)Ru(CO)]^+$. Second, these ligands will coordinate whether or not there is an agostic interaction in $[(PCP)Ru(CO)]^+$. Finally, the catalyst resting state is the agostic-$[(PCP)Ru(CO)(L)]^+$ (L = CH_2Cl_2) complex in the chemistry that is described next.

3.3.2 The Formation of the [(PCP-CHPh)Ru(CO)][BAr'$_4$] Complex

The complex $[(PCP)Ru(CO)(\eta^1\text{-}ClCH_2Cl)][BAr'_4]$ is an interesting synthetic precursor in Ru-PCP chemistry due to the presence of its labile CH_2Cl_2 ligand. Gunnoe *et al.*[47] reacted the complex $[(PCP)Ru(CO)(\eta^1\text{-}ClCH_2Cl)][BAr'_4]$ in a solution of CH_2Cl_2 with an excess of phenyldiazomethane ($PhCHN_2$), a carbene precursor. This reaction produced a single ruthenium-containing product. Full experimental characterization of the product that it is [(PCP-CHPh)Ru(CO)][BAr'$_4$] (PCP-CHPh = κ^4-*P,P,C,C*-1-CHPh-2,6-$(CH_2P^tBu_2)_2$-C_6H_3).[47] The complex [(PCP-CHPh)Ru(CO)][BAr'$_4$] had the carbene moiety (C(H)Ph) inserted into the ruthenium-*ipso* carbon bond of the PCP ligand (in the following discussion, we will call this the bridging carbene isomer), rather than a terminal ruthenium alkylidene (*i.e.*, (PCP)Ru(CO)(=C(H)Ph) complex). Furthermore, the

Ru-C_{ipso} bond distance (2.33 Å) was found to be longer than Ru-C_{ipso} bond distances in PCP complexes (*e.g.*, 2.05 Å in the [(PCP)Ru(CO)(η^1-$ClCH_2Cl$)][BAr'_4] discussed in the previous section of this dissertation). There was also evidence of a single weak agostic interaction in the bridging carbene complex, similar to those in cationic (PCP)Ru(CO) complexes.[47]

Gunnoe and coworkers suggested a mechanism for the formation of [(PCP-CHPh)Ru(CO)][BAr'_4] from [(PCP)Ru(CO)(η^1-$ClCH_2Cl$)][BAr'_4] and $PhCHN_2$, which begins with formation of a Ru terminal benzylidene complex, $L_nRu{=}C(H)Ph$, then intramolecular C-C coupling occurs via insertion of the terminal benzylidene ligand into the Ru-C_{ipso} bond.[47] Hence one may consider the isolated complex [(PCP-CHPh)Ru(CO)][BAr'_4] as a trapped intermediate arising from incorporation of a carbene moiety into a Ru-C_{aryl} bond. Such conversions are important models of ruthenium-catalyzed C-C bond coupling.[120,121,122,123] Variable temperature ^{1}H NMR spectroscopy in suggested a terminal benzylidene intermediate, [(PCP)(CO)Ru=CHPh)][BAr'_4], but this species could not be isolated experimentally. Literature reports in the literature for similar complexes revealed evidence of a carbene insertion process for Rh-benzylidene complexes.[109,112,124] Therefore, Gunnoe *et al*. hypothesized that the final bridging product is produced from an intermediate terminal carbene instead of a direct attack on the Ru-C_{ipso}.[47]

3.3.3 Formation of the [(PCP-C=CHPh)Ru(CO)][BAr'_4] Complex

Bruce *et al.* reported that vinylidene ($L_nM{=}C{=}(R')R$) ligands form from the

reaction of transition metal complexes with terminal acetylenes (RC≡CH).[125,126] Hence, [(PCP)Ru(CO)(η^1-$ClCH_2Cl$)][BAr'_4] was reacted with phenylacetylene (PhC≡CH) in CD_2Cl_2 to give [(PCP-C=CHPh)Ru(CO)][BAr'_4] (PCP-C=CHPh = κ^4-*P,P,C,C*-1-(C=CHPh)-2,6-($CH_2P^tBu_2$)$_2$-C_6H_3). Gunnoe and coworkers explored the possibility of vinylidene-C_{ipso} bond coupling reaction to proceed in analogy to formation of the [(PCP-CHPh)Ru(CO)][BAr'_4] complex just discussed.[47]

The structures of both complexes [(PCP-C=CHPh)Ru(CO)][BAr'_4] and [(PCP-CHPh)Ru(CO)][BAr'_4] were expected to be similar. Nonetheless, prominent differences in their spectra were noticed.[47] For example, the ^{31}P NMR spectra of the bridging vinylidene and bridging carbene products suggested that the phenyl ring was in the equatorial plane and perpendicular to the equatorial plane, respectively, yielding two unequal phosphine groups for the latter.[47]

Coupling reactions of terminal acetylenes with ruthenium pincer complexes have been reported.[127,128,129,130] Given the inability to cleanly isolate and grow crystals of these systems, conclusive assignment of the intermediates in the reactions of N_2CHPh or phenylacetylene with "[(PCP)Ru(CO)]$^+$" was not possible based on the experimental results alone.[47] However, results from the DFT calculations as will be discussed below, indicate that the most plausible identity of these intermediates are complexes with terminal multiple bonds.

3.3.4 DFT Calculations for [(PCP-CHPh)Ru(CO)][BAr'_4] and [(PCP-C=CHPh)Ru(CO)][BAr'_4] Complexes

Calculations employing hybrid QM/MM and DFT methodologies were used to

study the experimentally proposed mechanisms leading to the formation of the two complexes [(PCP-CHPh)Ru(CO)][BAr'$_4$] and [(PCP-C=CHPh)Ru(CO)][BAr'$_4$]. The proper transition states for the insertion of both carbene and vinylidene into Ru-C_{ipso} bonds were difficult to isolate for the full PCP models, so that analogous DFT-only calculations on truncated PCP' models (*vide supra)* were also performed.

Hybrid QM/MM calculations indicate that terminal [(PCP)(CO)Ru=$(C)_{0,1}$=CHPh]$^+$ complexes are viable reaction intermediates, since both moieties were characterized as stable minima on their respective potential energy surfaces through calculation of their energy Hessians. Hybrid QM/MM calculations on full experimental models for the proposed formation pathway of [(PCP-CHPh)Ru(CO)]$^+$ plus methylene chloride and dinitrogen by reacting [(PCP)Ru(CO)(η^1-$ClCH_2Cl$)]$^+$ with $PhCHN_2$, portrayed a highly exothermic process, downhill in enthalpy by more than 30 kcal/mol. The energetics for reaction of [(PCP)Ru(CO)(η^1-$ClCH_2Cl$)]$^+$ with phenyl-acetylene are discussed below. In addition, the calculated enthalpies for the Ru-C_{ipso} insertion reactions were: ΔH = -8 kcal/mol for =C(H)Ph insertion to form [(PCP-CHPh)Ru(CO)]$^+$ and ΔH = –27 kcal/mol for =C=C(H)Ph insertion to form [(PCP-C=CHPh)Ru(CO)]$^+$, supporting their thermodynamic propensity. The related calculations for the analogous truncated PCP' models produced enthalpy values of -17 kcal/mol for the carbene insertion and -22 kcal/mol for the vinylidene insertion. Combining the analysis of the QM part of the QM/MM extrapolated energies along with the QM energetics on small models, hinted at the importance of steric features in the insertion reactions. It was found that the insertion of carbene was impeded by roughly 4 - 5 kcal/mol by steric factors whilst the

vinylidene insertion was facilitated by a similar amount also due to steric factors. The results for full PCP versus PCP' models indicate that while the disparity in the energetics of carbene and vinylidene encompasses an electronic component, there are significant steric factors to this reaction as well (Figure 3.3). Apparently, the presence of the additional carbon atom in the vinylidene versus the carbene leads to less steric encumbrance between the phenyl substituent and the phosphine tert-butyl groups of complex $[(PCP\text{-}C{=}CHPh)Ru(CO)]^+$ when evaluated versus the complex $[(PCP\text{-}CHPh)Ru(CO)]^+$ where this extra carbon is absent.

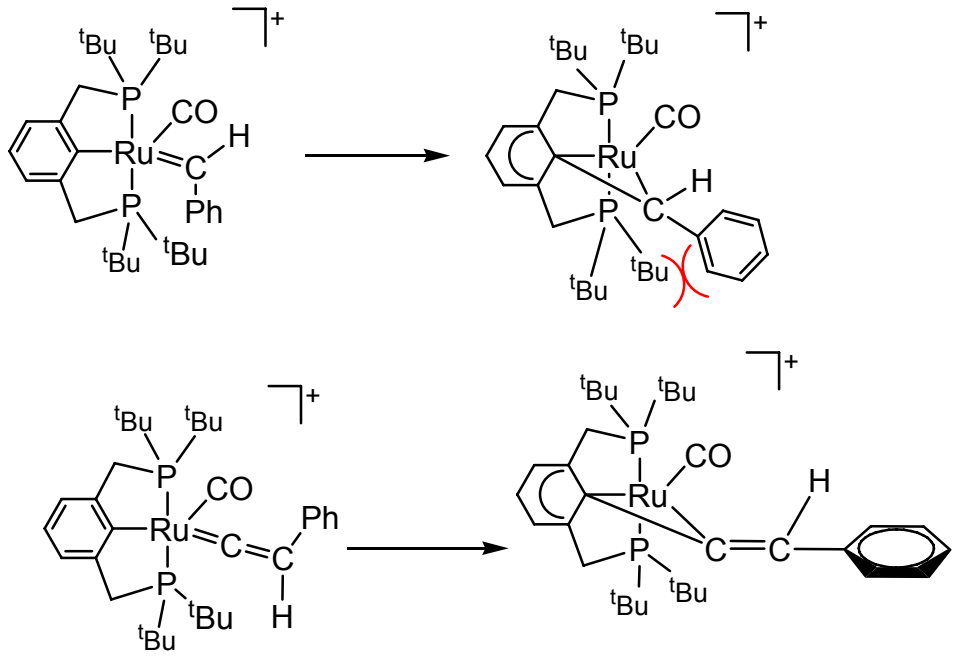

Figure 3.3. Steric features in the insertion reactions.

[Reproduced in part with permission from: (Zhang, J.; Barakat, K. A.; Cundari, T. R.; Gunnoe, T. B.; Boyle, P. D.; Petersen, J. L.; Day, C. S. *Inorg. Chem.* 2005, 44, 8379.) Copyright 2005 American Chemical Society.]

Furthermore, the vinylidene complex has the Ph substituent in the equatorial plane, away from the bulk phosphine substituents, giving it a further steric advantage

over the carbene analogue.

The supposition of the terminal alkyne complex as a likely intermediate in the formation of [(PCP-C=CHPh)Ru(CO)][BAr'$_4$] was investigated employing QM/MM calculations. The complex [(PCP)(CO)Ru(η^2-HC≡CPh)]$^+$ with the alkyne oriented in equatorial plane, was modeled and optimized. The resultant geometry was a high energy intermediate of about 13 kcal/mol above [(PCP-C=CHPh)Ru(CO)][BAr'$_4$], which corresponds to the triple bond of the alkyne being inserted into the Ru-C_{ipso} of the PCP ligand. Similar calculations on the smaller model [(PCP')(CO)Ru(η^2-HC≡CH)]$^+$ produced a stationary point, however, this moiety was a transition state with an imaginary frequency related to the rotation of the acetylene ligand with the C≡C bond to a conformation oriented perpendicular to the equatorial plane, with an energy value of about 23 kcal/mol more than the vinylidene model [(PCP')(CO)Ru=C=CH_2]$^+$. Given the steric repulsion between the phenyl and tert-butyl ligands, and this perpendicular conformation, the experimentally proposed [(PCP)(CO)Ru(η^2-HC≡CPh)]$^+$ would appear to be untenable.

Thus, reacting [(PCP)Ru(CO)(η^1-$ClCH_2Cl$)][BAr'$_4$] with N_2CHPh or phenylacetylene results in C-C bond formation of the PCP phenyl ring. The QM/MM and DFT calculations on [(PCP)(CO)Ru=$(C)_{0,1}$=CHPh]$^+$ and on [(PCP')(CO)Ru=$(C)_{0,1}$=CH_2]$^+$ respectively, presented data that support the thermodynamic feasibility of the experimentally proposed mechanisms: (1) the reaction with N_2CHPh is through the formation of a terminal ruthenium benzylidene complex, and (2) a terminal vinylidene complex is an intermediate in the reaction with phenylacetylene.

3.4 Summary and Conclusions

Collaborative computational and experimental efforts were employed to investigate exciting challenges involved in ruthenium catalysis. The studied catalytic pathways involved the oxidation of ruthenium (from the +2 to +3 oxidation state), C-H bond activation by 1,2-addition/reductive elimination pathways, and the possible intermediacy of highly coordinatively unsaturated (*i.e.*, 14-electron) complexes in catalytic hydroarylation of olefins.

Single-electron oxidation of Ru^{II} complexes of the type TpRu(CO)(NCMe)(R) (R = CH_3) leads to alkyl elimination and organic products that are expected to be a consequence of Ru-C_{alkyl} bond homolysis. The calculations indicate a significant decrease in the Ru-CH_3 homolytic bond dissociation enthalpy upon the oxidation of TpRu(CO)(NCMe)(Me) to its Ru^{III} cation both product stabilization and reactant destabilization. This oxidation could, therefore, instigate olefin polymerization since it would afford quick access to alkyl radical species.

The calculations support and extend experimental proposals in terms of probable pathways for the activation of C-H bonds, even though, not all the C-H activation proceedings are thermodynamically favorable. The proposed pathways studied in our simulations involve late transition metal (Ru in this case) complexes with non-dative heteroatom-based ligands (OH) to cleave a C-H bond of benzene. Our computed results indicate the net addition of aromatic C-H bonds across a Ru^{II}-OH bond in a process that is thermodynamically unfavorable but kinetically accessible. Such reactions could eventually lead to novel routes for metal mediated hydrocarbon functionalization, and

result in the discovery of various mechanisms for the breaking of C-H bond by transition metals.

Attempts to access a four-coordinate ruthenium complex starting from the five-coordinate precursor (PCP)Ru(CO)(Cl) led to the formation of complexes of the type $[(PCP)Ru(CO)(L)]^+$ {L = η^1-$ClCH_2Cl$, η^1-N_2, C_6H_5F, or μ-Cl-Ru(PCP)(CO)}. Additionally, reacting $[(PCP)Ru(CO)(ClCH_2Cl)]^+$ with a carbene source or phenylacetylene produced intermediates for carbene or vinylidene insertion into the Ru-C_{aryl} bond of the PCP ligand.

Both experimental observations and calculations support the suggestion that Binding of the weakly coordinating ligands such as dinitrogen, methylene chloride and fluorobenzene seemed favored by the 14-electron complex $[(PCP)Ru(CO)]^+$ over the formation of agostic interactions. Reactions of $[(PCP)Ru(CO)(\eta^1\text{-}ClCH_2Cl)][BAr'_4]$ with N_2CHPh or phenylacetylene yielded conversions involving C-C bond formation of the PCP phenyl ring. Experimental mechanisms leading to the formation of [(PCP-CHPh)Ru(CO)][BAr'$_4$] and [(PCP-C=CHPh)Ru(CO)][BAr'$_4$] were suggested and supported by the calculations. The QM/MM and DFT calculations on $[(PCP)(CO)Ru=(C)_{0,1}=CHPh]^+$ and on $[(PCP')(CO)Ru=(C)_{0,1}=CH_2]^+$ respectively, offered data supportive of the thermodynamic feasibility of the suggested experimental mechanisms, that the reaction with N_2CHPh develops through the formation of a ruthenium benzylidene intermediate complex, and a vinylidene intermediate complex for the reaction with phenylacetylene .

Therefore, the computations outlined thus far in this dissertation indicate that modifying the coordination environment of ruthenium catalysts (specifically, Ru^{II}

catalyst type), could lead to enhanced control of their catalysis pathways and novel mechanisms of reactivity.

CHAPTER 4

DISPROPORTIONATION OF GOLD(II) COMPLEXES: A DENSITY FUNCTIONAL STUDY OF LIGAND AND SOLVENT EFFECTS

4.1 Introduction

The chemistry of gold is dominated by the chemistry of the monovalent (Au^{I}) and trivalent (Au^{III}) ions. The former tend to be linear, two-coordinate complexes, while the latter are typically square planar, four-coordinate complexes. The chemistry of the intermediate formal oxidation state – divalent gold (*i.e.*, Au^{II}) – has come under increasing scrutiny in terms of its chemical applications as well as the novelty of this chemical state of gold.[131] The majority of complexes identified as Au^{II} in the Cambridge Structural Database and the literature are bimetallic, some with Au-Au bonds as short as 2.47 Å.[132] Many binuclear complexes contain phosphorus-ylide ligands, *e.g.*, $[IAu(CH_2PMe_2CH_2)_2AuI]$ and $[NCAu(CH_2PPh_2CH_2)_2AuCN]$.[131] In such cases, the assignment of a 2+ oxidation state to gold is not without ambiguity. Even compounds such as "$AuCl_2$" (Au_4Cl_8) or $Au(SO_3F)_2$ have been formulated in terms of a mixed valence Au^{I}/Au^{III} description,[133,134] as has AgO.[135] Such compounds have been termed "pseudogold(II)".[136] Wieghardt, Neese and their coworkers have published elegant theoretical-experimental analyses of dithiolene oxidation states, including "pseudogold(II)" complexes such as $[Au(mnt)_2]^{2-}$.[137] In many cases, assignments such as Au^{II} are inappropriate as the dithiolene ligands are not fully reduced.

The effect of the chemical environment upon the disproportionation reaction is a worthy topic of consideration. For example, $AuCl_2$ is stable with respect to disproportionation in the gas phase (as determined from DFT calculations by Schröder

et al.[138] and Blackmore *et al.*)[139] although solid $AuCl_2$ does disproportionate.[133] Schwerdtfeger and coworkers have used computational chemistry methods to study a different gold disproportionation reaction, *i.e.*, disproportionation of monovalent gold complexes to elemental gold and trivalent gold complexes.[140]

Monometallic Au^{II} complexes are rare with notable examples including $[Au\{S_2C_2(CN)_2\}_2]^{2-}$,[141] and related complexes,[142,143] *bis*(dicarbollido) gold(II) complexes such as $[Au(C_2B_9H_{11})_2]^{2-}$,[144] and the neutral Au^{II} complex with phthalocyanine.[145] Although these complexes are paramagnetic, EPR studies suggest that in many cases the unpaired electron resides primarily on the ligands while the spin density on gold is typically only 15%,[134,141,146] obscuring assignment of the correct oxidation state of gold. Other examples suggesting a localized unpaired electron on an Au^{II} center have been reported as transient species or impurities.[134,147] A remarkable noble gas complex has also been isolated, formulated as $[AuXe_4]^{2+}(Sb_2F_{11}^-)_2$.[148]

El-Sayed[149] and coworkers studied the chemistry of Au^{II} chlorides in connection with the deposition of gold nanoclusters. Stace and coworkers studied the entire series of divalent coinage-metal (Cu^{II}, Ag^{II} and Au^{II}) complexes in the gas phase with prototypical organic (*e.g.*, acetone and 2-butanone)[150] and inorganic (*e.g.*, water and ammonia) ligands. It was concluded, on the basis of mass spectrometric studies, that σ-donor and π-acceptor ligands will best stabilize gold in the 2+ oxidation state,[151] which is the same conclusion reached earlier by Herring *et al.*[134]

Recent research on the formation of gold nanoparticles has given added impetus to the study of gold disproportionation and hence Au^{II} chemistry.[149] El-Sayed *et al.* have

recently reported the use of gold nanoparticles for biomedical imaging, whereupon these materials display a variety of photochemical, photophysical and cytotoxic advantages versus competing technologies.[152] Caruso *et al.* have discussed Au^{II} disproportionation to Au^{I} and Au^{III} in the formation of colloidal gold under sonochemical conditions.[153]

In a previous paper from our group,[154] it was deduced through density functional theory that cationic *tris*(phosphine)gold(I) complexes undergo a Jahn-Teller distortion from a trigonal-planar toward a T-shaped geometry (P-Au-P ~ 2 × 90° and 180°) in the lowest triplet excited state. Omary and coworkers[155] showed this conclusion could be extended to neutral, three-coordinate Au^{I} complexes of the type $Au(phosphine)_2X$ (X = univalent anion, *e.g.*, chloride, bromide or iodide). The results of these theoretical predictions have been utilized by the experimental group of Omary to design series of novel luminescent materials with tunable emission colors, including a highly coveted blue phosphor with brightness and lifetimes that are suitable for molecular light-emitting diodes (LEDs).[155] As part of this research on the triplet excited states of $Au^{I}L_3$ complexes, it was hypothesized that the promotion of an electron from the 5*d* to the 6*p* manifold, which provides the driving force for the photoinduced Jahn-Teller distortion, was akin to a one-electron oxidation of the *d* orbital manifold of the d^{10} gold(I) ion (*i.e.*, $^{1}Au^{I} - 5d^{10}6p^{0} \rightarrow {}^{3}Au^{I} - 5d^{9}6p^{1}$).[154] Our earlier work further suggested that d^{9}-$Au^{II}L_3$ complexes would possess a T-shape in the doublet ground states, a supposition supported by density functional calculations on the parent model ($[Au(PH_3)_3]^{2+}$) and hybrid quantum mechanical/molecular mechanical (QM/MM) calculations on larger

phosphine complex models ($[Au^{II}(PR_3)_3]^{2+}$, PR_3 = TPA, PMe_3, PPh_3, PCy_2Ph, Cy = cyclohexyl, TPA = 1,3,5-triaza-7-phospha-adamantane).[154] Hence, Au^{II} complexes can be seen as ground-state models of excited-state Au^{I} complexes, and thus may possess interesting spectroscopic, magnetic, and other physicochemical properties.

For the above reasons, we have undertaken density functional theory studies of Au^{II} complexes, in particular disproportionation (also known as dismutation) reactions to Au^{I} and Au^{III} species, and to assess the stability and extent of paramagnetism in Au^{II} complexes. Ligands studied include water, ammonia, carbon monoxide, acetonitrile, methyl isonitrile, phosphines, pyridine, and chloride. For the gold-chloride complexes, our collaborator, Dr. H. Rabaâ (Ibn Tofail University, Morocco) probed the mechanism (dissociative versus associative) and the transition states for the disproportionation of Au^{II} to Au^{I} and Au^{III} complexes. This part of the research will not be presented in this dissertation.

4.2 Computational Methods

The Gaussian 98 program[49] was used for the calculations described herein. The B3PW91 hybrid functional[156] was employed along with the LANL pseudopotentials and their attendant valence basis sets.[157] The basis set of gold was augmented by two *f* functions (as per Pyykkö)[158] and one Couty-Hall outer *p* function[159] (contracted). Main group basis sets were augmented with a *d* polarization function taken from the 6-31G* basis set. We term this basis set combination LANL2DZ(2f,p)*. For modeling solvent effects, we employed the CPCM (conductor polarizable continuum method) technique[160]

for solvents of moderate (acetonitrile, ε = 36.64) and high (water, ε = 78.39) dielectric constants. All $Au^{I}L_2$ and $Au^{III}L_4$ complexes are singlets, and were studied using restricted Kohn-Sham methods. The d^9-$Au^{II}L_x$ complexes are open-shell entities (doublets) and their calculation employed unrestricted Kohn-Sham methods; spin contamination as measured by the $<S^2>$ expectation value was minimal.

Other stationary points (all minima, *i.e.*, zero imaginary frequencies as confirmed by calculation of the energy Hessian at the calculated stationary point) are obtained by gradient-driven geometry optimization using analytical gradients. Quoted free energies are obtained through the use of DFT-derived vibrational frequencies (unscaled) and are calculated at STP.

4.3 Results and Discussion

4.3.1 Disproportionation of Atomic Ions

4.3.1.1 Gas-Phase Ionization Potentials

Before embarking on the study of molecular species, atomic species were investigated because experimental data are rare for Au^{II} in a molecular environment. Korgaonkar and coworkers[161] reported the higher ionization potentials of gold in 1981. These workers deduced values (in kcal/mol) of 213 (IP_1), 473 (IP_2) and 784 (IP_3). Extremely high-level calculations (large basis sets, coupled cluster single and double excitation wavefunction built upon a Dirac-Coulomb-Breit Hamiltonian) have been reported by Eliav *et al.* and provide insight into the effort that needs to be expended for quantitative calculations of atomic IPs.[162]

Two sets of calculations were performed in this dissertation research upon the series $^{2}Au^{0}$, $^{1}Au^{+}$, $^{2}Au^{2+}$, $^{3}Au^{3+}$ (leading superscript refers to the ground state multiplicity) to calculate $IP_{1,2,3}$ using the DFT approach employed in our previous research on gold chemistry[154] (B3PW91/LANLDZ(2f,p)*). The more expensive post-Hartree-Fock method (CCSD(T))[163] is also utilized in the present research to study atoms and atomic ions. The calculated ionization potentials are in good agreement with experiment (kcal/mol): IP_1 = 215 (DFT), 205 (CCSD(T)); IP_2 = 481 (DFT), 462 (CCSD(T)); IP_3 = 764 (DFT), 759 (CCSD(T)).

For atomic species, the difference between the second (Equation 1) and third (Equation 2) ionization potentials is the disproportionation of two Au^{2+} ions into Au^{+} and Au^{3+} (Equation 3). As gas-phase ionization potentials increase with increasing charge on the atomic species, the quantity "IP_3 - IP_2" will be positive. Utilizing experimental ionization potentials[162] yields a disproportionation energy of 311 kcal/mol for atomic ions. The disproportionation energy computed at the B3PW91/LANL2DZ(2f,p)* level of theory is 283 kcal/mol, with the CCSD(T) value being 296 kcal/mol, both in reasonable agreement with experiment.[162]

$Au^{2+} + 1e^{-} \rightarrow Au^{+}$	$-IP_2$	(1)
$Au^{2+} \rightarrow Au^{3+} + 1e^{-}$	$+IP_3$	(2)
$2\ Au^{2+} \rightarrow Au^{+} + Au^{3+}$	$IP_3 - IP_2$	(3)

4.3.1.2 Solvent Effects

Solvent effects are expected to play a significant role in a process such as

disproportionation given the presence of ionic complexes and the importance of electrostatics in describing the metal-ligand bonds. Utilizing the PCM methodology (a simplistic solvation model for atomic metal ions)[164] to simulate an aqueous reaction field, it is calculated that solvation substantially alters the energetics of the disproportionation reaction. The gas-phase energy of Equation 3 calculated by B3PW91/LANL2DZ(2f,p)* is more than halved, going from 283 kcal/mol in the gas phase to 119 kcal/mol in aqueous environment (PCM-H_2O). While a lack of reliable redox data for Au^{2+} species plus the simplicity of the solvation model conspire against quantitative comparisons, the calculations reasonably indicate that the greater favorability of Au^{2+} disproportionation in water is driven by the large solvation energy of the 3+ gold ion: PCM calculated ΔG_{solv} in water (kcal/mol) = -4 ($^2Au^0$), -79 ($^1Au^+$), -326 ($^2Au^{2+}$), and -736 ($^3Au^{3+}$). In terms of synthesizing stable, *bona fide* Au^{2+} monometallic complexes, our results imply that solvent effects will be important in synthetic efforts.

4.3.1.3 Effect of Relativity on Disproportionation

Relativistic effects are known to be substantial in the chemistry of gold.[165] Schwerdtfeger and coworkers have compared IPs calculated with nonrelativistic Hartree-Fock calculations and relativistic Dirac-Fock calculations.[140] Hence, we sought to estimate the magnitude of relativistic effects upon the disproportionation of gold(II). To this end, the relativistic (R) and nonrelativistic (NR) pseudopotentials and basis sets of Hay, Wadt, Kahn and Bobrowicz (HWKB) were utilized.[166] Both schemes were employed

in conjunction with DFT[167] and CCSD(T)[164] methods. The results are organized in Table 4.1.

The largest effect of relativity is on the first ionization potential of gold, Table 4.1. With both DFT and CCSD(T) methods, the inclusion of relativistic effects increases IP_1 by ~50 kcal/mol. Interestingly, relativistic effects for IP_2 and IP_3, which are more pertinent to disproportionation, are much smaller. For both the B3PW91 and CCSD(T) methods, relativity decreases IP_2 (22 kcal/mol for the former, 9 kcal/mol for the latter) and also IP_3 (30 kcal/mol for DFT, 10 kcal/mol for CCSD(T)). The same relative changes, although different in magnitude, of gold IPs with respect to relativistic effects have been observed by Schwerdtfeger *et al.*[140] As the NR-HWKB calculations overestimate both IP_2 and IP_3 by roughly the same magnitude as seen in Table 4.1, the resultant difference (*i.e.*, the gas-phase disproportionation energy, ΔE_{disp}) is remarkably unaffected by relativity: ΔE_{disp} (kcal/mol) = 334 (B3PW91/NR-HWKB) versus 326 (B3PW91/R-HWKB); 312 (CCSD(T)/ NR-HWKB) versus 311 (CCSD(T)/ R-HWKB).

Table 4.1. Relativistic Effects and Gold Ionization Potentials[a]

Property	$IP(NR)_{DFT}$	$IP(R)_{DFT}$	$IP(NR)_{CC}$	$IP(R)_{CC}$
IP_1	154.1	196.0	156.8	210.6
IP_2	542.7	520.7	505.1	496.0
IP_3	876.6	846.9	817.0	807.2

[a] Ionization potentials (kcal/mol) calculated as differences in electronic energies of appropriate atomic and atomic ion states. NR and R denote nonrelativistic and relativistic pseudopotentials, respectively;[167] DFT and CC denote B3PW91 and CCSD(T) methods, respectively. [Reproduced in part with permission from: Barakat, K. A.; Cundari, T. R.; Rabaâ, H.; Omary, M. A. *J. Phys. Chem*. 2006, 110, 14645. Copyright 2006 American Chemical Society.]

Table 4.2. Disproportionation Free Energies (kcal/mol) of $Au^{II}L_3$ Complexes in Aqueous Media

L	$\Delta G_{rxn,gas}$	$\Delta G_{(1,aq)}$	$\Delta G_{(2,aq)}$	$\Delta G_{(3,aq)}$	ΔG_{solv}	$\Delta G_{rxn,aq}$	ρ_{spin} [b]
PH_3	43.8	-39.8	-173.2	-375.7	-69.0	-25.2	0.35
CO	72.6	-54.3	-208.8	-432.5	-69.2	+3.4	0.50
MeCN	41.4	-36.5	-148.7	-314.1	-53.2	-11.8	0.64
MeNC	21.5	-39.4	-154.3	-322.4	-53.2	-31.7	0.50
NH_3	59.2	-56.3	-207.4	-444.8	-86.3	-27.1	0.52
OH_2	88.0	-53.0	-242.6	-514.6	-92.4	-4.3	0.63
Py	23.7	-45.1	-150.1	-282.1	-27.0	-3.3	0.48

[a] $\Delta G_{rxn,gas}$ is the energy of the disproportionation reaction (Equation 4) in the gas phase; $\Delta G_{(1,aq)}$ is the calculated free energy of aquation of $^1[Au^IL_2]$; $\Delta G_{(2,aq)}$ is the calculated free energy of aquation of $^2[Au^{II}L_3]$; $\Delta G_{(3,aq)}$ is the calculated free energy of aquation of $^1[Au^{III}L_4]$; $\Delta G_{solv} = \Delta G_{(3,aq)} + \Delta G_{(1,aq)} - 2\,\Delta G_{(1,aq)}$; $\Delta G_{rxn,aq} = \Delta G_{rxn,gas} + \Delta G_{solv}$. Py = pyridine.

[b] Spin density (in e^-) on the Au atom in $^2Au^{II}L_3$ (gas-phase). CPCM spin densities are nearly identical to gas-phase spin densities.

4.3.2 Disproportionation of $Au^{II}L_3$ Complexes

In this section we investigate ligand and solvent effects on our model disproportionation reaction, Equation 4, for neutral ligands (L = PH_3, CO, NH_3, OH_2, pyridine, MeCN, MeNC). Calculated free energies in the gas phase and solution (CPCM water and acetonitrile) are compiled in Table 4.2, along with calculated solvation free energies for individual complexes.

$$2\ ^2[Au^{II}L_3] \rightarrow\ ^1[Au^IL_2] + {}^1[Au^{III}L_4] \qquad (4)$$

There are several interesting conclusions that emerge from the data in Table 4.2. First, the disproportionation reaction is highly endergonic in the gas phase, ranging from +21.5 kcal/mol for the isonitrile complex $[Au(MeNC)_3]^{2+}$ to +88.0 kcal/mol for disproportionation of the aqua complex $[Au(H_2O)_3]^{2+}$. No obvious trends with electron donating/accepting behavior of the ligands are obvious, and indeed may not be expected as disproportionation involves a subtle balance of factors due to the requirement for electron and ligand transfer. The latter is expected to be favored for weakly bonding ligands. The former is more complicated as ligands that make the Au^{I} complex a better electron donor may also make the Au^{III} complex a worse electron acceptor. Comparison of the data in Table 4.2 with the earlier results given for atomic ion species does indicate that the ligands do ameliorate the endergonicity of the gas-phase disproportionation reaction.

As computed in a previous study[154] of *tris*(phosphine)gold(I) complexes, $[Au^{II}L_3]$ complexes have a T-shape coordination geometry. Analysis of the spin densities highlights the difficulties in assigning oxidation states to formally divalent gold complexes.[133-135] In the crystal field limit, one expects a single unpaired electron on a d^9-Au^{II} ion. However, spin density values from a Mulliken population analysis are substantially less than one electron, ranging from 0.35 e^- for the complex with L = PH_3 to 0.64 e^- with L = MeCN, Table 4.2. Analyses of EPR spectra of magnetically dilute Au^{II} complexes have indicated delocalization of the unpaired electron onto the ligands; in some cases this delocalization is very substantial.[134,141,145,146] Schlupp and Maki propose that only 15% of the spin density resides on the gold in their *bis*(maleonitriledithiolato)-

gold(II) complex;[141] we have obtained a very similar value computationally for this complex.[168] While the partitioning of total electron density is always arbitrary to some extent, the results emphasize the inherent instability of the Au^{II} oxidation state. The low value of ρ_{spin} for PH_3, and comparison of the gold spin density of the MeCN complex (ρ_{spin} = 0.64 e^-) with the isomeric MeNC complex (ρ_{spin} = 0.50 e^-) makes it tempting to interpret the results in terms of the ability of σ-donor/π-acceptor ligands to stabilize Au^{II} complexes.[150,151] However, the computed results are not always so straightforward. For example, CO is a σ-donor/π-acceptor ligand; yet, its Au^{II} complex has a spin density on Au that is essentially the same as the Au^{II} complex with ammonia (a σ-donor), *i.e.*, ρ_{spin} ~ 0.5 e^- in both.

Linear correlations with prototypical frontier orbital properties and the calculated spin density on gold (ρ_{spin}) were investigated. There is very poor linear correlation with either the KS-HOMO (Kohn-Sham highest occupied molecular orbital) or KS-LUMO (Kohn-Sham lowest unoccupied molecular orbital) energy and ρ_{spin}.[169] Correlation is slightly better between ρ_{spin} and the KS-HOMO/KS-LUMO gap although pyridine is an obvious outlier for reasons that are not apparent. We also found no correlation between the free energies of the disproportionation reaction with neither the IP nor the KS-HOMO/KS-LUMO gap of the different L ligands. All these data suggest no apparent relationship between the stability of the $Au^{II}L_3$ complex and the electronic factor of the ligand alone.

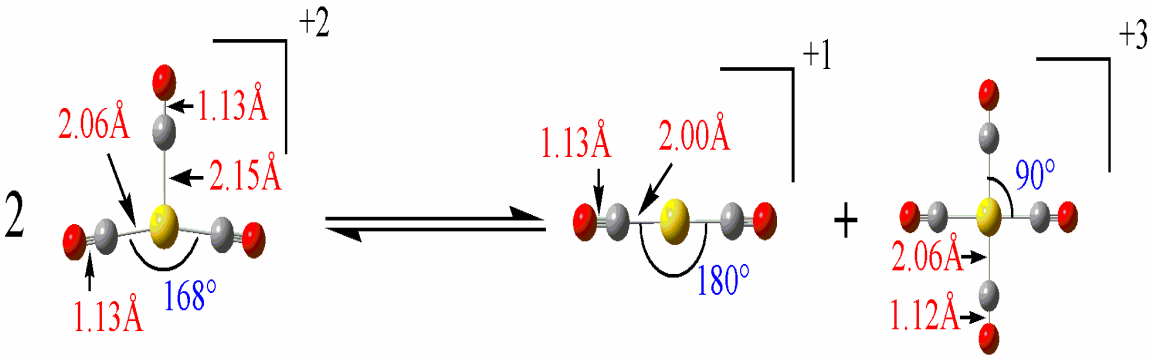

Figure 4.1. Disproportionation reaction for L = CO. Bond lengths in Å; bond angles in °. Reaction is calculated to be endergonic both in aqueous ($\Delta G_{rxn,aq}$ = +3.4 kcal/mol) and acetonitrile ($\Delta G_{rxn,aq}$ = +5.1 kcal/mol) solution.
[Reproduced in part with permission from: Barakat, K. A.; Cundari, T. R.; Rabaâ, H.; Omary, M. A. *J. Phys. Chem*. 2006, 110, 14645. Copyright 2006 American Chemical Society.]

The data in Table 4.2 indicate that the aqueous disproportionation reaction is considerably more favorable than the corresponding gas phase reaction. Disproportionation is now endergonic for the carbonyl complex (Figure 4.1). The remaining ligands have exergonic disproportionation reactions in aqueous media. The driving force for this shift in thermodynamics of disproportionation is the very large negative values for the free energies of aquation of the $^{1}[Au^{III}L_4]$ complexes. The solvation free energy contribution to the reaction (ΔG_{solv}) is very large for small, polar ligands such as ammonia and water. For the pyridine complex, the ΔG_{solv} is the least negative (-27.0 kcal/mol), a result consistent with the large size of the ligand (aquation energy is expected to vary inversely with the volume of the solute) and the low-polarity of the CH groups that are presented to the solvent. As a result, $\Delta G_{rxn,aq}$ for the disproportionation of $[Au(Py)_3]^{2+}$ is only moderately exergonic, -3.3 kcal/mol. For the aqua complex, the aqueous-phase disproportionation is also mildly exergonic, although,

unlike the pyridine complex, this reflects a very unfavorable gas-phase disproportionation counteracted by a very negative solvation free energy, Table 4.2.

The present results suggest that synthetic efforts toward a monometallic Au^{II} complex should utilize as nonpolar a solvent as is feasible, in order to thwart decomposition to univalent and trivalent gold complexes via disproportionation. This contention is further supported by the data in Table 4.3 regarding the calculated disproportionation energies and solvation free energies in acetonitrile (ε = 36.64). However, the CPCM calculations indicate several exceptions to this generalization due to the variations that exist in the solvation free energies of the various cationic complexes. Disproportionation can be more exergonic in acetonitrile than in water: $\Delta G_{rxn,an}$ = -34 kcal/mol vs. $\Delta G_{rxn,aq}$ = -32 kcal/mol for $[Au(MeNC)_3]^{2+}$; $\Delta G_{rxn,an}$ = -21 kcal/mol vs. $\Delta G_{rxn,aq}$ = -3 kcal/mol for $[Au(Py)_3]^{2+}$. However, for the majority of complexes, the switch from water to acetonitrile thermodynamically inhibits the disproportionation by 1 to 8 kcal/mol.

Tables 4.2 and 4.3 indicate that a polar environment provides enhanced driving force for the disproportionation of Au^{II} complexes, echoing the conclusions of the atomic calculations reported above. While the choice of solvent in a synthesis is, of course, dictated by a variety of factors, the present calculations indicate that lower polarity solvents may inhibit disproportionation toward the synthesis of stable Au^{II} mononuclear complexes.

Table 4.3. Disproportionation Free Energies (kcal/mol) of $Au^{II}L_3$ Complexes in Acetonitrile Solution[a]

Ligand	$\Delta G_{rxn,gas}$	$\Delta G_{(1,an)}$	$\Delta G_{(2,an)}$	$\Delta G_{(3,an)}$	ΔG_a	$\Delta G_{rxn,an}$
PH_3	43.8	-33.3	-151.1	-330.8	-61.9	-18.1
CO	72.6	-44.5	-179.6	-382.3	-67.5	5.1
MeCN	41.4	-29.7	-128.8	-280.5	-52.5	-11.1
MeNC	21.5	-32.3	-133	-289.1	-55.4	-34
NH_3	59.2	-46.4	-180.3	-392.6	-78.4	-19.2
OH_2	88	-51.1	-202.9	-443.5	-88.8	-0.8
Py	23.7	-32	-124.9	-262.5	-44.5	-20.8

[a] $\Delta G_{rxn,gas}$ is the energy of the disproportionation reaction (eq 4) in the gas phase; $\Delta G_{(1,an)}$ is the calculated free energy of solvation in acetonitrile of $^1[Au^IL_2]$; $\Delta G_{(2,an)}$ is the calculated free energy of solvation in acetonitrile of $^2[Au^{II}L_3]$; $\Delta G_{(3,an)}$ is the calculated free energy of solvation in acetonitrile of $^1[Au^IL_3]$; $\Delta G_{an} = \Delta G_{(3,an)} + \Delta G_{(1,an)} - 2\Delta G_{(1,an)}$; $\Delta G_{rxn,an} = \Delta G_{rxn,gas} + \Delta G_{an}$.

4.4 Summary and Conclusions

A computational study of gold(II) disproportionation reactions is presented. The effects of ligand, solvent and relativity are investigated. Several important conclusions have resulted from this research, the most important of which are summarized here.

1) Solvation significantly changes the energetics of the disproportionation reaction. The gas phase energy of disproportionation for atomic ions is more than halved, going from 283 kcal/mol in the gas-phase to 119 kcal/mol in aqueous environment (PCM-H_2O). The greater favorability of the disproportionation in aqueous media is driven by the big solvation energy of the trivalent gold ion. Thus, solvent choice will play an essential role in any synthetic effort aimed at Au^{II} monometallic complexes.

2) Relativistic effects on the energetics of atomic gold disproportionation are nominal.

3) For the disproportionation of $Au^{II}L_3$ complexes with neutral ligands, disproportionation is greatly endergonic in the gas phase.

4) The solvation free energy contribution to the reaction (ΔG_{solv}) is influenced by the ligand characteristics. For small and polar ligands like ammonia and water, ΔG_{solv} is very large. Calculations entail that for a monometallic Au^{II} complex to be synthesized; a nonpolar solvent is preferred over a polar solvent.

5) Disproportionation is considerably more favorable in solution than in the gas phase. With the exception of $[Au(CO)_3]^{2+}$, disproportionation of $Au^{II}L_3$ complexes to $Au^{I}L$ and $Au^{III}L_3$ is exergonic for the ligands probed. As with the atomic species, the driving force arises from the very complimentary solvation free energy of the trivalent gold complex.

The present calculations thus imply that choosing ligands that would lead to neutral species upon disproportionation (*e.g.*, $2\ AuX_2L \rightarrow AuXL + AuX_3L$; X = univalent ligand, L = neutral ligand) could afford an effective route to prevent this decomposition pathway for Au^{II} complexes. Likewise, bulkier ligands that yield larger, more weakly solvated complex ions emerge to be desirable.

CHAPTER 5

COMPUTATIONAL STUDIES OF $Hg[Mo(OH)_2(\equiv NH)]_2$

The following calculations were performed to investigate the electronic nature of the d^2 transition metal complex $Hg[Mo(\equiv NH)(OH)_2]_2$, and its proposed decomposition products. The calculations were performed in conjunction with experimental efforts by the group of Peter T. Wolczanski (Chemistry Department, Cornell University). The present chapter addresses only the computations performed in our research group.

5.1 Computational Methods

The model complex, $Hg[Mo(\equiv NH)(OH)_2]_2$, hereafter abbreviated as "$HgMo_2$", and its potential decomposition products – Hg atom, $Hg[Mo(\equiv NH)(OH)_2]$ (or "HgMo"), and $Mo(\equiv NH)(OH)_2$ – were studied with a variety of pure (BP86 and BLYP) and hybrid (B3LYP and B3PW91) functionals with different effective core potential basis sets. The following is a brief discussion of these studies. There were negligible differences in the calculated Hg-Mo equilibrium bond lengths and Hg-Mo bond dissociation enthalpies. Hence, the present results focus on the B3PW91 hybrid functional[156] and the Stevens effective core potential scheme.[52] The Steven valence basis sets (CEP-31G) for main group elements were supplemented by a d polarization function. All stationary points were evaluated by calculation of the vibrational frequencies to ascertain that they are true minima, *i.e.*, no imaginary frequencies. Enthalpic and entropic corrections to the total electronic energy were calculated using harmonic vibrational frequencies determined at the same level of theory employed for geometry optimization, and are

estimated at 1 atm and 298.15 K. Open-shell species were modeled using an unrestricted Kohn-Sham formalism; spin contamination was insignificant. All calculations employed the Gaussian 98 package.[49]

5.2 Results

5.2.1 Electronic Structure of $Mo(\equiv NH)(OH)_2$

The electronic structure of the model complex $Mo(\equiv NH)(OH)_2$ is more reminiscent of $Nb(OH)_3$ rather than its congener, $W(\equiv NH)(OH)_2$.[170,171] $Nb(OH)_3$ has near degenerate singlet and triplet ground states.[170] The complex $W(\equiv N^tBu)(silox)_2$, silox = O^tBu_3, is a stable diamagnetic complex;[172] calculations on a $W(\equiv NH)(OH)_2$ model also indicated a singlet ground state.[171] The ground state of $Mo(\equiv NH)(OH)_2$ is predicted to be a triplet by several density functional methods used in conjunction with the CEP-31G(d) valence basis set. The only exception is the BLYP functional, which predicts the singlet and triplet states to be degenerate. The singly occupied orbitals of $Mo(\equiv NH)(OH)_2$ are $d\sigma$ and $d\pi$ in character, the remaining two $d\pi$ orbitals of molybdenum being involved in forming the in- and out-of-plane MoN π bonds. See Figure 5.1 for frontier orbital plots.

The calculated singlet-triplet free energy splittings (ΔG_{ST}) for $Mo(\equiv NH)(OH)_2$ range from +0.4 (BLYP/CEP-31G(d)) to –8.2 (BHandHLYP/CEP-31G(d)) kcal/mol. The average ΔG_{ST} for the six functionals investigated (B3LYP, B3PW91, BLYP, BP86, BHandHLYP, and MPW1PW91) is –4 ± 3 kcal/mol; the negative sign indicates that S < T. Taking the B3PW91/CEP-31G(d) optimized geometry and carrying out a CCSD(T)

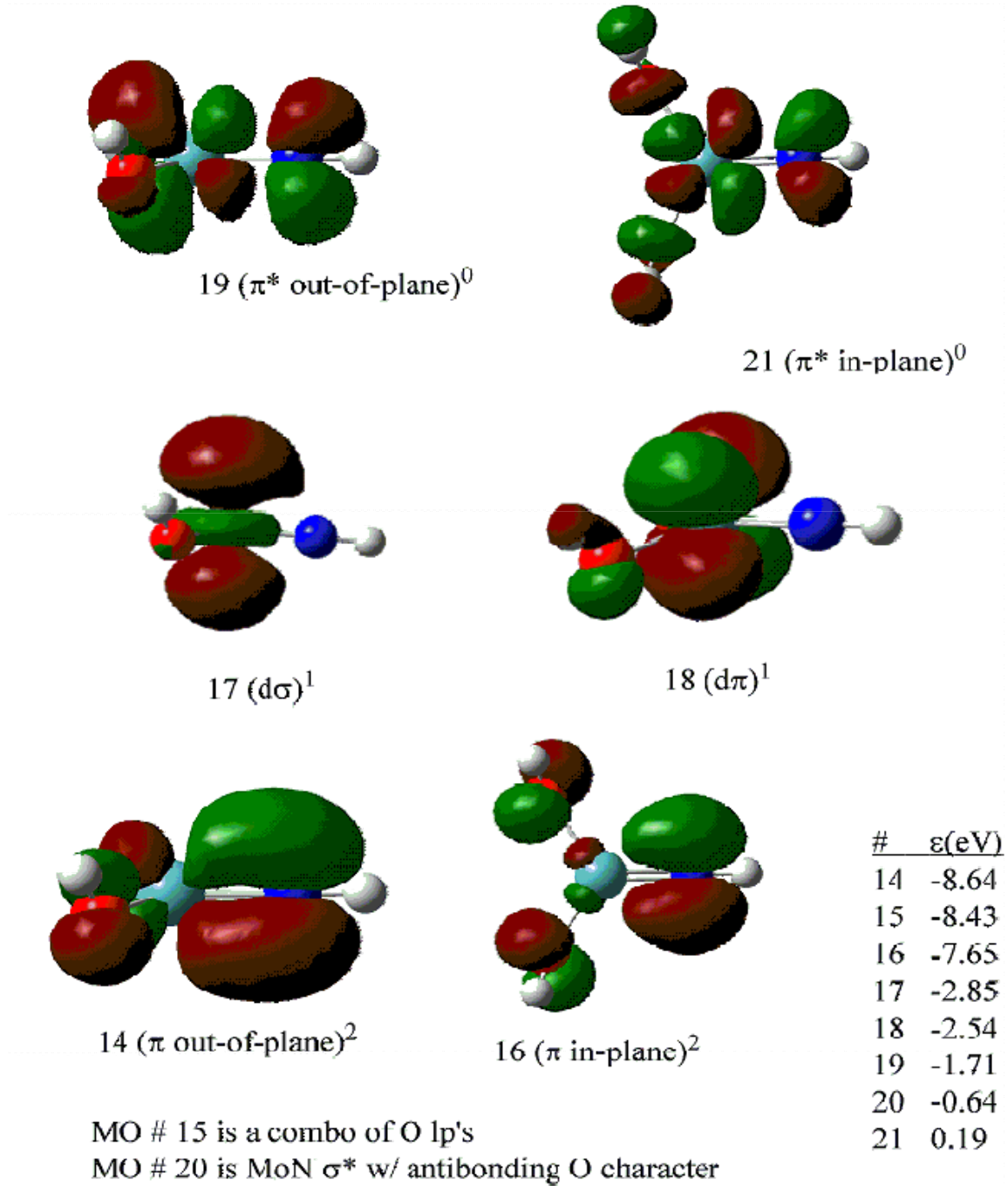

Figure 5.1. B3PW91/CEP-31G(d) frontier orbitals of triplet Mo(≡NH)$(OH)_2$.

[Reproduced in part with permission from: Rosenfeld, D. C.; Wolczanski, P. T.; Barakat, K. A.; Buda, C.; Cundari, T. R. *J. Am. Chem. Soc.* 2005, 127, 8262. Copyright 2006 American Chemical Society.]

single point energy evaluation (B3PW91/CEP-31G(d) computed frequencies used for calculation enthalpic and entropic corrections) yields an estimated ΔG_{ST} of -0.7 kcal/mol at the coupled cluster level of theory. To summarize, calculations indicate a triplet ground state for $Mo(\equiv NH)(OH)_2$, consistent with experimental data for transient $Mo(\equiv N^tBu)(silox)_2$. Perhaps more interestingly, the calculations also indicate a thermally accessible low energy excited singlet state.

5.2.2 $Hg[Mo(=NH)(OH)_2]_2$, "$HgMo_2$"

The complex $Hg[Mo(=N^tBu)(silox)_2]_2$ is very interesting. A survey of the Cambridge Structural Database[173] yields no other entities with a bond between a two-coordinate mercury and a four-coordinate molybdenum. The most similar species are $Hg[M(=NAr)_3]$, M = Tc, Re; Ar = 2,6-$C_6H_3{}^iPr_2$,[174,175] which are complexes of mercury and a high-valent metal-imido fragment; these complexes have been studied previously using ECP methods similar to those employed in the present research.[176]

Geometry optimization of $HgMo_2$ at the B3PW91/CEP-31G(d) level of theory indicates that the ground state is a triplet. Predicted Hg-Mo bond lengths are 2.76 Å, longer than experiment: 2.6810(5) Å. The average Hg-Mo bond length (limited to two-coordinate mercury complexes) in the Cambridge Structural Database is 2.73 ± 0.03 Å for 18 examples.[173] The symmetry of the $Hg[Mo(\equiv NH)(OH)_2]_2$ model is ~C_{2h} with the imido groups anti to each other. Other pertinent bond lengths (Å) and bond angles (°) are given in Figure 5.2.

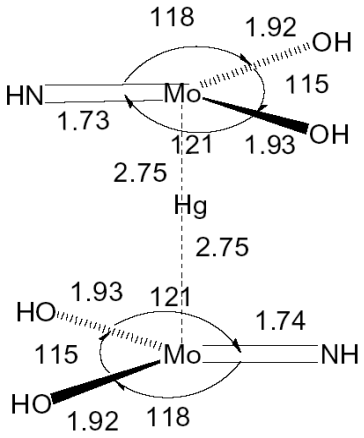

Figure 5.2. Pertinent bond lengths (Å) and bond angles (°) for $Hg[Mo(\equiv NH)(OH)_2]_2$.

[Reproduced in part with permission from: Rosenfeld, D. C.; Wolczanski, P. T.; Barakat, K. A.; Buda, C.; Cundari, T. R. *J. Am. Chem. Soc.* 2005, 127, 8262. Copyright 2006 American Chemical Society.]

In its simplest terms the bonding in $HgMo_2$ can be described as follows. First, the ground state of triplet d^2-$Mo(OH)_2(\equiv NH)$ is $(d\sigma)^1(d\pi)^1$. Each of the $d\sigma$ orbitals from both $Mo(OH)_2(\equiv NH)$ fragments participates in a singlet-coupled, three-center, four-electron interaction with the $6s^2$ of Hg – resulting in bonding, nonbonding, and antibonding combinations. The $d\pi$ orbitals of the Mo(OH)2(≡NH) fragments interact only weakly with Hg-based orbitals, and thus maintain their triplet coupling.

5.2.3 $Hg[Mo(=NH)(OH)_2]_2$ Thermochemistry

Given the apparent robustness of $Hg[Mo(=N^tBu)(silox)_2]_2$, calculation of the Hg-Mo bond dissociation enthalpies was of interest. The reactions studied are

$$^3HgMo_2 \rightarrow {}^3HgMo + {}^3Mo$$

$$^3HgMo \rightarrow {}^1Hg + {}^3Mo$$

where the superscript refers to the calculated ground state multiplicity. The B3PW91/CEP-31G(d) estimated enthalpies are 22.4 kcal/mol for the first Hg-Mo bond dissociation, and 3.1 kcal/mol for the second Hg-Mo bond dissociation.

5.2.4 Other Spin States with $HgMo_2$ Stoichiometry

Other isomeric and spin states of $HgMo_2$ stoichiometry were investigated. For the $HgMo_2$, the lowest energy calculated state is a triplet as mentioned above. The lowest energy singlet state found is Hg + Mo_2; the latter complex is akin to the Mo-imido dimer reported by Schrock.[177] The stability of the singlet Mo_2 dimer makes it interesting that this material is not experimentally observed in any of the reactions of $HgMo_2$.The singlet state of Hg + Mo_2 is 42.1 kcal/mol lower in energy than triplet $HgMo_2$. As for a possible quintet state, the most plausible candidates for such a multiplicity would seem to be the products of Hg-Mo bond dissociation, *i.e.,* $\{^3HgMo + {}^3Mo\}$ and $\{^1Hg + 2\ {}^3Mo\}$. Assuming no substantial interaction among the fragments these product states are calculated to be 22.4 and 25.5 kcal/mol, respectively, above triplet $HgMo_2$.

Given that the products of the dissociation of the first Hg-Mo bond of $HgMo_2$ are both triplets, the spin state evolution along this reaction coordinate was investigated. An energy scan of one Hg-Mo bond (keeping the other constant at the value calculated in its optimized minimum energy geometry) from 2.5 to 4.5 Å in 0.1 Å increments was performed, (Figure 5.3). The enthalpic and entropic corrections were determined at every point, (Figure 5.4). As is evident from (Figure 5.4), the crossing point (Hg-Mo ~ 4.0 Å, *ca.* 26 kcal/mol above the lowest energy triplet) is similar whether the electronic

energy, enthalpy or free energy is used. More importantly, there is a crossing between the triplet and quintet surfaces as one Hg-Mo bond is stretched; as this is not a full optimization, the estimated T-Q crossing point of 26 kcal/mol should be an upper limit to the real triplet-quintet crossing point.

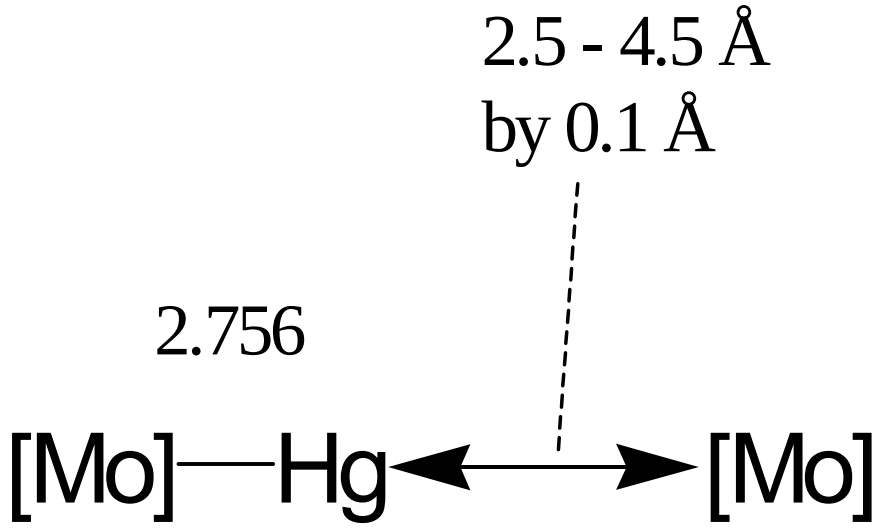

Figure 5.3. Energy scan of one Hg-Mo bond.

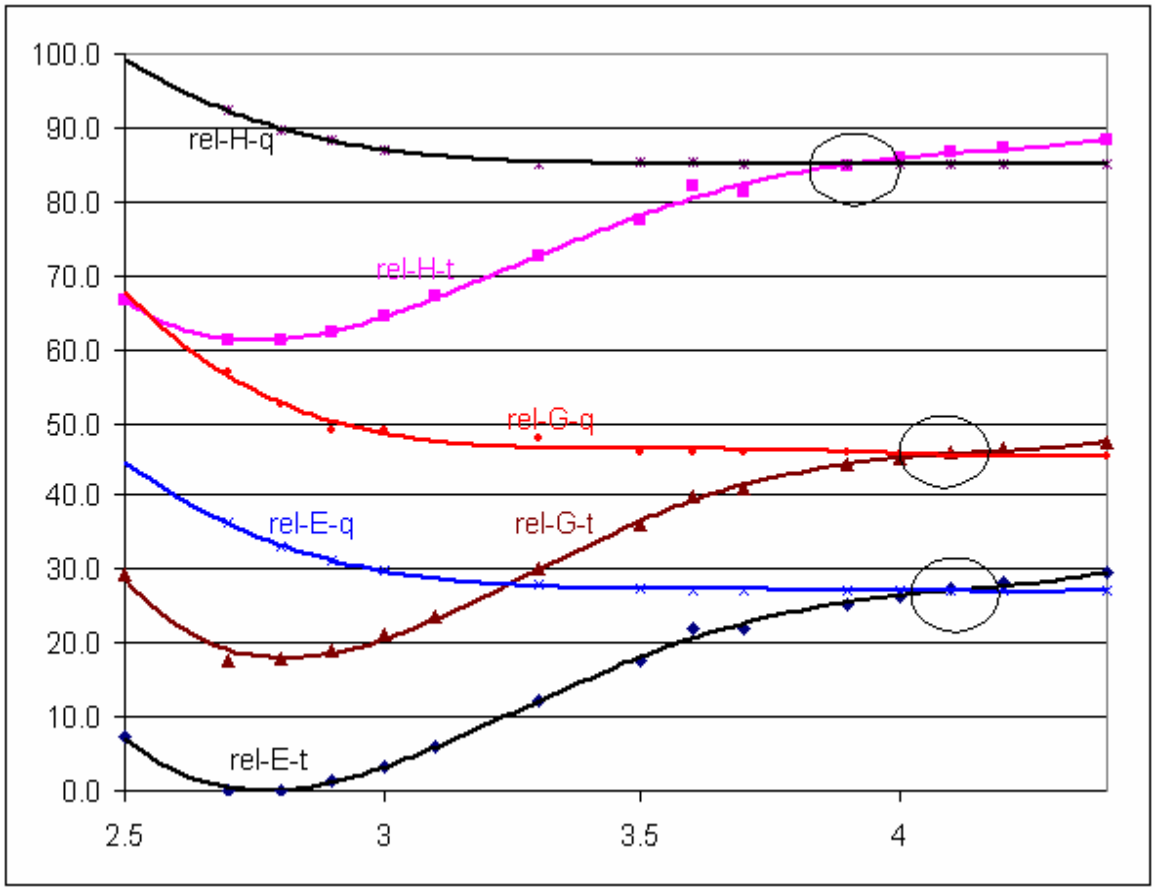

Figure 5.4. Evolution triplet (t) and quintet (q) states of $HgMo_2$ in terms of relative energy (E), enthalpy (H) and free energy (G) as a single as a single Hg-Mo bond is stretched from 2.5 to 4.5 Å. The t-q crossing points are circled for E, H and G.

To summarize, the calculations were performed to complement experimental studies by Wolczanski and coworkers and to investigate the electronic nature of the d^2 transition metal complex $Hg[Mo(\equiv NH)(OH)_2]_2$, and its proposed decomposition products.. The calculations indicate a triplet ground state for $Mo(\equiv NH)(OH)_2$, and a thermally accessible low energy excited singlet state. Geometry optimization of $HgMo_2$ at the B3PW91/CEP-31G(d) level of theory indicates that the ground state is a triplet.

As for a possible quintet state, the most plausible candidates for such a multiplicity would seem to be the products of Hg-Mo bond dissociation, *i.e.,* $\{^3HgMo$ +

^{3}Mo} and {^{1}Hg + 2 ^{3}Mo}. Assuming no substantial interaction among the fragments these product states are calculated to be accessible relative to triplet $HgMo_2$ leading to the inference that such a pathway for decomposition of $Hg[Mo(=N^tBu)(silox)_2]_2$ should be feasible under ambient experimental conditions.

CHAPTER 6

IMPORTANT AMINO ACID INTERACTIONS AT THE DIMER INTERFACE OF HUMAN GLUTATHIONE SYNTHETASE, A NEGATIVELY COOPERATIVE ATP-GRASP ENZYME

6.1 Introduction

Negative cooperativity describes a situation in which the first substrate binding event in a multimeric enzyme inhibits the binding of a second substrate molecule to a different active site in another enzyme subunit. Koshland in his studies of aspartate receptors[178] showed that binding of the first aspartate molecule to a dimeric enzyme induces a structural change that "squeezes" the other receptor site, thus making binding of the second aspartate more difficult. Despite more than a century passing since the first recognition of cooperativity in enzymes (the classic case of positive cooperativity in O_2 binding to hemoglobin[179]), there is still discussion regarding the molecular-level events that yield cooperativity. Several theories of enzyme cooperativity have been proposed, notably the Koshland, Nemethy, Filmer (KNF or sequential[180]) and Monod-Wyman-Changeux (MWC or concerted[181]). In an interesting series of papers, Gutheil and coworkers have investigated negative cooperativity using thermodynamic models.[182,183,184] Abeliovich has presented a statistical analysis of negative cooperativity, particularly in relation to the Hill coefficient, the most common parameter for quantifying negative cooperativity.[185] Negative cooperativity, despite its rarity, is biologically important. To quote Koshland[178] "negative cooperativity gives a less sensitive response over a much broader range of stimulus." For important biological molecules whose concentrations can vary over a wide range, a negatively cooperative

enzyme tempers or moderates the response to mitigate potential physiological consequences. Koshland ends his review[178] with a call for more research, stating, "dimeric proteins with negative cooperativity are good potential systems for analyzing the quantification of conformational changes."

Human glutathione synthetase (*hGS*) is responsible for formation of glutathione (GSH), the body's most important natural antioxidant.[186] Glutathione synthetase's significance is heightened by it being the only human member of an important enzyme family, ATP-Grasp,[187] which has been structurally characterized. Other ATP-Grasp enzymes play a role in bacterial cell wall and purine biosynthesis, common targets for antibiotics. Furthermore, GS and GSH in important crops have been implicated for their role in drought-induced stress and herbicide interactions.[188] Others in our research group have focused on the mechanism of human glutathione synthetase (*hGS*), its catalytic action, and deducing the important amino acids that control its reactivity.[189,190] Dinescu *et al.* concluded on the basis of sequence and structural comparison of *hGS* with other ATP-Grasp members shows that within the ATP binding site that Glu144 is fully conserved, Lys364 and Lys305 are charge conserved, and Asn146 is backbone-conserved.[189] Experiments (site-directed mutagenesis, kinetic analysis) show that when Glu144, Asn146, Lys305 and Lys364 are replaced with amino acids that cannot interact favorably with substrates, the resulting mutant enzymes show little to no activity.[189] Optical circular dichroism (OCD) spectra and molecular dynamics simulations suggest that the loss of activity is due to changes in ATP binding rather than a substantial change in the tertiary structure of *hGS*. Bioinformatics techniques indicate several other

regions of high amino acid identity in GS from humans and other eukaryotes. These regions are termed the substrate (S), glycine-rich (G), and alanine-rich (A) loops, (Figure 6.1). In terms of the interest in negative cooperativity, human glutathione synthetase is a dimeric enzyme that has been shown to display negative cooperativity with a Hill coefficient of 0.5.[191,192]

In the present research, important amino acid interactions at the dimer interface of human glutathione synthetase are investigated. Another point of interest is possible mechanisms by which the active sites communicate across the dimer interface, despite their *ca.* 50 Å separation. Computational techniques are thus utilized to probe the nature of negative cooperativity in *hGS.*

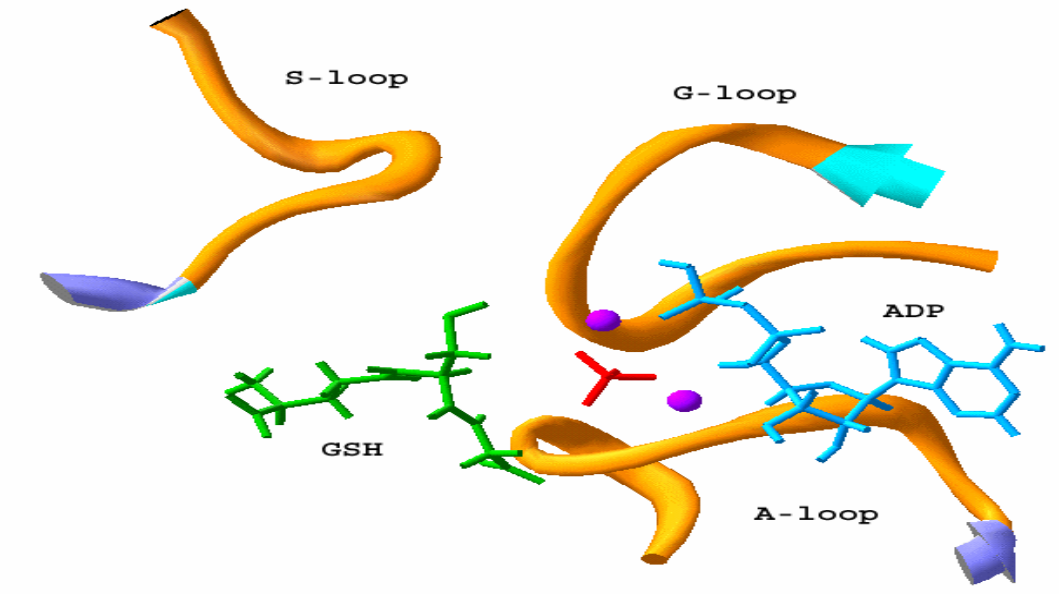

Figure 6.1. Location of GAS loops around active site of *hGS*.

6.2 Computational Methods

6.2.1 Structural Analysis of *hGS*

The crystallographic coordinates from the X-ray structure analysis of dimeric human glutathione synthetase (*hGS*, glutathione synthetase, human form) (PDB code = 2HGS)[193] were visualized and analyzed with DeepView.[194,195] DeepView was used to identify amino acid residues within a chosen distance of the dimer interface of *hGS*. These are defined as amino acids that have interchain interactions between chain A and chain B of 2HGS. Analyses of the protein-contacts were carried out for both wild type and mutant 2HGS. Contact types (*i.e.*, hydrogen bonds, hydrophobic contacts, *etc.*) and pertinent atomic distances were computed with the MOE (Molecular Operating Environment) program.[196]

Potential sites within 2HGS were identified using the Site Finder functionality within MOE, and which was based upon the alpha shape methodology.[197,198] Operational settings employed in this research were as follows: Probe Radius 1 = 1.4 Å (radius of a hypothetical hydrophilic, hydrogen-bonding atom), Probe Radius 2 = 1.8 Å (radius of a hypothetical hydrophobic atom), isolated Donor/Acceptor = 3 Å (if a hydrophilic alpha sphere had no hydrophobic alpha sphere within the specified distance, then the former was discarded; this minimized sites likely to bind only water), Connection Distance = 2.5 Å (if individual clusters had two alpha spheres within this distance they were combined), Minimum Site Size = 3 (minimum number of alpha spheres that comprised a suitable site), Radius = 2 Å (sites smaller than this size were eliminated). Solvent and salts were excluded in the simulations.

6.2.2 *Ab Initio* Calculation of Amino Acid Interactions

The GaussView visualization program was used to construct models of interacting residue pairs found at the dimer interface of *hGS*. After their construction, a conformational search was performed using the MOE (Molecular Operating Environment, software and the Amber94 force field[199] to find the lowest energy conformer, which was subsequently refined using *ab initio* calculations. The lowest energy conformer obtained from the molecular mechanics-based conformational search was then fully optimized with the GAMESS program[200] with hybrid density functional theory (DFT) methods (B3LYP functional[51] both in the gas phase and in solution (water)). For the latter simulations, the PCM (polarizable continuum model[160]) methodology was employed to compute the solvent effect. The basis set used for gas-phase and PCM simulations was 6-31+G(d).[201]

6.2.3 Analysis of Dimeric *hGS* Mutants

To explore dimer interaction energies (*i.e.*, ΔE_{dimer}, the energy of interaction between chain A and chain B) of mutant *hGS*, these were constructed from wild-type *hGS* and modeled with the MOE software[196] using the Amber94 force field.[199] Starting with the crystal structure coordinates of *hGS*, hydrogen atoms were first added, and with heavy atoms fixed in position, the resulting hydrogen-decorated enzyme structure was energy minimized with the Amber94 force field. Subsequently, the fixed heavy atoms were then allowed to move and then the resulting enzyme structure was fully geometry optimized, again with the Amber94 force field. Mutants were built by altering

individual residues of the energy minimized wild-type dimer *hGS*. Subsequently, the appropriate hydrogens were added, followed by Amber94 energy minimization. Water molecules were removed from the final optimized structures prior to dimer interface analysis so that the calculated ΔE_{dimer} are solely the energy between the amino acids that comprise chain A and the amino acids that comprise chain B of the *hGS* dimer or its mutants.

6.3 Results and Discussion

6.3.1 Structural Analysis of *hGS*

Analysis of dimeric *hGS* was initiated by looking for strong contacts between chain A amino acids and chain B amino acids across the dimer interface of 2HGS. Initial screens started with long-range interactions of (4 Å or less) and the residue sets were subsequently culled by reducing the threshold distance. Selected distances used are as follows (the number of residues within the specified distance is also denoted): (a) ≤3.95 Å, 28 residues per monomer, (b) ≤3.50 Å, 24 residues from each monomer, and (c) ≤3.00 Å, 5 residues from each monomer.

From these data it can be seen that the number of amino acid residues that are close to the dimer interface falls off very rapidly as the threshold distance is reduced from ~3.5 Å to ~3 Å. Moreover, the closest chain A:chain B interactions, and thus presumably those most chemically and biologically significant, are small in number. The latter pairs of five residues (Asp24, Ser42, Glu43, Tyr47, and Arg221 in both chains A and B of *hGS*) with the most significant bonding across the dimer interface were

considered the initial target residues for further study. These important interchain contacts are organized in Table 6.1.

Seven residues participate in five significant dimer interface interactions (Ser42•••Asp24, Tyr47•••Glu43, Arg221•••Asp24, $Val44_A$•••$Val44_B$ and $Val45_A$•••$Val45_B$) with subscripts denoting the chain to which the residue belongs. As *hGS* is a dimer, each of the three asymmetric interacting amino acid pairs must be doubled. For example, the Ser42•••Asp24 interaction signifies both $Ser42_A$•••$Asp24_B$ and $Ser42_B$•••$Asp24_A$. The symmetric $Val44_A$•••$Val44_B$ and $Val45_A$•••$Val45_B$ contacts are the closest hydrophobic contacts across the dimer interface. The prominent interchain contacts are depicted in Figures 6.2 and 6.3.

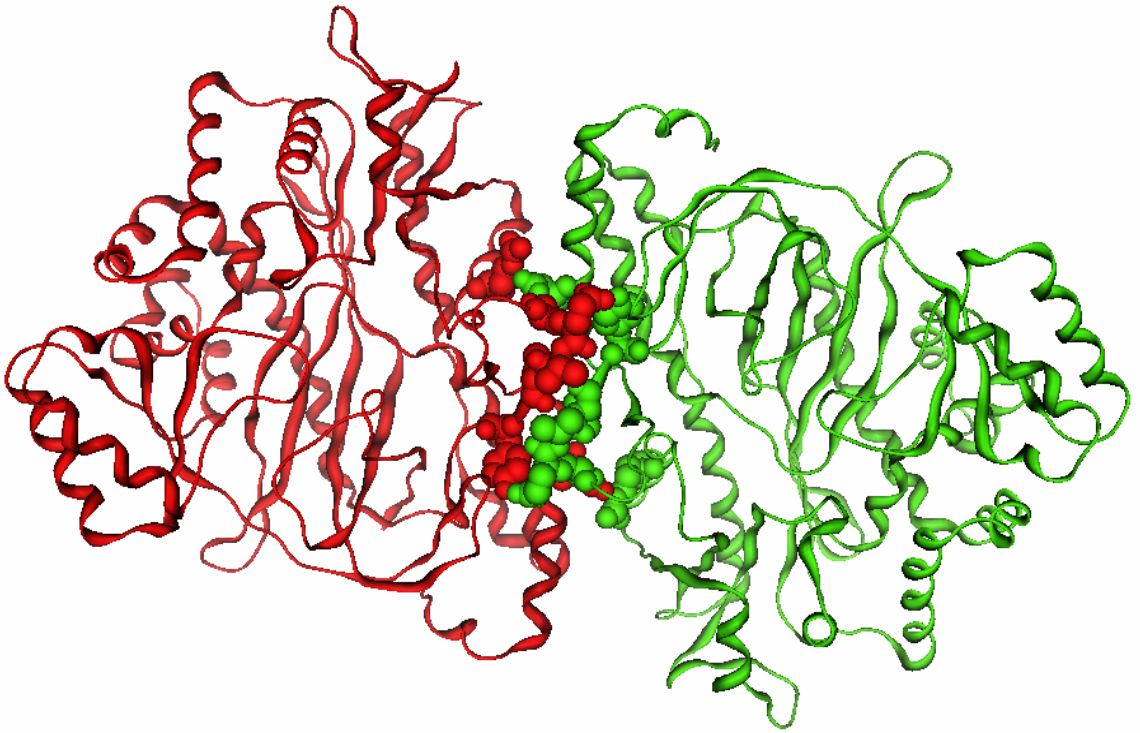

Figure 6.2. Ribbon diagram of human glutathione synthetase. Chain A is red; chain B is green. Amino acids that participate in close contacts across the dimer interface are indicated by space filling models.

Table 6.1. Protein Contacts: Wild-Type versus Mutant *hGS* Dimer

	S42 | D24	D24 | R221	E43 | Y47	$V44_A$ | $V44_B$	$V45_A$ | $V45_B$
Interaction Type[d]	HB	ION	HB	HYD	HYD
WT[e]	2.9	2.6	2.6	3.3	3.4
S42A	[a]	2.6	2.6	3.4	3.5
Y47F	2.9	2.6	[a]	3.4	3.4
E43A	3	2.6	[a]	3.3	3.4
R221A	2.8	[a]	2.6	3.3	3.4
D24A	[a]	[a]	2.6	3.3	3.4
ΔE_{int}-gas[b]	-18.3	-116.4	-24.6	-5.2	-5.2
ΔE_{int}-pcm[c]	-6.1	-13.5	-7.4	2.9	2.9

[a] This chain A:chain B interaction is lost due to mutation.
[b] Gas-phase interaction energy (kcal/mol) calculated at the B3LYP/6-31+G(d) level of theory.
[c] Aqueous-phase interaction energy (kcal/mol) calculated at the B3LYP/6-31+G(d) level of theory utilizing the polarizable continuum model (PCM).
[d] Interaction types: HB (hydrogen-bond), ION (ionic hydrogen bond), and HYD (hydrophobic).
[e] WT = wild-type *hGS*; for others, the single point mutation is designated by the original residue, then the residue number, and finally the residue (alanine) to which the residue was mutated to.

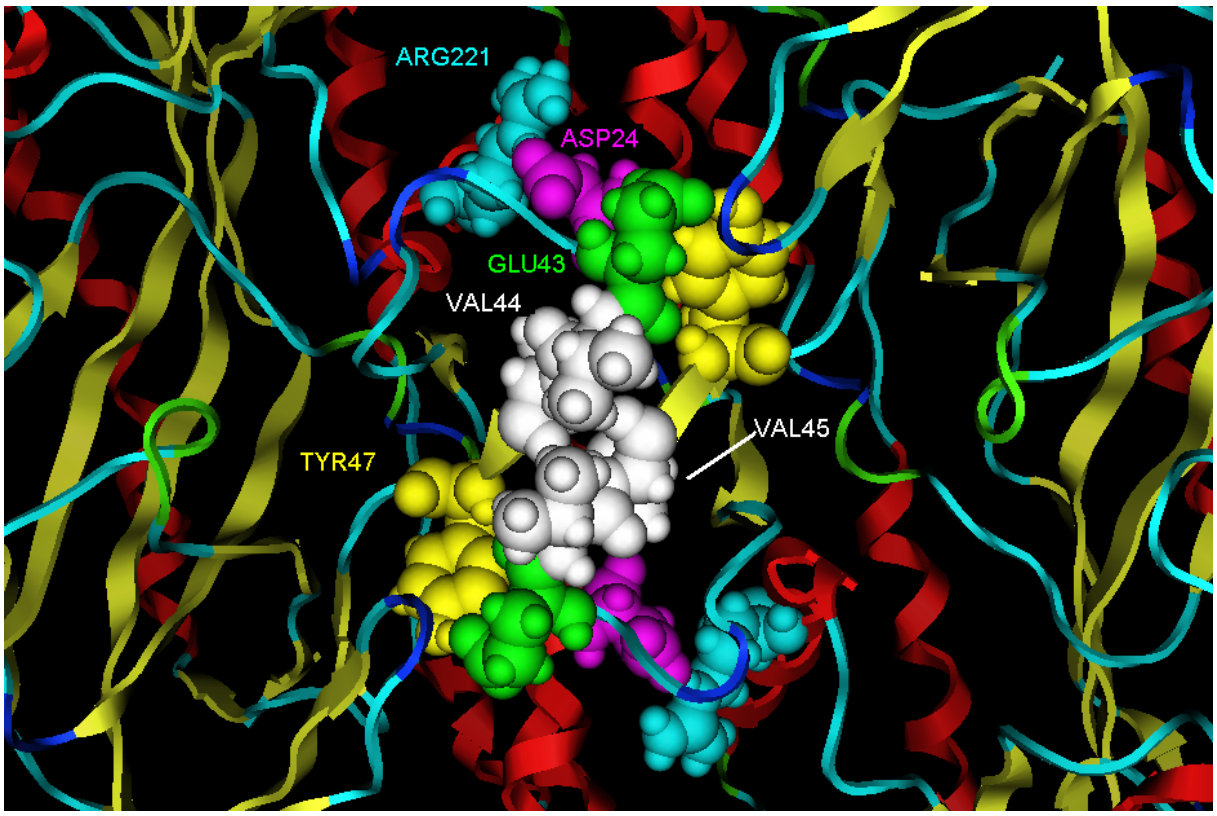

Figure 6.3. Close up of dimer interface of diagram of human glutathione synthetase. Color-coded space filling models indicate amino acids that participate in close contacts across the dimer interface.

The shortest amino acid contacts across the dimer interface are summarized in Table 6.1. The Ser42(O_γ)•••Asp24(O_δ) (2.9 Å) and Tyr47(O_H)•••Glu43(O_ε) (2.6 Å) interactions are categorized as hydrogen bond interactions. As both involve a hydrogen bond between a neutral donor and an anionic receptor, the shorter distance for the latter suggests that it is a stronger contact. Note that the distances indicated are heavy atom - heavy atom distances since hydrogen atoms are not located in the X-ray crystallography experiment. The Arg221(N_ε)•••Asp24(O_δ) (2.6 Å) is characterized by MOE as an ionic-hydrogen bond (salt bridge). The hydrophobic interactions are longer

distance than the other interactions just discussed - $Val44_A$•••$Val44_B$ and $Val44_A$•••$Val44_B$, ~3.6 Å distance between the respective C_γ of each valine side chain.

6.3.2 *Ab Initio* Calculation of Amino Acid Interactions

To better quantify the energetic magnitude of the important dimer interface contacts revealed by analysis of the structure of the *hGS* dimer, *ab initio* calculations were performed on amino acid pairs. The computational expense of *ab initio* methods requires the use of chemical approximations to make the calculations tractable. For this reason, interacting amino acid pairs are analyzed in the absence of the surrounding amino acids and the residues are truncated at the alpha carbon, which is replaced by a methyl group (Figure 6.4). The level of theory used for these calculations is B3LYP/6-31+G(d), which has been used with success in previous studies of hydrogen-bonding.[202] The interacting amino acid models are geometry optimized in both gas-phase and aqueous phase, the latter using a polarizable continuum model.[160]

The aqueous-phase geometries are shown in Figure 6.4. Each shows evidence of strong hydrogen-bonding interactions, as typified by close heavy atom - heavy atom distances ($O^{\cdots}O$ for Ser42•••Asp24 and Tyr47•••Glu43; $N^{\cdots}O$ for Arg221•••Asp24) of 2.5 to 2.7 Å and linear angles about the hydrogen-bonded hydrogen. It is encouraging that the calculated distances compare well with the experimental estimates from the crystal structure of 2HGS (see Table 6.1) despite the lack of the surrounding protein environment in the *ab initio* calculations. B3LYP/6-31+G(d) calculations are also carried out on the individual amino acid models shown in Figure 6.4.

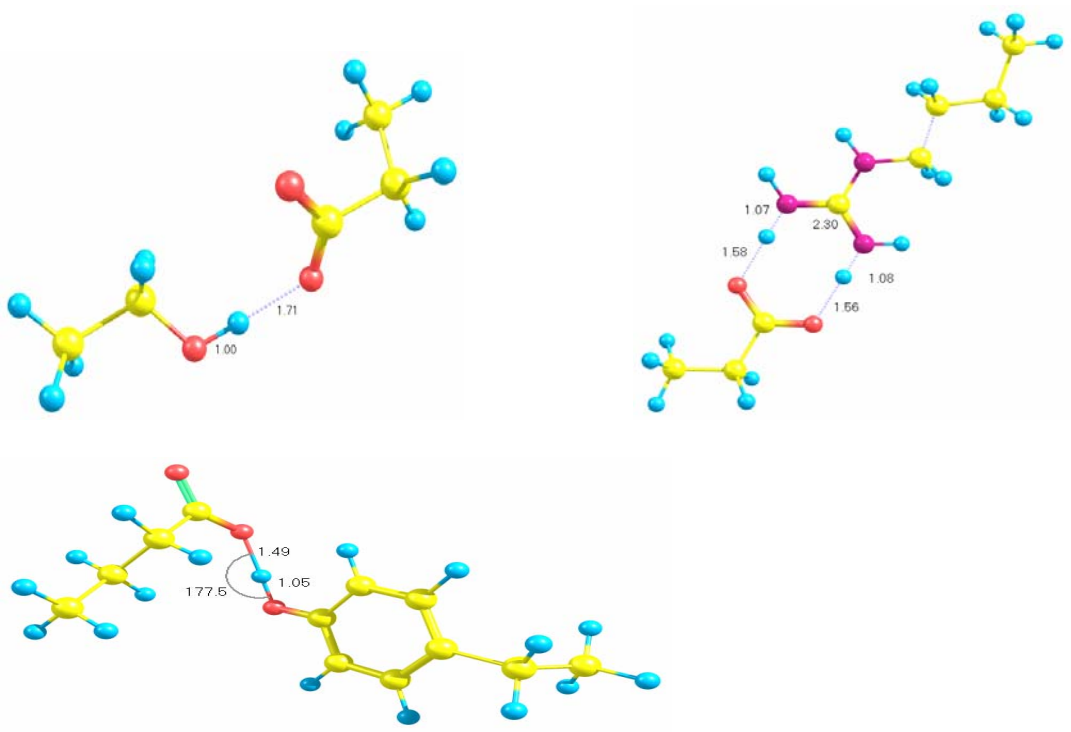

Figure 6.4. Calculated interacting amino acid models for Ser42•••Asp24 (top left), Tyr47•••Glu43 (bottom left) and Arg221•••Asp24 (top right). B3LYP/6-31+G(d) geometries optimized in PCM water; pertinent bond lengths (in Å) are given.

These energies are then subtracted from the energy of the amino acid pairs to determine the binding energies of the three interacting amino acid models in Figure 6.4. The calculated binding energies thus obtained in the gas-phase (ΔE_{int}-gas) and aqueous solution (ΔE_{int}-pcm) are summarized in Table 6.1 and Figure 6.5. The $Val44_A$•••$Val44_B$ and $Val45_A$•••$Val45_B$ interactions are also modeled with B3LYP/6-31+G(d) methods.[203] As before, a methyl group replaces the C_α of the amino acid residues.

Several important points emerge from the binding energy data. First, the effect of the medium (*cf.* the gas-phase and PCM/aqueous interaction energies) is significant. The shielding effected by the solvent, particularly on the salt bridge interaction, is substantial. Hence, the presence of solvent molecules (either *in vivo* or *in vitro*) or

solvent polarity is predicted to significantly attenuate the dimer interface interactions in *hGS*. Second, the calculated salt bridge (Arg221•••Asp24) binding energy is double the

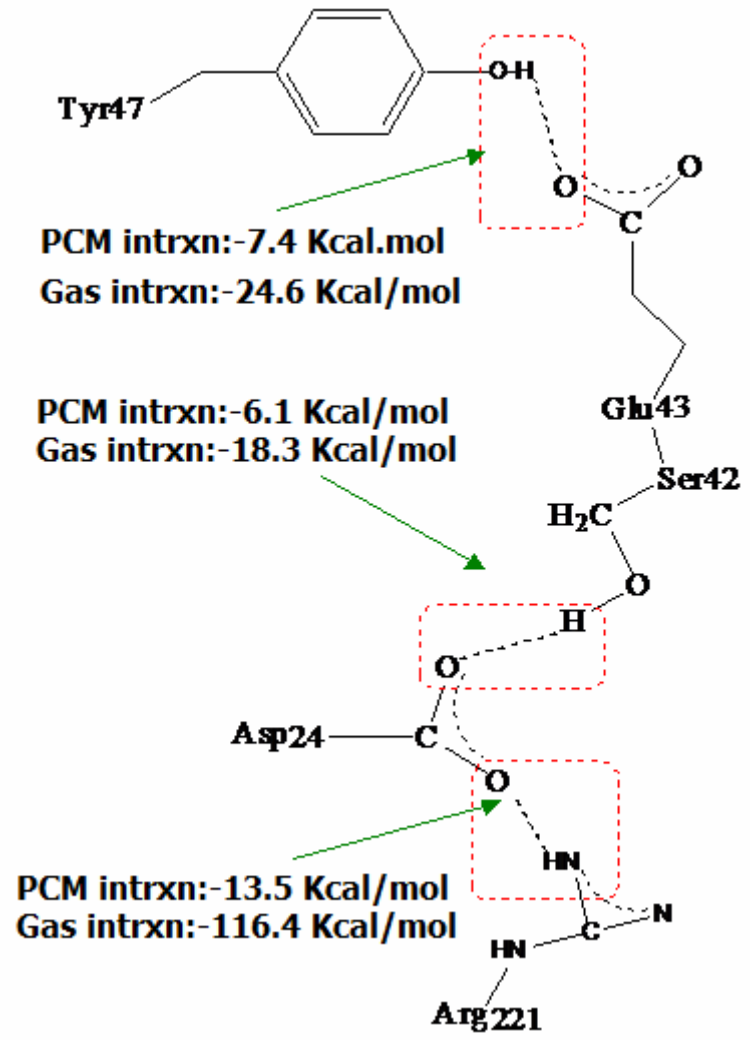

Figure 6.5. B3LYP/6-31+G(d) calculated interaction energies for amino acid across the dimer interface of *hGS* in the gas and PCM (aqueous) phase.

binding energy of the hydrogen bonds in aqueous environment, suggesting that on the basis of its close distance (see Table 6.1) and strong interaction energy (see Figure 6.5) that this contact is the most substantial across the dimer interface of *hGS*. Third, the

hydrophobic interactions are substantially weaker than the other bonds, as expected given their greater distances and the nature of this type of chemical interaction. Weak hydrophobic interactions are seen in the gas phase calculations that disappear upon the incorporation of continuum solvent effects. Fourth, Asp24 participates in both a strong salt bridge with Arg221, and a strong hydrogen bond with Ser42. Hence, Asp24 is the most interesting target for site directed mutagenesis experiments, and its mutation is expected to engender more substantial changes to hGS than the other interactions at the dimer interface.

6.3.3 Analysis of Dimeric *hGS* Mutants

The analysis of protein contacts and *ab initio* studies of amino acid models has indicated several profitable targets for site directed mutagenesis, both experiments and simulations. The accumulated structural and energetic data indicate that the interchain interactions can be prioritized as follows in terms of their expected impact on *hGS*: Arg221•••Asp24 > Ser42•••Asp24 ~ Tyr47•••Glu43 > $Val44_A$•••$Val44_B$ ~ $Val45_A$•••$Val45_B$. Furthermore, the participation of Asp24 in two significant interactions suggests it as the most profitable target for mutation. To this end, an *in silico* site directed mutagenesis "alanine scan" is performed. Two notes are germane before discussion of these simulations. First, Tyr47 was mutated to the non-hydrogen bonding residue phenylalanine rather than alanine to most closely maintain the steric impact of the Tyr residue. Second, all mutations are symmetric, *e.g.*, in the case of the S42A mutation, the Ser42 from chain A and chain B are both mutated to alanine.

The data in Table 6.1 indicate that there is little structural change on the other significant dimer interface contacts when a single point mutation is made. Indeed, massive structural changes are not expected on the basis of previous spectroscopic experiments.[189] Thus, given these structural similarities, analysis of the chain A:chain B interaction with molecular mechanics methods (Amber94 force field[199]) was deemed prudent. To further enhance the reliability of the simulations, the dimer interface interaction energies (ΔE_{dimer}) are indexed relative to that of the wild-type enzyme (ΔE_{rel}). These data are summarized in Table 6.2.

Table 6.2. Chain A:Chain B Interaction Energies: Wild-Type versus Mutant *hGS*

Enzyme[a]	ΔE_{dimer}[b]	ΔE_{rel}[c]
WT	-391.464	0
S42A	-387.674	4
Y47F	-374.599	17
E43A	-336.624	55
R221A	-273.924	118
D24A	-237.221	154

[a] WT = wild-type *hGS*; for others, the single point mutation is designated by the original residue then the residue number and finally the residue (alanine) to which the residue was mutated to.

[b] Interaction energy (kcal/mol) between chain A and chain B of dimeric *hGS* calculated with Amber94 force field.[199]

[c] This is ΔE_{dimer} (kcal/mol) for the mutant *hGS* relative to wild-type *hGS*.[199]

From the analysis thus far, it is hypothesized that mutation of Ser43, Tyr47, Glu43, Arg221 and Asp24 to residues incapable of participating in hydrogen-bonding and/or salt bridges (in the case of Asp24 and Arg221) will weaken the dimer interface interaction of *hGS*. These hypotheses are supported by the data in Table 6.2. Mutation of Ser42 to alanine leaves the dimer binding energy essentially unchanged (ΔE_{rel} = 4

kcal/mol) as compared to wild-type *hGS*. Tyr47, like Ser42, participates in a single hydrogen-bonding interaction across the dimer interface. The *ab initio* calculated interaction energies (Figure 6.5) suggest that the contact involving Tyr47 is stronger than that involving Ser42, as does the shorter distance (2.6 versus 2.9 Å, Table 6.1) found in the crystal structure of 2HGS. Mutation of Tyr47 yields minimal changes on the dimer interaction energy when mutated to phenylalanine (ΔE_{rel} = 17 kcal/mol), but the effect of the Y47F mutation is more substantial than that that realized by S42A mutation (ΔE_{rel} = 4 kcal/mol).

Mutation of the Glu43 residue on the dimer interface interaction is expected to be more significant than the mutations of Ser42 and Tyr47 given the negative charge on the glutamate residue. Also, Glu43 participates in a short, strong 2.6 Å hydrogen bond, Table 6.1. The data in Table 6.2 corroborate such predictions, yielding a ΔE_{rel} = 53 kcal/mol for E43A mutation, a value much larger than the S42A and Y47F mutations just discussed.

The final two single point mutations investigated by simulation are R221A and D24A.[204] Both of these modifications are expected to abolish the Arg221•••Asp24 salt bridge in wild-type *hGS*. Also, the mutation of Asp24 is expected to be most consequential since it also participates in a strong hydrogen bond with Ser42. These suppositions are supported by the dimer interaction energies. The dimer binding energy is weakened by 118 kcal/mol relative to the wild-type dimer upon R221A mutation. The effect of D24A mutation on weakening of the dimer interaction is ~40% higher than the R221A mutation, ΔE_{rel} = 154 kcal/mol.

6.3.4 Possible Avenues for Active Site Interactions

The active site for *hGS* is "buried" in each of the monomer units. The active sites are ~50 Å separated using the Mg_A•••Mg_B distances as a metric. Thus, the active site is ~25 Å away from the dimer interface. Negative cooperativity implies that a binding event in one subunit affects the other active site in a different subunit in a conformational and energetic sense. Hence, the question arises, what residues provide a possible line of communication between the two *hGS* active sites? To probe this issue, an active site analysis of the *hGS* dimer is undertaken. The technique finds "voids" in the enzyme and is routinely used in drug design to isolate likely receptor sites.[197,198] In the present research, the active site analysis is employed to answer the question – are there amino residues in dimeric *hGS* that are close to both the active site and the dimer interface residues?

The site finder technique excludes solvent molecules (water) and ligands (two Mg^{2+}, GS, ADP and phosphate) in its analysis. Hence, it is not surprising that the ATP-binding sites (since *hGS* is a dimer each active site found occurs in pairs) are the largest sites found. The ATP-binding site is surrounded by, among other residues, the four conserved residues indicated in previous studies of *hGS* and other ATP-Grasp superfamily of enzymes, *viz.* Glu144, Asn146, Lys305 and Lys364 (see Figure 6.1). Other notable residues nearest to the ATP-binding sites are residues from the S-loop (Arg267, Tyr270, Met271 and Arg273), G-loop (Arg367, Glu368, Gly369, Gly370, Gly371, Asn372 and Asn373) and the A-loop (all residues from Ile454 through Ala463 as well as Ala466).

The largest active site in *hGS* is intrachain (*i.e.*, no close contacts exist between residues in chain A and chain B of 2HGS), which is expected given their large separation distance. What is more interesting, however, are the four pairs of sites identified as *interchain*. Only two of the sites identified by the software are close to residues in the vicinity of the active site, and close to residues at the dimer interface. In both of these cases, these residues are from the A-loop. Specifically, these A-loop residues are Glu455, His456, Val461, Ala462, Gly464 and Val465. These sites, the A-loop and dimer interface are plotted in (Figure 6.6).

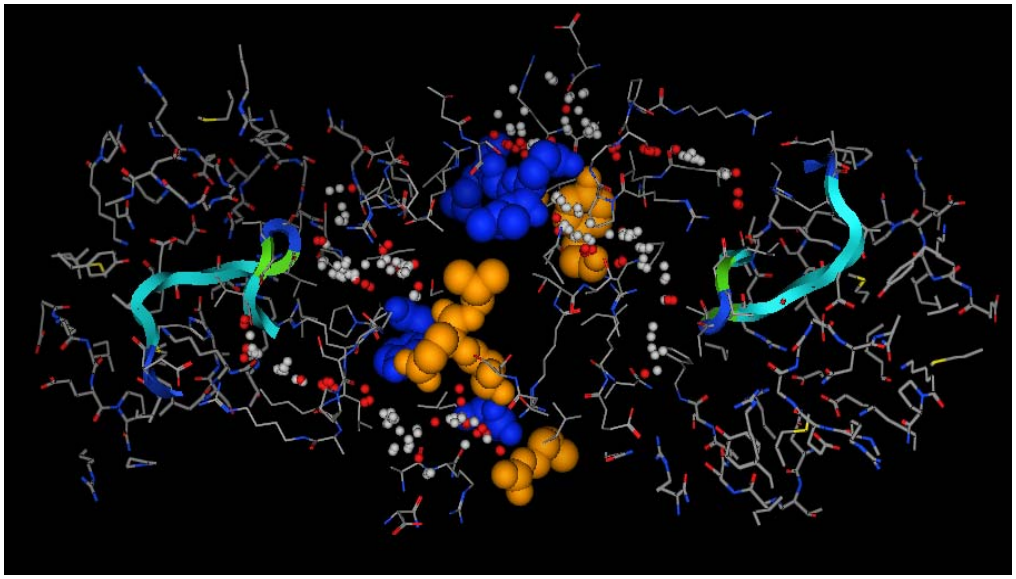

Figure 6.6. Important dimer interface residues Asp24, Ser42, Glu43, Val44, Val45, Tyr47, Arg221 (blue = chain 1; orange = chain 2). The A-loop backbone is shown as a ribbon. Alpha spheres are shown for important intrachain sites; alpha spheres for the ATP-Grasp binding site are not shown.

In summary, important amino acid interactions at the dimer interface of human glutathione synthetase, along with possible mechanisms by which the *ca.* 50 Å separated active sites communicate across the dimer interface were investigated. Computational techniques were utilized to probe the nature of negative cooperativity in

hGS. Analysis of dimeric *hGS* was initiated by looking for strong contacts between chain A amino acids and chain B amino acids across the dimer interface of 2HGS. Pairs of five residues (Asp24, Ser42, Glu43, Tyr47, and Arg221 in both chains A and B of *hGS*) with the most significant bonding across the dimer interface were found. Seven residues participate in the five significant dimer interface interactions (Ser42•••Asp24, Tyr47•••Glu43, Arg221•••Asp24, $Val44_A$•••$Val44_B$ and $Val45_A$•••$Val45_B$) with subscripts denoting which chain the residue belongs to. For the salt bridge (Arg221•••Asp24) the calculated binding energy is double the binding energy of the hydrogen bonds in aqueous environment, suggesting that on the basis of its close distance and strong interaction energy that this contact is the most substantial across the dimer interface of *hGS*. Asp24 participates in both a strong salt bridge with Arg221, and a strong hydrogen bond with Ser42. Hence, Asp24 is the most interesting target for site directed mutagenesis experiments, and its mutation is expected to engender more substantial changes to hGS than the other interactions at the dimer interface. The analysis of protein contacts and *ab initio* studies of amino acid models has indicated several profitable targets for site directed mutagenesis, both experiments and simulations. The structural and energetic data thus far accumulated indicate that the interchain interactions can be prioritized as follows in terms of their expected impact on *hGS*: Arg221•••Asp24 > Ser42•••Asp24 ~ Tyr47•••Glu43 > $Val44_A$•••$Val44_B$ ~ $Val45_A$•••$Val45_B$. Experimental studies by the group of Anderson (Texas Woman's University, Department of Chemistry) are currently underway to further support the above mentioned findings in *hGS*.

ENDNOTES

1 Hunter, T. *Cell.* 1995, 80, 225.

2 Clark, J. H.; Macquarrie, D. J. *Chem. Soc. Rev.* 1996, 25, 303.

3 Trost, B. M. *Acc. Chem. Res*. 2002, 35, 695.

4 Sanford, M. S.; Ulman, M.; Grubbs, R. H. *J. Am. Chem. Soc*. 2001,123, 749.

5 Trnka, T. M.; Grubbs, R. H. *Acc. Chem. Res*. 2001, 34, 18.

6 Louie, J.; Grubbs, R. H. *Organometallics*. 2002, 21, 2153.

7 Lail, M.; Bell, C. M.; Cundari, T. R.; Corner, D.; Gunnoe, T. B.; Petersen, J. L. *Organometallics*. 2004, 23, 5007.

8 Lail, M.; Arrowood, B. N.; Gunnoe, T. B. *J. Am. Chem. Soc*. 2003, 125, 7506.

9 Pittard, K. A.; Lee, J. P.; Cundari, T. R.; Gunnoe, T. B.; Petersen, J. L. *Organometallics*. 2004, 23, 5514.

10 Halpern, J. *Inorg. Chim. Acta* 1982, 62, 31.

11 Halpern, J. *Acc. Chem. Res.* 1982, 15, 332.

12 Vollhardt, K. P. C.; Cammack, J. K.; Matzger, A. J.; Bauer, A.; Capps, K. B.; Hoff, C. D. *Inorg. Chem.* 1999, 38, 2624.

13 Heyduk, A. F.; Nocera, D. G. *J. Am. Chem. Soc.* 2000, 122, 9415.

14 Riordan, C. G.; Halpern, J. *Inorg. Chim. Acta*. 1996, 243, 19.

15 Ng, F. T. T.; Rempel, G. L.; Mancuso, C.; Halpern, J. *Organometallics*. 1990, 9, 2762.

16 Collman, J. P.; McElwee-White, L.; Brothers, P. J.; Rose, E. *J Am. Chem. Soc*. 1986, 108, 1332.

17 Tilset, M.; Fjeldahl, I.; Hamon, J.-R.; Hamon, P.; Toupet, L.; Saillard, J.-Y.; Costuas, K.; Haynes, A. *J. Am. Chem. Soc*. 2001, 123, 9984.

18 Sherry, A. E.; Wayland, B. B. *J. Am. Chem. Soc.* 1990, 112, 1259.

19 Cui, W.; Zhang, X. P.; Wayland, B. B. *J. Am. Chem. Soc.* 2003, 125, 4994.

20 Arrowood, B. N.; Lail, M.; Gunnoe, T. B.; Boyle, P. D. *Organometallics*. 2003, 22, 4692.

21 Labinger, J. A.; Bercaw, J. E. *Nature* 2002, 417, 507.

22 Arndtsen, B. A.; Bergman, R. G.; Mobley, T. A.; Peterson, T. H. *Acc.Chem. Res.* 1995, 28, 154.

23 Jones, W. D.; Feher, F. J. *Acc. Chem. Res*. 1989, 22, 91.

24 Crabtree, R. H. *Chem. Rev*. 1985, 85, 245.

25 Crabtree, R. H. *Chem. Rev*. 1995, 95, 987.

26 Goldberg, K. I.; Goldman, A. S. *Activation and Functionalization of C-H Bonds*; Oxford University Press: Washington, DC, 2004.

27 Crabtree, R. H. *J. Chem. Soc., Dalton Trans.* 2001, 2437.

28 Periana, R. A.; Bhalla, G.; William J. Tenn, I.; Young, K. J. H.; Liu, X. Y.; Mironov, O.; Jones, C.; Ziatdinov, V. R. *J. Mol. Catal. A: Chem.* 2004, 220, 7.

29 Labinger, J. A. *J. Mol. Catal. A: Chem.* 2004, 220, 27.

30 Tenaglia, A.; Heumann, A. *Angew. Chem., Int. Ed.* 1998, 38, 2180.

31 Dyker, G. *Handbook of C-H Transformations*; Wiley-VCH: Weinheim, 2005.

32 Ritleng, V.; Sirlin, C.; Pfeffer, M. *Chem. Rev*. 2002, 102, 1731.

33 Dyker, G. *Angew. Chem., Int. Ed.* 1999, 38, 1698.

34 Goj, L. A.; Gunnoe, T. B. *Curr. Org. Chem.* 2005, 9, 671.

35 Walsh, P. J.; Hollander, F. J.; Bergman, R. G. *J. Am. Chem. Soc.* 1988, 110, 8729.

36 Hoyt, H. M.; Michael, F. E.; Bergman, R. G. *J. Am. Chem. Soc.* 2004, 126, 1018.

37 Bennett, J. L.; Wolczanski, P. T. *J. Am. Chem. Soc.* 1997, 119, 10696.

38 Cummins, C. C.; Baxter, S. M.; Wolczanski, P. T. *J. Am. Chem. Soc.* 1988, 110, 8731.

39 Fulton, J. R.; Sklenak, S.; Bouwkamp, M. W.; Bergman, R. G. *J. Am.Chem. Soc.* 2002, 124, 4722.

52 Stevens, W. J.; Basch, H.; Krauss, M. *J. Chem. Phys.* 1984, 81, 6026; Stevens, W. J.; Krauss, M.; Basch, H.; Jasien, P. G. *Can. J. Chem.* 1992, 70, 612.

53 Cundari, T. R.; Klinckman, T. R.; Wolczanski, P. T. *J. Am. Chem. Soc.* 2002, 124, 1481.

54 Holland, P. L.; Cundari, T. R.; Perez, L. L.; Eckert, N. A.; Lachicotte, R. J. *J. Am. Chem. Soc.* 2002, 124, 14416.

55 Veige, A. S.; Slaughter, L. M.; Wolczanski, P. T.; Matsunaga, N.; Decker, S. A.; Cundari, T. R. *J. Am. Chem. Soc.* 2001, 123, 6419.

56 Bergman, R. G.; Cundari, T. R.; Gillespie, A. M.; Gunnoe, T. B.; Harman, W. D.; Klinckman, T. R.; Temple, M. D.; White, D. P. *Organometallics*. 2003, 22, 2331.

57 Vreven, T.; Morokuma, K. *J. Comp. Chem*. 2000, 21, 1419.

58 Rappé, A. K.; Casewit, C. J.; Colwell, K. S.; Goddard III, K. S.; Skiff, W. M. *J. Am. Chem. Soc*. 1992, 114, 10024.

59 Lazarou, Y. G.; Prosmitis, A. V.; Papadimitriou, V. C.; Papagiannakopoulos, P. *J. Phys. Chem. A*. 2001, 105, 6729.

60 Huheey, J. E. *Inorganic Chemistry: Principles of Structure and Reactivity*, 3rd ed.; Harper & Row: New York, 1983.

61 Simões, J. A. M.; Beauchamp, J. L. *Chem. Rev.* 1990, 90, 629.

62 Marks, T. J.; Gagne, M. R.; Nolan, S. P.; Schock, L. E.; Seyam, A.; Stern, D. *Pure Appl. Chem.* 1989, 61, 1665.

63 Marks, T. J. *Bonding Energetics in Organometallic Compounds*; American Chemical Society: Washington, DC, 1990; Vol. 428.

64 Hay, B. P.; Finke, R. G. *Polyhedron.* 1988, 7, 1469.

65 Hartwig, J. F. *Angew. Chem., Int. Ed.* 1998, 37, 2046.

66 Wolfe, J. P.; Wagaw, S.; Marcoux, J. F.; Buchwald, S. L. *Acc. Chem.Res.* 1998, 31, 805.

67 Mayer, J. M. *Acc. Chem. Res*. 1998, 31, 441.

68 Klei, S. R.; Golden, J. T.; Tilley, T. D.; Bergman, R. G. *J. Am. Chem.Soc.* 2002, 124, 2092.

69 Collman, J. P.; Hegedus, L. S.; Norton, J. R.; Finke, R. G. *Principles and Applications of Organotransition Metal Chemistry*; University Science: Mill Valley, CA, 1987.

70 Grubbs, R. H.; Chang, S. *Tetrahedron.* 1998, 54, 4413.

71 Grubbs, R. H. *Tetrahedron.* 2004, 60, 7117.

72 Nagashima, H.; Kondo, H.; Hayashida, T.; Yamaguchi, Y.; Gondo, M.; Masuda, S.; Miyazaki, K.; Matsubara, K.; Kirchner, K. *Coord. Chem. Rev.* 2003, 245, 177.

73 Aneetha, H.; Jime´nez-Tenorio, M.; Puerta, M. C.; Valerga, P.; Sapunov, V. N.; Schmid, R.; Kirchner, K.; Mereiter, K. *Organometallics*. 2002, 21, 5334.

74 Tenorio, M. J.; Puerta, M. C.; Valerga, P. *J. Organomet. Chem*. 2000, 609, 161.

75 Kolle, U.; Rietmann, C.; Raabe, G. *Organometallics*. 1997, 16, 3273.

76 Campion, B. K.; Heyn, R. H.; Tilley, T. D. *J. Chem. Soc., Chem.Commun*. 1988, 278.

77 Johnson, T. J.; Huffman, J. C.; Caulton, K. G. *J. Am. Chem. Soc*. 1992, 114, 2725.

78 Bickford, C. C.; Johnson, T. J.; Davidson, E. R.; Caulton, K. G. *Inorg. Chem*. 1994, 33, 1080.

79 Huang, J.; Stevens, E. D.; Nolan, S. P.; Petersen, J. L. *J. Am. Chem. Soc*. 1999, 121, 2674.

80 Huang, D.; Streib, W. E.; Eisenstein, O.; Caulton, K. G. *Angew. Chem.,Int. Ed. Engl.* 1997, 36, 2004.

81 Tenorio, M. J.; Tenorio, M. A. J.; Puerta, M. C.; Valerga, P. *Inorg. Chim. Acta*. 1997, 259, 77.

82 Baratta, W.; Herdtweck, E.; Rigo, P. *Angew. Chem., Int. Ed.* 1999, 38, 1629.

83 Tenorio, M. J.; Mereiter, K.; Puerta, M. C.; Valerga, P. *J. Am. Chem. Soc.* 2000, 122, 11230.

84 Huang, D.; Streib, W. E.; Bollinger, J. C.; Caulton, K. G.; Winter, R. F.; Scheiring, T. *J. Am. Chem. Soc.* 1999, 121, 8087.

85 Huang, D.; Bollinger, J. C.; Streib, W. E.; Folting, K.; Young, V., Jr.; Eisenstein, O.; Caulton, K. G. *Organometallics.* 2000, 19, 2281.

86 Watson, L. A.; Coalter, J. N., III; Ozerov, O. V.; Pink, M.; Huffman, J. C.; Caulton, K. G. *New J. Chem.* 2003, 263.

87 Watson, L. A.; Ozerov, O. V.; Pink, M.; Caulton, K. G. *J. Am. Chem. Soc.* 2003, 125, 8426.

88 Walstrom, A. N.; Watson, L. A.; Pink, M.; Caulton, K. G. *Organometallics.* 2004, 23, 4814.

89 Walstrom, A.; Pink, M.; Yang, X.; Tomaszewski, J.; Baik, M. H.; Caulton, K. G. *J. Am. Chem. Soc.* 2005, 127, 5330.

90 Gusev, D. G.; Madott, M.; Dolgushin, F. M.; Lyssenko, K. A.; Antipin, M. Y. *Organometallics.* 2000, 19, 1734.

91 van der Boom, M. E.; Iron, M. A.; Atasoylu, O.; Shimon, L. J. W.; Rozenberg, H.; Ben-David, Y.; Konstantinovski, L.; Martin, J. M. L.; Milstein, D. *Inorg. Chim. Acta.* 2004, 357, 1854.

92 Kulawiec, R. J.; Crabtree, R. H. *Coord. Chem. Rev.* 1990, 99, 89.

93 Arndtsen, B. A.; Bergman, R. G. *Science.* 1995, 270, 1970.

94 Butts, M. D.; Scott, B. L.; Kubas, G. J. *J. Am. Chem. Soc.* 1996, 118, 11831.

95 Huhmann-Vincent, J.; Scott, B. L.; Kubas, G. J. *J. Am. Chem. Soc.* 1998, 120, 6808.

96 Peng, T. S.; Winter, C. H.; Gladysz, J. A. *Inorg. Chem.* 1994, 33, 2534.

97 Colsman, M. R.; Newbound, T. D.; Marshall, L. J.; Noirot, M. D.; Miller, M. M.; Wulfsberg, G. P.; Frye, J. S.; Anderson, O. P.; Strauss, S. H. *J. Am. Chem. Soc.* 1990, 112, 2349.

98 Newbound, T. D.; Colsman, M. R.; Miller, M. M.; Wulfsberg, G. P.; Anderson, O. P.; Strauss, S. H. *J. Am. Chem. Soc.* 1989, 111, 3762.

99 Bown, M.; Waters, J. M. *J. Am. Chem. Soc.* 1990, 112, 2442.

100 Van Seggen, D. M.; Anderson, O. P.; Strauss, S. H. *Inorg. Chem.* 1992, 31, 2987.

101 Wu, F.; Dash, A. K.; Jordan, R. F. *J. Am. Chem. Soc.* 2004, 126, 15360.

102 Ben-Ari, E.; Gandelman, M.; Rozenberg, H.; Shimon, L. J. W.; Milstein, D. *J. Am. Chem. Soc.* 2003, 125, 4714.

103 Fryzuk, M. D.; Johnson, S. A. *Coord. Chem. Rev.* 2000, 200, 379.

104 Vigalok, A.; Kraatz, H. B.; Konstantinovski, L.; Milstein, D. *Chem. Eur. J.* 1997, 3, 253.

105 Ibers, J. A.; Mingos, D. M. P. *Inorg. Chem.* 1971, 10, 1035.

106 Hoffman, P. R.; Yoshida, T.; Okano, T.; Otsuka, S.; Ibers, J. A. *Inorg. Chem.* 1976, 15, 2462.

107 Thorn, D. L.; Tulip, T. H.; Ibers, J. A. *J. Chem. Soc., Dalton Trans.* 1979, 2022.

108 Gusev, D. G.; Lough, A. J. *Organometallics.* 2002, 21, 5091.

109 van der Boom, M. E.; Milstein, D. *Chem. Rev.* 2003, 103, 1759.

110 van der Boom, M. E.; Liou, S. Y.; Ben-David, Y.; Shimon, L. J. W.; Milstein, D. *J. Am. Chem. Soc.* 1998, 120, 6531.

111 Vigalok, A.; Ben-David, Y.; Milstein, D. *Organometallics.* 1996, 15, 1839.

112 Vigalok, A.; Milstein, D. *Organometallics.* 2000, 19, 2061.

113 Jensen, C. M. *Chem. Commun.* 1998, 2443.

114 Lee, D. W.; Kaska, W. C.; Jensen, C. M. *Organometallics.* 1998, 17, 1.

115 Gusev, D. G.; Dolgushin, F. M.; Antipin, M. Y. *Organometallics.* 2000, 19, 3429.

116 Abbenhuis, R. A. T. M.; del Rio, I.; Bergshoef, M. M.; Boersma, J.; Veldman, N.; Spek, A. L.; van Koten, G. *Inorg. Chem.* 1998, 37, 1749.

117 Scott, A. P.; Radom, L. *J. Phys. Chem.* 1996, 100(41), 16502.

118 Brookhart, M.; Green, M. L. H.; Wong, L. L. *Prog. Inorg. Chem.* 1988, 36, 1.

119 Brookhart, M.; Green, M. L. H. *J. Organomet. Chem.* 1983, 250, 395.

120 Hoover, J. F.; Stryker, J. M. *J. Am. Chem. Soc.* 1990, 112, 464.

121 Bergamini, P.; Costa, E.; Cramer, P.; Hogg, J.; Orpen, A. G.; Pringle, P. G. *Organometallics.* 1994, 13, 1058.

122 Trace, R. L.; Sanchez, J.; Yang, J.; Yin, J.; Jones, W. M. *Organometallics.*1992, 11, 1440.

123 Tan, K. L.; Bergman, R. G.; Ellman, J. A. *J. Am. Chem. Soc.* 2002, 124, 3202.

124 Cohen, R.; Rybtchinski, B.; Gandelman, M.; Rozenberg, H.; Martin, J. M. L.; Milstein, D. *J. Am. Chem. Soc.* 2003, 125, 6532.

125 Bruce, M. I. *Chem. Rev.* 1991, 91, 197.

126 Selegue, J. P. *Coord. Chem. Rev.* 248(15-16), 1543.

127 Lee, H. M.; Yao, J.; Jia, G. *Organometallics.* 1997, 16, 3927.

128 Jia, G.; Lee, H. M.; Xia, H. P.; Williams, I. D. *Organometallics.* 1996, 15, 5453.

129 Gusev, D. G.; Maxwell, T.; Dolgushin, F. M.; Lyssenko, M.; Lough, A. J. *Organometallics.* 2002, 21, 1095.

130 Wen, T. B.; Cheung, Y. K.; Yao, J.; Wong, W. T.; Zhou, Z. Y.; Jia, G. *Organometallics.* 2000, 19, 3803.

131 Laguna, A.; Laguna, M. *Coord. Chem. Rev.* 1999, 837, 193.

132 Irwin, M. D.; Abdou, H. E.; Mohamed, A. A.; Fackler, J. P., Jr. *Chem. Commun.* 2003, 2882.

133 (a) Dell'Amico, D. B.; Calderazzo, F.; Marchetti, F. *J. Chem. Soc. Dalton Trans.* 1976, 1829. (b) Dell'Amico, D. B.; Calderazzo, F.; Marchetti, F.; Merlino, S.; Perego, G. *J. Chem. Soc. Chem. Commun.* 1977, 31. (c) Dell'Amico, D. B.; Calderazzo, F.; Marchetti, F.; Merlino, S. *J. Chem. Soc. Dalton Trans.* 1982, 2257.

134 Herring, F. G.; Hwang, G.; Lee, K. C.; Mistry, F.; Phillips, P. S.; Willner, H.; Aubke, F. *J. Am. Chem. Soc.* 1992, 114, 1271.

135 McMillan, J. A. *Chem. Rev.* 1962, 62, 65 and references therein.

136 Schmidbaur, H.; Dash, K. C. *Adv. Inorg. Chem. Radiochem.* 1982, 25, 39.

137 (a) Petrenko, T.; Ray, K.; Wieghardt, K. E.; Neese, F.. *J. Am. Chem. Soc.* 2006, 128, 4422. (b) Ray, K.; Weyhermueller, T.; Neese, F.; Wieghardt, K. *Inorg. Chem.* 2005, 44, 5345. (c) Kay, K.; Weyhermueller, T.; Goossens, A.; Craje, M. W. J.; Wieghardt, K. *Inorg. Chem.* 2003, 42, 4082.

138 Schröder, D.; Brown, R.; Schwerdtfeger, P.; Wang, X. B.; Yang, X.; Wang, L. S.; Schwarz, H. *Angew. Chem. Int. Ed.* 2003, 42, 311.

139 Blackmore, I. J.; Bridgeman, A. J.; Harris, N.; Holdaway, M. A.; Rooms, J. F.; Thompson, E. L. Young, N. A. *Angew. Chem. Int. Ed.* 2005, 44, 6746.

140 Schwerdtfeger, P.; Boyd, P. D. W.; Brienne, S.; Burrell, A. K. *Inorg. Chem*. 1992, 31, 3411.

141 Schlupp, R. L.; Maki, A. H. *Inorg. Chem.* 1974, 13, 44. See footnote 40.

142 Vänngard, T.; Kerström, S. A. *Nature* 1959, 184,183.

143 Bergendahl, T. J.; Bergendahl, E. M.; *Inorg. Chem.* 1972, 11, 638..

144 Warren, L. F.; Hawthorne, M. F. *J. Am. Chem. Soc.* 1968, 90*,* 4823.

145 (a) MacCragh, A,; Koski, W. S. *J. Am. Chem. Soc.* 1963, 85, 2375. (b) MacCragh, A.; Koski, W. S. *J. Am. Chem. Soc.* 1965, 87, 2496.

146 See also Waters, J. H.; Gray, H. B. *J. Am. Chem. Soc.* 1965, 87, 3534 and Elder, S. H.; Lucier, G. M.; Hollander, F. J.; Bartlett, N. *J. Am. Chem. Soc.* 1997, 119, 1020.

147 Johnson, W. M.; Dev, R.; Cady, G. H. *Inorg. Chem.* 1972, 11, 2260.

148 Seidel, S.; Seppelt, K. *Science.* 2000, 290, 117.

149 Eustis, S.; Hsu, H-Y.; El-Sayed, M. A.; *J. Phys. Chem. Let. B.* 2005, 109, 4811 and references therein.

150 Walker, N.; Wright, R.; Barren, P.; Murrell, J,; Stace. A. *J. Am. Chem. Soc*. 2001, 123, 4223.

151 Walker, N. R.; Wright, R. R.; Barran, P. E.; Stace, A. *J. Organometallics*. 1999, 18, 3569.

152 El-Sayed, I. H.; Huang, X.; El-Sayed, M. A. *Nano Lett.* 2005, 5, 829.

153 Caruso, R. A.; Ashokkumar, M.; Grieser, F. *Langmuir.* 2002, 18, 7831. See also Gachard, E.; Remita, H.; Khatouri, J.; Keita, B.; Nadjo, L.; Belloni, J*. New J. Chem.* 1998, 22, 1257.

154 Barakat, K. A.; Cundari, T. R.; Omary, M. A.; *J. Am. Chem. Soc*. 2003, 125, 14228. See also Barakat, K. A.; Cundari, T. R. *Chem. Phys.* 2005, 311, 3 for a brief analysis of disproportionation without ligand exchange (*i.e.*, 2 $^{2}[Au^{II}L_3] \rightarrow {}^{1}[Au^{I}L_3] + {}^{1}[Au^{III}L_3]$).

155 Sinha, P.; Wilson, A. K.; Omary, M. A. *J. Am. Chem. Soc.* 2005, 127, 12488.

156 Parr, R. G.; Yang. W. Density-functional Theory of Atoms and Molecules, Oxford Univ. Press, Oxford, (1989). Becke, A. D. *J. Chem. Phys*. 1993, 98, 5648. Burke, K.; Perdew, J. P.; Wang, Y. Electronic Density Functional Theory: Recent Progress and New Directions. Dobson, J. F.; Vignale, G.; Das, M. P., Eds. Plenum, New York, (1998).

157 Hay, P. J.; Wadt, W. R. *J. Chem. Phys*. 1985, 82, 270.

158 Pyykkö, P.; Mendizabal, F. *Inorg. Chem*. 1998, 37, 3018.

159 Couty, M.; Hall, M. B. *J. Comp. Chem*. 1996, 17, 1359.

160 Tomasi, J.; Mennucci, B.; Cammi, R. *Chem. Rev.* 2005, 105, 2999.

161 Korgaonkar, A. V.; Gopalaraman, C. P.; Rohatgi, V. K. *Int. J. Mass. Spec. Ion Phys*. 1981, 40, 127.

162 Eliav, E.; Kaldor, U.; Ishikawa, Y. *Phys. Rev. A.* 1994, 49, 1724.

163 Bartlett, R. J.; Stanton, J. F. *Rev. Comp. Chem.* 1995, 5, 65. Crawford, T. D.; Schaefer III, H. F. *Rev. Comp. Chem.* 2000, 14, 33.

164 For more sophisticated approaches to the issue of calculating the redox potentials and solvation spheres of metal ions see, for example, Uudsemaa, M.; Tamm, T. *J. Phys. Chem. A.* 2003, 107, 9997. Baik, M-H.; Freisner, R. A. *J. Phys. Chem. A.* 2002, 106, 7407. and Li, J.; Fisher, C. L.; Chen, J.; Bashford, D.; Noodleman, L. *Inorg. Chem.* 1996, 35, 4694.

165 Pyykkö, P. *Chem. Rev*. 1988, 88, 563.

166 Hay, P. J.; Wadt, W. R.; Kahn, L. R.; Bobrowicz, F. W. *J. Chem. Phys.* 1978, 69, 984.

167 Parr, R. G.; Yang, W. In *Density-functional Theory of Atoms and Molecules*, Oxford Univ. Press, Oxford, 1989.

168 Using the B3PW91/LANL2DZ(2f,d) level of theory, spin density on gold in *bis*(maleonitriledithiolato)-gold(II) dianion is calculated to be 18% by a Mulliken population analysis and 13% by a natural bond orbital analysis. Schlupp and Maki determine a value of 15% from an analysis of EPR spectra of magnetically dilute samples.

169 Correlation was likewise poor with the ionization potential calculated directly for the reaction: ^{1}Ligand → ^{2}Ligand^{+}.

170 Veige, A. S.; Slaughter, L. M.; Lobkovsky, E. B.; Wolczanski, P. T.; Matsunaga, N.; Decker, S. A.; Cundari, T. R. *Inorg. Chem.* 2003, 42, 6204.

171 Cundari, T. R. *Organometallics.* 1993, 12, 4971.

172 Eppley, D. F.; Wolczanski, P. T.; Van Duyne, G. D. *Angew. Chem. Int. Ed. Engl.* 1991, 30, 584-585.

173 Allen, F. H. *Acta Crystallogr.* 2002, B58, 380.

174 Burrell, A. K.; Clark, D. L.; Gordon, P. L.; Sattelberger, A. P.; Bryan, J. C. *J. Am. Chem. Soc.* 1994, 116, 3813.

175 Williams, D S.; Schofield, M. H.; Schrock, R. R.; Davis, W. M.; Anhaus, J. T. *J. Am. Chem. Soc.* 1991, 113, 5480.

176 (a) Bryan, J. C.; Burrell, A. K.; Benson, M. T.; Cundari, T. R.; Barrera, J.; Hall, K. A. in "Technetium in Chemistry and Nuclear Medicine," Nicolini, M.; Bandoli, G.; Mazzi, U. (Eds.) SGE Ditoriali, Padova, 1995. (b) Benson, M. T.; Bryan, J. C.; Burrell, A. K.; Cundari, T. R. *Inorg. Chem.* 1995, 34, 2348.

177 Robbins, J.; Bazan, G. C.; Murdzek, J. S.; O'Regan, M. B.; Schrock, R. R. *Organometallics.* 1991, 10, 2902.

178 Koshland, Jr., D. E. *Curr. Opinion Struct. Bio.* 1996, 6, 757.

179 Bohr, C.; Hasselbach, K. A.; Krogh A. *Skand. Arch. Physiol.* 1904, 16, 402. Quoted in Koshland, D. E. Jr.; Hamadani, K. *J. Biol. Chem.* 2002, 277*,* 46841.

180 Koshland, D. E.; Nemethy, G.; Filmer, D. Biochemistry 1966, 5, 365.

181 Monod, J.; Wyman, J.; Changeux, J. P. *J. Mol. Bio.* 1965, 12, 88.

182 Gutheil, W. G.; and McKenna, C. E. *Biophys. Chem.* 1992, 45, 171.

183 Gutheil, W. G. *Biophys. Chem.* 1992, 45, 181.

184 Gutheil, W. G. *Biophys. Chem.* 1994, 52, 83.

185 Abeliovich, H. *Biophys. J.* 2005, 89, 76.

186 Anderson, M. E. *Chemico-Biological Interactions* 1998, 111-112, 1.

187 Galperin, M. Y., and Koonin, E. V. *Protein Sci.* 1997, 6, 2639.

188 Camper, N. D.; Keese, R. J.; Coker, P. S. *J. Enviro. Sci. Health* 2004, B39, 665; Gossett, D. R.; Banks, S. W.; Millhollon, E. P.; Lucas, M. C. *Plant Physiol.* 1996, 112, 803.

189 Dinescu, A.; Cundari, T. R.; Bhansali, V. S.; Luo, J. L.; Anderson, M. E. *J. Biol. Chem.* 2004, 279, 22412.

190 Dinescu, A.; Anderson, M. E.; Cundari, T. R. *Biochem. Biophys. Res. Comm.* 2007, 353, 450.

191 Njalsson, R.; Norgren, S.; Larsson, A.; Huang, C. S.; Anderson, M. E.; Luo, J. L. *Biochem. Biophys. Res. Comm.* 2001, 289, 80.

192 Luo, J. L.; Huang, C. S.; Babaoglu, K.; Anderson, M. E. *Biochem. Biophys. Res. Comm.* 2000, 275, 577.

193 Polekhina, G.; Board, P. C.; Gali, R.; Rossjohn, J.; Parker, M. W. *EMBO J.* 1999, 12, 3204.

194 Guex, N.; Peitsch, M. C. *Electrophoresis.* 1997, 18, 2714.

195 Sobolev, S.; Sorokine, A.; Prilusky, A.; Abola, E. E.; Edelman, M. *Bioinformatics.* 1999, 15, 327.

196 MOE (Molecular Operating Environment) Chemical Computing Group Inc., http://www.chemcomp.com.

197 Liang J.; Edelsbrunner H.; Fu P.; Sudhakar P. V.; Subramaniam S. *Proteins.* 1998, 33, 1.

198 Liang J.; Edelsbrunner H.; Fu P.; Sudhakar P. V.; Subramaniam S. *Proteins.* 1998, 33, 18.

199 Cornell, W. D.; Cieplak, P.; Bayly, C. I.; Gould, I. R.; Merz, K. M., Jr.; Ferguson, D. M.; Spellmeyer, D. C.; Fox, T.; Caldwell, J. W.; Kollman, P. A. *J. Am. Chem. Soc.* 1995, 117, 5179.

200 Schmidt, M. W.; Baldridge, K. K.; Boatz, J. A.; Elbert, S. T.; Gordon, M. S.; Jensen, J. J.; Koseki, S.; Matsunaga, N.; Nguyen, K. A.; Su, S.; Windus, T. L.; Dupuis, M., and Montgomery, J. A. *J. Comput. Chem.* 1993, 14, 1347.

201 Hehre, W. J.; Ditchfield, R.; Pople, J. A. *J. Chem. Phys.* 1972, 56, 2257. Francl, M. M.; Petro, W. J.; Hehre, W. J.; Binkley, J. S.; Gordon, M. S.; DeFrees, D. J.; Pople, J. A. *J. Chem. Phys.* 1982, 77, 3654.

202 Jensen, J. H. – personal communication.

40 Collman, J. P.; Hegedus, L. S.; Norton, J. R.; Finke, R. G. *Principles and Applications of Organotransition Metal Chemistry*; University Science: Mill Valley, CA, 1987.

41 Crabtree, R. H. *The Organometallic Chemistry of the Transition Metals*, 2nd ed.; John Wiley and Sons: New York, 1994.

42 Conner, D.; Jayaprakash, K. N.; Cundari, T. R.; Gunnoe, T. B. *Organometallics* 2004, 23, 2724.

43 Zhang, J.; Gunnoe, T. B.; Boyle, P. D. *Organometallics.* 2004, 23, 3094.

44 Zhang, J.; Gunnoe, T. B.; Petersen, J. L. *Inorg. Chem.* 2005, 44, 2895.

45 Lail, M.; Gunnoe, T. B.; Barakat, K. A.; Cundari, T. R. *Organometallics*. 2005, 24, 1301.

46 Feng, Y.; Lail, M.; Barakat, K. A.; Cundari, T. R.; Gunnoe, T. B.; Petersen, J. L. *J. Am. Chem. Soc.* 2005, 127, 14174.

47 Zhang, J.; Barakat, K. A.; Cundari, T. R.; Gunnoe, T. B.; Boyle, P. D.; Petersen, J. L.; Day, C. S. *Inorg. Chem*. 2005, 44, 8379.

48 Feng, Y.; Lail, M.; Foley, N. A.; Gunnoe, T. B.; Barakat, K. A.; Cundari, T. R.; Petersen, J. L. *J. Am. Chem. Soc*. 2006, 128, 7982.

49 Frisch, M. J.; Trucks, G. W.; Schlegel, H. B.; Scuseria, G. E.; Robb, M. A.; Cheeseman, J. R.; Zakrzewski, V. G.; Montgomery, Jr., J. A.; Stratmann, R. E.; Burant, J. C.; Dapprich, S.; Millam, J. M.; Daniels, A. D.; Kudin, K. N.; Strain, M. C.; Farkas, O.; Tomasi, J.; Barone, V.; Cossi, M.; Cammi, R.; Mennucci, B.; Pomelli,C.; Adamo, C.; Clifford, S.; Ochterski, J.; Petersson, G. A.; Ayala, P. Y.; Cui, Q.; Morokuma, K.; Rega, N.; Salvador, P.; Dannenberg, J. J.; Malick, D. K.; Rabuck, A. D.; Ragavachari, K.; Foresman, J. B.; Cioslowski, J.; Ortiz, J. V.; Baboul, A. G.; Stefanov, B. B.; Liu, G.; Liashenko, A.; Piskorz, P.; Komaromi, I.; Gomperts, R.; Martin, R. L.; Fox, D. J.; Keith, T.; Al-Laham, M. A.; Peng, C. Y.; Nanayakkara, A.; Challacombe, M.; Gill, P. M. W.; Johnson, B.; Chen, W.; Wong, M. W.; Andres, J. L.; Gonzalez, C.; Head-Gordon, M.; Replogle, E. S.; Pople, J. A. Gaussian 98, Revision A.11.3. , Gaussian, Inc., Pittsburgh PA 2002.

50 Parr, R. G.; Yang, W. *Density-functional Theory of Atoms and Molecules*, Oxford Univ. Press, Oxford, 1989.

51 (a) Becke, A. D. *Phys*. *Rev.* 1998, A38, 3098. (b) Becke, A. D. *J. Chem. Phys*. 1993, 98, 1372. (c) Becke, A. D. *J. Chem. Phys*. 1993, 98, 5648; Lee, C.; Yang, W.; Parr, R. G. *Phys. Rev.* 1998, B37, 785.

203 Many researchers have discussed the suitability of density functional theory for describing weak nonbonded (van der Waals, London dispersion forces, *etc.*) interactions such as are expected in hydrophobic interactions. So, these calculations must be viewed as approximate.

204 Given the small magnitude of the Val…Val interactions, mutation of these residues was not pursued.

REFERENCES

Abbenhuis, R. A. T. M.; del Rio, I.; Bergshoef, M. M.; Boersma, J.; Veldman, N.; Spek, A. L.; van Koten, G. *Inorg. Chem.* 1998, 37, 1749.

Abeliovich, H. *Biophys. J.* 2005, 89, 76.

Allen, F. H. *Acta Crystallogr.* 2002, B58, 380.

Anderson, M. E. *Chemico-Biological Interactions* 1998, 111-112, 1.

Aneetha, H.; Jime´nez-Tenorio, M.; Puerta, M. C.; Valerga, P.; Sapunov, V. N.; Schmid, R.; Kirchner, K.; Mereiter, K. *Organometallics*. 2002, 21, 5334.

Arndtsen, B. A.; Bergman, R. G. *Science.* 1995, 270, 1970.

Arndtsen, B. A.; Bergman, R. G.; Mobley, T. A.; Peterson, T. H. *Acc.Chem. Res.* 1995, 28, 154.

Arrowood, B. N.; Lail, M.; Gunnoe, T. B.; Boyle, P. D. *Organometallics*. 2003, 22, 4692.

Baik, M-H.; Freisner, R. A. *J. Phys. Chem. A.* 2002, 106, 7407.

Barakat, K. A.; Cundari, T. R. *Chem. Phys.* 2005, 311, 3.

Barakat, K. A.; Cundari, T. R.; Omary, M. A.; *J. Am. Chem. Soc*. 2003, 125, 14228.

Baratta, W.; Herdtweck, E.; Rigo, P. *Angew. Chem., Int. Ed.* 1999, 38, 1629.

Bartlett, R. J.; Stanton, J. F. *Rev. Comp. Chem.* 1995, 5, 65.

Becke, A. D. *Phys*. *Rev.* 1998, A38, 3098.

Becke, A. D. *J. Chem. Phys*. 1993, 98, 1372.

Becke, A. D. *J. Chem. Phys*. 1993, 98, 5648.

Ben-Ari, E.; Gandelman, M.; Rozenberg, H.; Shimon, L. J. W.; Milstein, D. *J. Am. Chem. Soc.* 2003, 125, 4714.

Bennett, J. L.; Wolczanski, P. T. *J. Am. Chem. Soc.* 1997, 119, 10696.

Benson, M. T.; Bryan, J. C.; Burrell, A. K.; Cundari, T. R. *Inorg. Chem.* 1995, 34, 2348.

Bergamini, P.; Costa, E.; Cramer, P.; Hogg, J.; Orpen, A. G.; Pringle, P. G. *Organometallics.* 1994, 13, 1058.

Bergendahl, T. J.; Bergendahl, E. M.; *Inorg. Chem.* 1972, 11, 638.

Bergman, R. G.; Cundari, T. R.; Gillespie, A. M.; Gunnoe, T. B.; Harman, W. D.; Klinckman, T. R.; Temple, M. D.; White, D. P. *Organometallics*. 2003, 22, 2331.

Bickford, C. C.; Johnson, T. J.; Davidson, E. R.; Caulton, K. G. *Inorg. Chem*. 1994, 33, 1080.

Blackmore, I. J.; Bridgeman, A. J.; Harris, N.; Holdaway, M. A.; Rooms, J. F.; Thompson, E. L. Young, N. A. *Angew. Chem. Int. Ed.* 2005, 44, 6746.

Bohr, C.; Hasselbach, K. A.; Krogh A. *Skand. Arch. Physiol.* 1904, 16, 402. Quoted in Koshland, D. E. Jr.; Hamadani, K. *J. Biol. Chem.* 2002, 277*,* 46841.

Bown, M.; Waters, J. M. *J. Am. Chem. Soc.* 1990, 112, 2442.

Brookhart, M.; Green, M. L. H. *J. Organomet. Chem.* 1983, 250, 395.

Brookhart, M.; Green, M. L. H.; Wong, L. L. *Prog. Inorg. Chem.* 1988, 36, 1.

Bruce, M. I. *Chem. Rev.* 1991, 91, 197.

Bryan, J. C.; Burrell, A. K.; Benson, M. T.; Cundari, T. R.; Barrera, J.; Hall, K. A. in "Technetium in Chemistry and Nuclear Medicine," Nicolini, M.; Bandoli, G.; Mazzi, U. (Eds.) SGE Ditoriali, Padova, 1995.

Burke, K.; Perdew, J. P.; Wang, Y. Electronic Density Functional Theory: Recent Progress and New Directions. Dobson, J. F.; Vignale, G.; Das, M. P., Eds. Plenum, New York, (1998).

Burrell, A. K.; Clark, D. L.; Gordon, P. L.; Sattelberger, A. P.; Bryan, J. C. *J. Am. Chem. Soc.* 1994, 116, 3813.

Butts, M. D.; Scott, B. L.; Kubas, G. J. *J. Am. Chem. Soc.* 1996, 118, 11831.

Camper, N. D.; Keese, R. J.; Coker, P. S. *J. Enviro. Sci. Health* 2004, B39, 665.

Campion, B. K.; Heyn, R. H.; Tilley, T. D. *J. Chem. Soc., Chem.Commun*. 1988, 278.

Caruso, R. A.; Ashokkumar, M.; Grieser, F. *Langmuir.* 2002, 18, 7831.

Clark, J. H.; Macquarrie, D. J. *Chem. Soc. Rev.* 1996, 25, 303.

Cohen, R.; Rybtchinski, B.; Gandelman, M.; Rozenberg, H.; Martin, J. M. L.; Milstein, D. *J. Am. Chem. Soc.* 2003, 125, 6532.

Collman, J. P.; Hegedus, L. S.; Norton, J. R.; Finke, R. G. *Principles and Applications of Organotransition Metal Chemistry*; University Science: Mill Valley, CA, 1987.

Collman, J. P.; McElwee-White, L.; Brothers, P. J.; Rose, E. *J Am. Chem. Soc*. 1986, 108, 1332.

Colsman, M. R.; Newbound, T. D.; Marshall, L. J.; Noirot, M. D.; Miller, M. M.; Wulfsberg, G. P.; Frye, J. S.; Anderson, O. P.; Strauss, S. H. *J. Am. Chem. Soc.* 1990, 112, 2349.

Conner, D.; Jayaprakash, K. N.; Cundari, T. R.; Gunnoe, T. B. *Organometallics* 2004, 23, 2724.

Cornell, W. D.; Cieplak, P.; Bayly, C. I.; Gould, I. R.; Merz, K. M., Jr.; Ferguson, D. M.; Spellmeyer, D. C.; Fox, T.; Caldwell, J. W.; Kollman, P. A. *J. Am. Chem. Soc.* 1995, 117, 5179.

Couty, M.; Hall, M. B. *J. Comp. Chem*. 1996, 17, 1359.

Crabtree, R. H. *J. Chem. Soc., Dalton Trans.* 2001, 2437.

Crabtree, R. H. *Chem. Rev*. 1995, 95, 987.

Crabtree, R. H. *The Organometallic Chemistry of the Transition Metals*, 2nd ed.; John Wiley and Sons: New York, 1994.

Crabtree, R. H. *Chem. Rev*. 1985, 85, 245.

Crawford, T. D.; Schaefer III, H. F. *Rev. Comp. Chem.* 2000, 14, 33.

Cui, W.; Zhang, X. P.; Wayland, B. B. *J. Am. Chem. Soc.* 2003, 125, 4994.

Cummins, C. C.; Baxter, S. M.; Wolczanski, P. T. *J. Am. Chem. Soc.* 1988, 110, 8731.

Cundari, T. R. *Organometallics.* 1993, 12, 4971.

Cundari, T. R.; Klinckman, T. R.; Wolczanski, P. T. *J. Am. Chem. Soc.* 2002, 124, 1481.

Dell'Amico, D. B.; Calderazzo, F.; Marchetti, F. *J. Chem. Soc. Dalton Trans.* 1976, 1829.

Dell'Amico, D. B.; Calderazzo, F.; Marchetti, F.; Merlino, S. *J. Chem. Soc. Dalton Trans.* 1982, 2257.

Dell'Amico, D. B.; Calderazzo, F.; Marchetti, F.; Merlino, S.; Perego, G. *J. Chem. Soc. Chem. Commun.* 1977, 31.

Dinescu, A.; Anderson, M. E.; Cundari, T. R. *Biochem. Biophys. Res. Comm.* 2007, 353, 450.

Dinescu, A.; Cundari, T. R.; Bhansali, V. S.; Luo, J. L.; Anderson, M. E. *J. Biol. Chem.* 2004, 279, 22412.

Dyker, G. *Handbook of C-H Transformations*; Wiley-VCH: Weinheim, 2005.

Dyker, G. *Angew. Chem., Int. Ed.* 1999, 38, 1698.

Elder, S. H.; Lucier, G. M.; Hollander, F. J.; Bartlett, N. *J. Am. Chem. Soc.* 1997, 119, 1020.

Eliav, E.; Kaldor, U.; Ishikawa, Y. *Phys. Rev. A.* 1994, 49, 1724.

El-Sayed, I. H.; Huang, X.; El-Sayed, M. A. *Nano Lett.* 2005, 5, 829.

Eppley, D. F.; Wolczanski, P. T.; Van Duyne, G. D. *Angew. Chem. Int. Ed. Engl.* 1991, 30, 584-585.

Eustis, S.; Hsu, H-Y.; El-Sayed, M. A.; *J. Phys. Chem. Let. B.* 2005, 109, 4811.

Feng, Y.; Lail, M.; Barakat, K. A.; Cundari, T. R.; Gunnoe, T. B.; Petersen, J. L. *J. Am. Chem. Soc.* 2005, 127, 14174.

Feng, Y.; Lail, M.; Foley, N. A.; Gunnoe, T. B.; Barakat, K. A.; Cundari, T. R.; Petersen, J. L. *J. Am. Chem. Soc*. 2006, 128, 7982.

Francl, M. M.; Petro, W. J.; Hehre, W. J.; Binkley, J. S.; Gordon, M. S.; DeFrees, D. J.; Pople, J. A. *J. Chem. Phys.* 1982, 77, 3654.

Frisch, M. J; et al. Gaussian 98, Revision A.11.3. , Gaussian, Inc., Pittsburgh PA 2002.

Fryzuk, M. D.; Johnson, S. A. *Coord. Chem. Rev.* 2000, 200, 379.

Fulton, J. R.; Sklenak, S.; Bouwkamp, M. W.; Bergman, R. G. *J. Am.Chem. Soc.* 2002, 124, 4722.

Gachard, E.; Remita, H.; Khatouri, J.; Keita, B.; Nadjo, L.; Belloni, J*. New J. Chem.* 1998, 22, 1257.

Galperin, M. Y., and Koonin, E. V. *Protein Sci.* 1997, 6, 2639.

Goj, L. A.; Gunnoe, T. B. *Curr. Org. Chem.* 2005, 9, 671.

Goldberg, K. I.; Goldman, A. S. *Activation and Functionalization of C-H Bonds*; Oxford University Press: Washington, DC, 2004.

Gossett, D. R.; Banks, S. W.; Millhollon, E. P.; Lucas, M. C. *Plant Physiol.* 1996*,* 112*,* 803*.*

Grubbs, R. H. *Tetrahedron.* 2004, 60, 7117.

Grubbs, R. H.; Chang, S. *Tetrahedron.* 1998, 54, 4413.

Guex, N.; Peitsch, M. C. *Electrophoresis.* 1997, 18, 2714.

Gusev, D. G.; Dolgushin, F. M.; Antipin, M. Y. *Organometallics.* 2000, 19, 3429.

Gusev, D. G.; Lough, A. J. *Organometallics.* 2002, 21, 5091.

Gusev, D. G.; Madott, M.; Dolgushin, F. M.; Lyssenko, K. A.; Antipin, M. Y. *Organometallics.* 2000, 19, 1734.

Gusev, D. G.; Maxwell, T.; Dolgushin, F. M.; Lyssenko, M.; Lough, A. J. *Organometallics.* 2002, 21, 1095.

Gutheil, W. G. *Biophys. Chem.* 1994, 52, 83.

Gutheil, W. G. *Biophys. Chem.* 1992, 45, 181.

Gutheil, W. G.; and McKenna, C. E. *Biophys. Chem.* 1992, 45, 171.

Halpern, J. *Inorg. Chim. Acta* 1982, 62, 31.

Halpern, J. *Acc. Chem. Res.* 1982, 15, 332.

Hartwig, J. F. *Angew. Chem., Int. Ed.* 1998, 37, 2046.

Hay, B. P.; Finke, R. G. *Polyhedron.* 1988, 7, 1469.

Hay, P. J.; Wadt, W. R. *J. Chem. Phys*. 1985, 82, 270.

Hay, P. J.; Wadt, W. R.; Kahn, L. R.; Bobrowicz, F. W. *J. Chem. Phys.* 1978, 69, 984.

Hehre, W. J.; Ditchfield, R.; Pople, J. A. *J. Chem. Phys.* 1972, 56, 2257.

Herring, F. G.; Hwang, G.; Lee, K. C.; Mistry, F.; Phillips, P. S.; Willner, H.; Aubke, F. *J. Am. Chem. Soc.* 1992, 114, 1271.

Heyduk, A. F.; Nocera, D. G. *J. Am. Chem. Soc.* 2000, 122, 9415.

Hoffman, P. R.; Yoshida, T.; Okano, T.; Otsuka, S.; Ibers, J. A. *Inorg. Chem.* 1976, 15, 2462.

Holland, P. L.; Cundari, T. R.; Perez, L. L.; Eckert, N. A.; Lachicotte, R. J. *J. Am. Chem. Soc.* 2002, 124, 14416.

Hoover, J. F.; Stryker, J. M. *J. Am. Chem. Soc.* 1990, 112, 464.

Hoyt, H. M.; Michael, F. E.; Bergman, R. G. *J. Am. Chem. Soc.* 2004, 126, 1018.

Huang, D.; Bollinger, J. C.; Streib, W. E.; Folting, K.; Young, V., Jr.; Eisenstein, O.; Caulton, K. G. *Organometallics.* 2000, 19, 2281.

Huang, D.; Streib, W. E.; Bollinger, J. C.; Caulton, K. G.; Winter, R. F.; Scheiring, T. *J. Am. Chem. Soc.* 1999, 121, 8087.

Huang, D.; Streib, W. E.; Eisenstein, O.; Caulton, K. G. *Angew. Chem.,Int. Ed. Engl.* 1997, 36, 2004.

Huang, J.; Stevens, E. D.; Nolan, S. P.; Petersen, J. L. *J. Am. Chem. Soc*. 1999, 121, 2674.

Huheey, J. E. *Inorganic Chemistry: Principles of Structure and Reactivity*, 3rd ed.; Harper & Row: New York, 1983.

Huhmann-Vincent, J.; Scott, B. L.; Kubas, G. J. *J. Am. Chem. Soc.* 1998, 120, 6808.

Hunter, T. *Cell.* 1995, 80, 225.

Ibers, J. A.; Mingos, D. M. P. *Inorg. Chem.* 1971, 10, 1035.

Irwin, M. D.; Abdou, H. E.; Mohamed, A. A.; Fackler, J. P., Jr. *Chem. Commun.* 2003, 2882.

Jensen, C. M. *Chem. Commun.* 1998, 2443.

Jia, G.; Lee, H. M.; Xia, H. P.; Williams, I. D. *Organometallics.* 1996, 15, 5453.

Johnson, T. J.; Huffman, J. C.; Caulton, K. G. *J. Am. Chem. Soc*. 1992, 114, 2725.

Johnson, W. M.; Dev, R.; Cady, G. H. *Inorg. Chem.* 1972, 11, 2260.

Jones, W. D.; Feher, F. J. *Acc. Chem. Res*. 1989, 22, 91.

Kay, K.; Weyhermueller, T.; Goossens, A.; Craje, M. W. J.; Wieghardt, K. *Inorg. Chem.* 2003, 42, 4082.

Klei, S. R.; Golden, J. T.; Tilley, T. D.; Bergman, R. G. *J. Am. Chem.Soc.* 2002, 124, 2092.

Kolle, U.; Rietmann, C.; Raabe, G. *Organometallics*. 1997, 16, 3273.

Korgaonkar, A. V.; Gopalaraman, C. P.; Rohatgi, V. K. *Int. J. Mass. Spec. Ion Phys*. 1981, 40, 127.

Koshland, Jr., D. E. *Curr. Opinion Struct. Bio.* 1996, 6, 757.

Koshland, D. E.; Nemethy, G.; Filmer, D. Biochemistry 1966, 5, 365.

Kulawiec, R. J.; Crabtree, R. H. *Coord. Chem. Rev.* 1990, 99, 89.

Labinger, J. A. *J. Mol. Catal. A: Chem.* 2004, 220, 27.

Labinger, J. A.; Bercaw, J. E. *Nature* 2002, 417, 507.

Laguna, A.; Laguna, M. *Coord. Chem. Rev.* 1999, 837, 193.

Lail, M.; Arrowood, B. N.; Gunnoe, T. B. *J. Am. Chem. Soc*. 2003, 125, 7506.

Lail, M.; Bell, C. M.; Cundari, T. R.; Corner, D.; Gunnoe, T. B.; Petersen, J. L. *Organometallics*. 2004, 23, 5007.

Lail, M.; Gunnoe, T. B.; Barakat, K. A.; Cundari, T. R. *Organometallics*. 2005, 24, 1301.

Lazarou, Y. G.; Prosmitis, A. V.; Papadimitriou, V. C.; Papagiannakopoulos, P. *J. Phys. Chem. A*. 2001, 105, 6729.

Lee, C.; Yang, W.; Parr, R. G. *Phys. Rev.* 1998, B37, 785.

Lee, D. W.; Kaska, W. C.; Jensen, C. M. *Organometallics.* 1998, 17, 1.

Lee, H. M.; Yao, J.; Jia, G. *Organometallics.* 1997, 16, 3927.

Li, J.; Fisher, C. L.; Chen, J.; Bashford, D.; Noodleman, L. *Inorg. Chem.* 1996, 35, 4694.

Liang J.; Edelsbrunner H.; Fu P.; Sudhakar P. V.; Subramaniam S. *Proteins.* 1998, 33, 1.

Louie, J.; Grubbs, R. H. *Organometallics*. 2002, 21, 2153.

Luo, J. L.; Huang, C. S.; Babaoglu, K.; Anderson, M. E. *Biochem. Biophys. Res. Comm.* 2000, 275, 577.

MacCragh, A.; Koski, W. S. *J. Am. Chem. Soc.* 1965, 87, 2496.

MacCragh, A,; Koski, W. S. *J. Am. Chem. Soc.* 1963, 85, 2375.

Marks, T. J. *Bonding Energetics in Organometallic Compounds*; American Chemical Society: Washington, DC, 1990; Vol. 428.

Marks, T. J.; Gagne, M. R.; Nolan, S. P.; Schock, L. E.; Seyam, A.; Stern, D. *Pure Appl. Chem.* 1989, 61, 1665.

Mayer, J. M. *Acc. Chem. Res*. 1998, 31, 441.

McMillan, J. A. *Chem. Rev.* 1962, 62, 65.

MOE (Molecular Operating Environment) Chemical Computing Group Inc., http://www.chemcomp.com.

Monod, J.; Wyman, J.; Changeux, J. P. *J. Mol. Bio.* 1965, 12, 88.

Nagashima, H.; Kondo, H.; Hayashida, T.; Yamaguchi, Y.; Gondo, M.; Masuda, S.; Miyazaki, K.; Matsubara, K.; Kirchner, K. *Coord. Chem. Rev.* 2003, 245, 177.

Njalsson, R.; Norgren, S.; Larsson, A.; Huang, C. S.; Anderson, M. E.; Luo, J. L. *Biochem. Biophys. Res. Comm.* 2001, 289, 80.

Newbound, T. D.; Colsman, M. R.; Miller, M. M.; Wulfsberg, G. P.; Anderson, O. P.; Strauss, S. H. *J. Am. Chem. Soc.* 1989, 111, 3762.

Ng, F. T. T.; Rempel, G. L.; Mancuso, C.; Halpern, J. *Organometallics*. 1990, 9, 2762.

Parr, R. G.; Yang, W. *Density-functional Theory of Atoms and Molecules*, Oxford Univ. Press, Oxford, 1989.

Peng, T. S.; Winter, C. H.; Gladysz, J. A. *Inorg. Chem.* 1994, 33, 2534.

Periana, R. A.; Bhalla, G.; William J. Tenn, I.; Young, K. J. H.; Liu, X. Y.; Mironov, O.; Jones, C.; Ziatdinov, V. R. *J. Mol. Catal. A: Chem.* 2004, 220, 7.

Petrenko, T.; Ray, K.; Wieghardt, K. E.; Neese, F.. *J. Am. Chem. Soc.* 2006, 128, 4422.

Pittard, K. A.; Lee, J. P.; Cundari, T. R.; Gunnoe, T. B.; Petersen, J. L. *Organometallics*. 2004, 23, 5514.

Polekhina, G.; Board, P. C.; Gali, R.; Rossjohn, J.; Parker, M. W. *EMBO J.* 1999, 12, 3204.

Pyykkö, P. *Chem. Rev*. 1988, 88, 563.

Pyykkö, P.; Mendizabal, F. *Inorg. Chem*. 1998, 37, 3018.

Rappé, A. K.; Casewit, C. J.; Colwell, K. S.; Goddard III, K. S.; Skiff, W. M. *J. Am. Chem. Soc*. 1992, 114, 10024.

Ray, K.; Weyhermueller, T.; Neese, F.; Wieghardt, K. *Inorg. Chem.* 2005, 44, 5345.

Riordan, C. G.; Halpern, J. *Inorg. Chim. Acta*. 1996, 243, 19.

Ritleng, V.; Sirlin, C.; Pfeffer, M. *Chem. Rev*. 2002, 102, 1731.

Robbins, J.; Bazan, G. C.; Murdzek, J. S.; O'Regan, M. B.; Schrock, R. R. *Organometallics.* 1991, 10, 2902.

Sanford, M. S.; Ulman, M.; Grubbs, R. H. *J. Am. Chem. Soc*. 2001,123, 749.

Schlupp, R. L.; Maki, A. H. *Inorg. Chem.* 1974, 13, 44. See footnote 40.

Schmidbaur, H.; Dash, K. C. *Adv. Inorg. Chem. Radiochem.* 1982, 25, 39.

Schmidt, M. W.; Baldridge, K. K.; Boatz, J. A.; Elbert, S. T.; Gordon, M. S.; Jensen, J. J.; Koseki, S.; Matsunaga, N.; Nguyen, K. A.; Su, S.; Windus, T. L.; Dupuis, M., and Montgomery, J. A. *J. Comput. Chem.* 1993, 14, 1347.

Schröder, D.; Brown, R.; Schwerdtfeger, P.; Wang, X. B.; Yang, X.; Wang, L. S.; Schwarz, H. *Angew. Chem. Int. Ed.* 2003, 42, 311.

Schwerdtfeger, P.; Boyd, P. D. W.; Brienne, S.; Burrell, A. K. *Inorg. Chem*. 1992, 31, 3411.

Scott, A. P.; Radom, L. *J. Phys. Chem.* 1996, 100(41), 16502.

Seidel, S.; Seppelt, K. *Science.* 2000, 290, 117.

Selegue, J. P. *Coord. Chem. Rev.* 248(15-16), 1543.

Sherry, A. E.; Wayland, B. B. *J. Am. Chem. Soc.* 1990, 112, 1259.

Simões, J. A. M.; Beauchamp, J. L. *Chem. Rev.* 1990, 90, 629.

Sinha, P.; Wilson, A. K.; Omary, M. A. *J. Am. Chem. Soc.* 2005, 127, 12488.

Sobolev, S.; Sorokine, A.; Prilusky, A.; Abola, E. E.; Edelman, M. *Bioinformatics.* 1999, 15, 327.

Stevens, W. J.; Basch, H.; Krauss, M. *J. Chem. Phys.* 1984, 81, 6026.

Stevens, W. J.; Krauss, M.; Basch, H.; Jasien, P. G. *Can. J. Chem.* 1992, 70, 612.

Tan, K. L.; Bergman, R. G.; Ellman, J. A. *J. Am. Chem. Soc.* 2002, 124, 3202.

Tenaglia, A.; Heumann, A. *Angew. Chem., Int. Ed.* 1998, 38, 2180.

Tenorio, M. J.; Mereiter, K.; Puerta, M. C.; Valerga, P. *J. Am. Chem. Soc.* 2000, 122, 11230.

Tenorio, M. J.; Puerta, M. C.; Valerga, P. *J. Organomet. Chem*. 2000, 609, 161.

Tenorio, M. J.; Tenorio, M. A. J.; Puerta, M. C.; Valerga, P. *Inorg. Chim. Acta*. 1997, 259, 77.

Thorn, D. L.; Tulip, T. H.; Ibers, J. A. *J. Chem. Soc., Dalton Trans.* 1979, 2022.

Tilset, M.; Fjeldahl, I.; Hamon, J.-R.; Hamon, P.; Toupet, L.; Saillard, J.-Y.; Costuas, K.; Haynes, A. *J. Am. Chem. Soc*. 2001, 123, 9984.

Tomasi, J.; Mennucci, B.; Cammi, R. *Chem. Rev.* 2005, 105, 2999.

Trace, R. L.; Sanchez, J.; Yang, J.; Yin, J.; Jones, W. M. *Organometallics.*1992, 11, 1440.

Trnka, T. M.; Grubbs, R. H. *Acc. Chem. Res*. 2001, 34, 18.

Trost, B. M. *Acc. Chem. Res*. 2002, 35, 695.

Uudsemaa, M.; Tamm, T. *J. Phys. Chem. A.* 2003, 107, 9997.

van der Boom, M. E.; Iron, M. A.; Atasoylu, O.; Shimon, L. J. W.; Rozenberg, H.; Ben-David, Y.; Konstantinovski, L.; Martin, J. M. L.; Milstein, D. *Inorg. Chim. Acta.* 2004, 357, 1854.

van der Boom, M. E.; Liou, S. Y.; Ben-David, Y.; Shimon, L. J. W.; Milstein, D. *J. Am. Chem. Soc.* 1998, 120, 6531.

van der Boom, M. E.; Milstein, D. *Chem. Rev.* 2003, 103, 1759.

Vänngard, T.; Kerström, S. A. *Nature* 1959, 184,183.

Van Seggen, D. M.; Anderson, O. P.; Strauss, S. H. *Inorg. Chem.* 1992, 31, 2987.

Veige, A. S.; Slaughter, L. M.; Lobkovsky, E. B.; Wolczanski, P. T.; Matsunaga, N.; Decker, S. A.; Cundari, T. R. *Inorg. Chem.* 2003, 42, 6204.

Veige, A. S.; Slaughter, L. M.; Wolczanski, P. T.; Matsunaga, N.; Decker, S. A.; Cundari, T. R. *J. Am. Chem. Soc.* 2001, 123, 6419.

Vigalok, A.; Ben-David, Y.; Milstein, D. *Organometallics.* 1996, 15, 1839.

Vigalok, A.; Kraatz, H. B.; Konstantinovski, L.; Milstein, D. *Chem. Eur. J.* 1997, 3, 253.

Vigalok, A.; Milstein, D. *Organometallics.* 2000, 19, 2061.

Vollhardt, K. P. C.; Cammack, J. K.; Matzger, A. J.; Bauer, A.; Capps, K. B.; Hoff, C. D. *Inorg. Chem.* 1999, 38, 2624.

Vreven, T.; Morokuma, K. *J. Comp. Chem*. 2000, 21, 1419.

Walker, N. R.; Wright, R. R.; Barran, P. E.; Stace, A. *J. Organometallics*. 1999, 18, 3569.

Walker, N.; Wright, R.; Barren, P.; Murrell, J,; Stace. A. *J. Am. Chem. Soc*. 2001, 123, 4223.

Walsh, P. J.; Hollander, F. J.; Bergman, R. G. *J. Am. Chem. Soc.* 1988, 110, 8729.

Walstrom, A.; Pink, M.; Yang, X.; Tomaszewski, J.; Baik, M. H.; Caulton, K. G. *J. Am. Chem. Soc.* 2005, 127, 5330.

Walstrom, A. N.; Watson, L. A.; Pink, M.; Caulton, K. G. *Organometallics.* 2004, 23, 4814.

Warren, L. F.; Hawthorne, M. F. *J. Am. Chem. Soc.* 1968, 90*,* 4823.

Waters, J. H.; Gray, H. B. *J. Am. Chem. Soc.* 1965, 87, 3534.

Watson, L. A.; Coalter, J. N., III; Ozerov, O. V.; Pink, M.; Huffman, J. C.; Caulton, K. G. *New J. Chem.* 2003, 263.

Watson, L. A.; Ozerov, O. V.; Pink, M.; Caulton, K. G. *J. Am. Chem. Soc.* 2003, 125, 8426.

Wen, T. B.; Cheung, Y. K.; Yao, J.; Wong, W. T.; Zhou, Z. Y.; Jia, G. *Organometallics.* 2000, 19, 3803.

Williams, D S.; Schofield, M. H.; Schrock, R. R.; Davis, W. M.; Anhaus, J. T. *J. Am. Chem. Soc.* 1991, 113, 5480.

Wolfe, J. P.; Wagaw, S.; Marcoux, J. F.; Buchwald, S. L. *Acc. Chem.Res.* 1998, 31, 805.

Wu, F.; Dash, A. K.; Jordan, R. F. *J. Am. Chem. Soc.* 2004, 126, 15360.

Zhang, J.; Barakat, K. A.; Cundari, T. R.; Gunnoe, T. B.; Boyle, P. D.; Petersen, J. L.; Day, C. S. *Inorg. Chem*. 2005, 44, 8379.

Zhang, J.; Gunnoe, T. B.; Boyle, P. D. *Organometallics.* 2004, 23, 3094.

Zhang, J.; Gunnoe, T. B.; Petersen, J. L. *Inorg. Chem.* 2005, 44, 2895.